

D-A100 333

NOTRE DAME UNIV IND DEPT OF AEROSPACE AND MECHANICA--ETC F/G 20/4  
HIGH SPEED SMOKE FLOW VISUALIZATION.(U)

MAR 81 S M BATILL, R C. NELSON, T J MUELLER

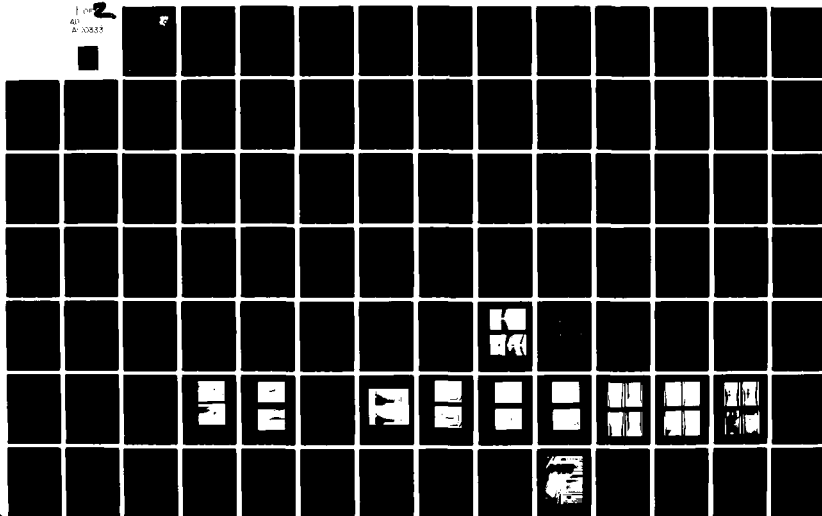
F33615-79-C-3034

AFWAL-TR-81-3002

NL

UNCLASSIFIED

1 of 2  
40  
A-10833



AD A100333

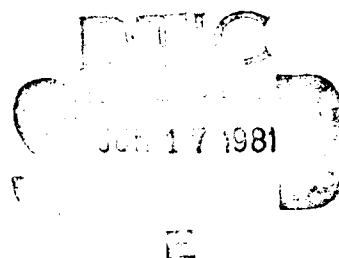
AFWAL-TR-81-3002

HIGH SPEED SMOKE FLOW VISUALIZATION

Stephen M. Batill  
Robert C. Nelson  
Thomas J. Mueller  
Department of Aerospace and Mechanical Engineering  
University of Notre Dame  
Notre Dame, IN 46556.



March 1981



TECHNICAL REPORT AFWAL-TR-81-3002

Final Report for Period September 1979 - October 1980

Approved for public release; distribution unlimited

DNC FILE COPY

FLIGHT DYNAMICS LABORATORY  
AIR FORCE WRIGHT AERONAUTICAL LABORATORIES  
AIR FORCE SYSTEMS COMMAND  
WRIGHT-PATTERSON AFB, OHIO 45433


81 6 16 118

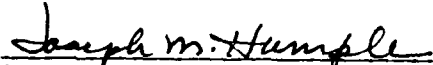
# NOTICE

When Government drawings, specifications, or other data are used for any purpose other than in connection with a definitely related Government procurement operation, the United States Government thereby incurs no responsibility nor any obligation whatsoever; and the fact that the Government may have formulated, furnished, or in any way supplied the said drawings, specifications, or other data, is not to be regarded by implication or otherwise as in any manner licensing the holder or any other person or corporation, or conveying any rights or permission to manufacture, use, or sell any patented invention that may in any way be related thereto.

This report has been reviewed by the Office of Public Affairs (ASD/PA) and is releasable to the National Technical Information Service (NTIS). At NTIS, it will be available to the general public, including foreign nations.

This technical report has been reviewed and is approved for publication.

  
WILEY C. WELLS  
Mechanical Engineer  
Mechanical Systems Group

  
JOSEPH M. HAMPLE, Chief  
Experimental Engineering Branch  
Aeromechanics Division

FOR THE COMMANDER

  
PETER J. BUTKEWICZ  
Colonel, USAF  
Chief, Aeromechanics Division

If your address has changed, if you wish to be removed from our mailing list, or if the addressee is no longer employed by your organization please notify AFWAL/FIMN, W-PAFB, OH 45433, to help us maintain a current mailing list.

Copies of this report should not be returned unless return is required by security considerations, contractual obligations, or notice on a specific document.

19 REPORT DOCUMENTATION PAGE		READ INSTRUCTIONS BEFORE COMPLETING FORM	
1. REPORT NUMBER	2. GOVT ACCESSION NO.	3. RECIPIENT'S CATALOG NUMBER	
AFWAL-TR-81-3002	AD-A200	333	
4. TITLE (and Subtitle)	5. TYPE OF REPORT & PERIOD COVERED	6. PERFORMING ORG. REPORT NUMBER	
HIGH SPEED SMOKE FLOW VISUALIZATION.	Final Rept. Sept 1979 - Oct 1980		
7. AUTHOR(s)	8. CONTRACT OR GRANT NUMBER(s)		
Stephen M. Batill Robert C. Nelson Thomas J. Mueller	F33615-79-C-3034		
9. PERFORMING ORGANIZATION NAME AND ADDRESS	10. PROGRAM ELEMENT, PROJECT, TASK AREA & WORK UNIT NUMBERS		
Dept. of Aerospace and Mechanical Engineering University of Notre Dame Notre Dame, IN 46556.	61102F 2703-N4-38		
11. CONTROLLING OFFICE NAME AND ADDRESS	12. REPORT DATE	13. NUMBER OF PAGES	
	March 1981	109	
14. MONITORING AGENCY NAME & ADDRESS (if different from Controlling Office)	15. SECURITY CLASS. (of this report)	15a. DECLASSIFICATION DOWNGRADING SCHEDULE	
FLIGHT DYNAMICS LABORATORY (AFWAL/FIMN) AIR FORCE WRIGHT AERONAUTICAL LABORATORIES (AFSC) WRIGHT-PATTERSON AIR FORCE BASE, OH 45433.	UNCLASSIFIED		
16. DISTRIBUTION STATEMENT (of this Report)			
Approved for public release; distribution unlimited.			
17. DISTRIBUTION STATEMENT (of the abstract entered in Block 20, if different from Report)			
18. SUPPLEMENTARY NOTES			
19. KEY WORDS (Continue on reverse side if necessary and identify by block number)			
Smoke Flow Visualization Wind Tunnel Design Transonic Smoke Visualization Supersonic Smoke Visualization			
20. ABSTRACT (Continue on reverse side if necessary and identify by block number)			
Dr. V.P. Goddard demonstrated that it was possible to use smoke flow visualization techniques, which had previously been considered the tools of the low speed aerodynamicist, in high speed and supersonic flows. This report documents a study to evaluate the techniques used by Goddard and to establish design criteria for a large high speed flow visualization facility. Included are discussions of the existing facilities at the University of Notre Dame, studies of the wind tunnel flow field and methods for smoke data acquisition.			

## PREFACE

The work documented in this report was performed by the Department of Aerospace and Mechanical Engineering, University of Notre Dame, for the Department of the Air Force, Air Force Wright Aeronautical Laboratories (AFSC), Flight Dynamics Laboratory, Wright-Patterson Air Force Base, Ohio, under contract F33615-79-C-3034. The Principal Investigators on the project were Dr. Stephen M. Batill, Dr. Robert C. Nelson and Dr. Thomas J. Mueller.

The authors wish to acknowledge the contributions of Mr. Nikolaos Adonakis and Mr. Carl Aumen as Graduate Research Assistants at the University of Notre Dame.

The report documents work conducted from September 1979 to October 1980. The final report was submitted in December 1980.

Accession No.	
NTIS	X
DTIC	
AD	
AS	
CS	
DS	
ES	
FS	
GS	
HS	
IS	
JS	
KS	
LS	
MS	
NS	
OS	
PS	
QS	
RS	
TS	
US	
VS	
WS	
XS	
YS	
ZS	
Dist	
A	

## TABLE OF CONTENTS

	<u>Page No.</u>
INTRODUCTION . . . . .	1
Historical Development . . . . .	1
Project Scope . . . . .	3
UNIVERSITY OF NOTRE DAME'S HIGH SPEED SMOKE VISUALIZATION FACILITIES . . . . .	7
Original Tunnel Design . . . . .	7
Smoke Generation Techniques . . . . .	9
Kerosene Smoke . . . . .	11
Alternative Methods . . . . .	12
Smoke Flow Photography . . . . .	14
Photographic Procedures . . . . .	15
Preliminary Visualization Studies . . . . .	16
Inlet Flow Field Study . . . . .	19
Optical Data Acquisition Techniques . . . . .	25
NEW FACILITIES AND DESIGN CRITERIA . . . . .	28
Inlet Design Methods . . . . .	28
Transonic Flow Visualization . . . . .	31
Facility Design Criteria . . . . .	34
Inlet/Screens . . . . .	35
Test Section . . . . .	36
CONCLUSIONS AND RECOMMENDATIONS . . . . .	40
REFERENCES . . . . .	42
APPENDIX: SYSTEM SAFETY HAZARD ANALYSIS . . . . .	45
TABLES . . . . .	48
FIGURES . . . . .	52

# LIST OF ILLUSTRATIONS

<u>Figure No.</u>	<u>Title</u>	<u>Page No.</u>
1.	Original Photographs by V.P. Goddard	52
2.	Schematic of Notre Dame's High Speed Aerodynamics Facilities, Planform View.	53
3.	Schematic of Pilot Supersonic Tunnel, Original Inlet.	54
4.	Schematic of 5" by 5" Supersonic Tunnel	55
5.	Range of Particle Size of Various Materials (from Ref. 38)	56
6.	Methods of Particle Detection, Range for Light Scattering.	57
7.	Distillation Curves for Hydrocarbon Mixtures (from Ref. 15)	58
8.	Kerosene Smoke Generator	59
9.	Schematic of Smoke Rake	60
10.	Photographs of Steam Visualization Experiment in Pilot Tunnel	61
11.	Photographs of Mineral Oil Smoke Generator Demonstration	62
12.	Lighting and Camera Arrangements	63
13.	High Speed Motion Picture Photograph, Right Circular Cylinder Model, $M_\infty = 0.55$ , 128 frames/second.	64
14.	High Speed Still Photograph, Right Circular Cylinder Model, 5" by 5" Tunnel.	65
15.	High Speed Still Photographs, Sphere Model.	66
16.	High Speed Still Photographs, Double Wedge Airfoil.	67
17.	Screen Influence Study, Pilot Tunnel, Original Smith/Wang Inlet, Top Lighting. (15.1 mm ID Smoke Rake)	68
18.	Screen Influence Study, Pilot Tunnel, Original Smith/Wang Inlet, Back Lighting. (15.1 mm ID Smoke Rake)	69

# LIST OF ILLUSTRATIONS (Cont.)

<u>Figure No.</u>	<u>Title</u>	<u>Page No.</u>
19.	Screen Influence Study, Pilot Tunnel, Original Smith/Wang Inlet. (9.5 mm ID Smoke Rake)	70
20.	Inlet Geometry Profile, Smith/Wang Inlet, Side View.	71
21.	Inlet Geometry Profile, Smith/Wang Inlet, Top View.	72
22.	Axial Distribution of Cross-Section Area, Smith/Wang Inlet.	73
23.	Axial Velocity Fluctuations, Smith/Wang Inlet, Port 1.	74
24.	Axial Velocity Fluctuations, Smith/Wang Inlet, Port 2.	75
25.	Axial Velocity Fluctuations, Smith/Wang Inlet, Port 3.	76
26.	Axial Turbulence Intensity Summary, Smith/Wang Inlet.	77
27.	Inlet Geometry Profile, MPT Inlet, Side View.	78
28.	Inlet Geometry Profile, MPT Inlet, Top View.	79
29.	Axial Distribution of Cross-Section Area, MPT Inlet.	80
30.	Photograph of MPT Inlet Installed on Pilot Tunnel	81
31.	Axial Velocity Fluctuations, MPT Inlet, Port 1.	82
32.	Axial Velocity Fluctuations, MPT Inlet, Port 2.	83
33.	Axial Velocity Fluctuations, MPT Inlet, Port 3.	84
34.	Axial Turbulence Intensity Summary, MPT Inlet, (Solid Symbols are X-Wire Measurements).	85
35.	Turbulence Intensity Summary, Transverse Component, MPT Inlet.	86
36.	Screen Influence Study, Pilot Tunnel, MPT Inlet, Top Lighting. (19.1 mm ID Smoke Rake)	87/88



# LIST OF ILLUSTRATIONS (Cont.)

<u>Figure No.</u>	<u>Title</u>	<u>Page No.</u>
37.	Influence of Honeycomb Insert on Smoke Visualization Data	89
38.	Axial Turbulence Intensity Summary, MPT Inlet with Honeycomb.	90
39.	Total Pressure Loss through Anti-Turbulence Screens	91
40.	Schematic of Single Pass Schlieren System	92
41.	Opaque Stop Schlieren Photograph; 9° Double Wedge Model, $M_\infty \approx 1.42$ .	93
42.	Simultaneous Smoke Flow/Opaque Stop Schlieren Photograph; 9° Double Wedge Model, $M_\infty \approx 1.42$ .	94
43.	Modified Opaque Stop Schlieren System	95
44.	Inlet Entrance and Exit Velocity Profiles (Data from Ref. 24)	96
45.	Inlet Wall Velocity Distribution, Comparison of One-Dimensional and Two-Dimensional Calculations.	97
46.	Geometry and Notation for Matched Cubic Inlet Shapes	97
47.	Non-Dimensional Inlet Length versus Contraction Ratio, Calculated Using Morel's Method.	98
48.	Location of Match Point versus Contraction Ratio, Calculated Using Morel's Method.	98
49.	Inlet Profile, CR = 75 Inlet, Transonic Tunnel.	99
50.	Inlet Profile, CR = 150 Inlet, Transonic Tunnel.	100
51.	Schematic of Transonic Test Section	101
52.	Screen Influence, Transonic Tunnel, CR = 75 Inlet, $M_\infty = 0.40$ .	102
53.	Transonic Smoke Flow Visualization, CR = 75 Inlet, $\alpha = 8^\circ$ , $M_\infty \approx 0.40$ .	103
54.	Transonic Smoke Flow Visualization, CR = 75 Inlet, $\alpha = 15^\circ$ , $M_\infty \approx 0.40$ .	104

# LIST OF ILLUSTRATIONS (Cont.)

<u>Figure No.</u>	<u>Title</u>	<u>Page No.</u>
55.	Transonic Smoke Flow Visualization, CR = 150 Inlet, $\alpha = 0^\circ$ , $M_\infty \approx 0.40$ .	105
56.	Transonic Smoke Flow Visualization, CR = 150 Inlet, $\alpha = 0^\circ$ .	106
57.	Transonic Smoke Flow Visualization, CR = 150 Inlet, 11 Screens, $M_\infty \approx 0.72$ .	107
58.	Transonic Smoke Flow Visualization, CR = 150 Inlet, 11 Screens, $M_\infty \approx 0.40$ .	108
59.	Transonic Smoke Flow Demonstration, Oblique View, CR = 150 Inlet, $M_\infty \approx 0.40$ .	109

# LIST OF TABLES

<u>Table No.</u>	<u>Title</u>	<u>Page No.</u>
I.	Wind Tunnel Geometric Properties	47
II.	Methods for Aerosol Generation (from Reference 15)	48
III.	Physical Properties of Hydrocarbons Used for Smoke Generation (from Reference 38)	49
IV.	Recommended Equipment for Smoke Flow Photography	50
V.	Sources of Problems in Flow Visualization Experiments	51
VI.	Photographic Procedures	51

## SUMMARY

Dr. V.P. Goddard demonstrated that it was possible to use smoke flow visualization techniques, which had previously been considered the tools of the low speed aerodynamicist, in high speed and supersonic flows. This report documents a study to evaluate the techniques used by Goddard and to establish design criteria for a large high speed flow visualization facility. Included are discussions of the existing facilities at the University of Notre Dame, studies of the wind tunnel flow field and methods for smoke data acquisition.

## INTRODUCTION

There has been a great interest throughout the history of aerodynamics in the development of techniques which can be used to help visualize a given flow phenomenon. This visualization of flow patterns has played a singularly important role in the advancement of our physical understanding of the mechanics of fluids. Flow visualization has led to the discovery of flow phenomena and has helped in the development of mathematical models for complex flow problems. It is also useful in the verification of existing principles and has been an important tool in the development of complicated engineering systems. Most visualization methods allow for detailed study of a problem without the introduction of probes which can influence the character of the flow.

### Historical Development

Flow visualization in wind tunnels closely followed the development of such tunnels and may be traced to Dr. Ludwig Mach of Vienna in 1893.<sup>1</sup> Mach's indraft tunnel had a cross-section of 180 by 250 mm (7 by 10 in.) and was driven by a centrifugal fan which could produce a speed of 10 m (33 ft) per second. A piece of wire mesh over the inlet was used to straighten the flow. One side of the test section was clear glass and the others were painted black. The flow was observed and photographed by using silk threads, cigarette smoke, and glowing iron particles. The only smoke flow photographs presented in Reference 1 are for the flow past a plate perpendicular to the flow. The smoke is faint and difficult to make out; nevertheless, it was a beginning.

In France, about 1899, E.J. Marey who was famous for his photographic studies of animal locomotion, turned his attention to photographing air in motion.<sup>2</sup> Marey, cognizant of the work of Mach, used a vertical wind tunnel with a 200 by 300 mm (8 by 12 in.) cross-section. The front and sides of the test section were glass and the back was covered with black velvet. Air was drawn into the tunnel by a small suction fan after passing through fine silk gauze at the inlet. Smoke obtained by burning wood shavings entered the wind tunnel upstream of the gauze straighteners through a row of fine tubes. Excellent smoke flow photographs were obtained using a magnesium flash.

Although the interest in smoke visualization continued during the first

thirty years of the twentieth century, significant improvements in the technique and results were not achieved until the 1930's.<sup>3</sup> The best of the early two-dimensional smoke tunnels was developed by A.M. Lippisch in Germany in the mid-1930's.<sup>4</sup> He obtained a large number of good smoke photographs for the flow around plates, cylinders, and airfoils, including the Lippisch rotor-wing. Many of these photographs indicate that the turbulence level was higher than desirable. Also, he began the development of an intermittent smoke delivery system.

Within this same time period, F.N.M. Brown, at the University of Notre Dame, began his research in flow visualization. His first smoke tunnel became operational in 1937.<sup>3,5</sup> It was an indraft, open circuit tunnel with a large inlet contraction section, and produced speeds of up to 3 m (10 ft) per second. The test section was 305 by 1219 by 1.58 mm (12 by 48 by 1/16 in.) deep. Photographs were obtained at about 3 m (10 ft) per second using titanium tetrachloride for smoke. This smoke tunnel was developed primarily for classroom demonstrations. He also developed a three-dimensional smoke tunnel which was operational in 1940. This indraft tunnel had a single 6.30 meshes per cm (16 per in.) screen followed by a 9:1 contraction in area. The test section which had a 610 by 610 mm (24 by 24 in.) cross-section was about 914 mm (36 in.) in length, and speeds of up to 12.2 m (40 ft) per second could be attained using a 1 hp DC motor. Smoke was produced by coking wheat straw and was introduced upstream of the anti-turbulence screen through a row of tubes, i.e., a rake. A new three-dimensional smoke tunnel was designed but little progress was made during World War II.

Work began in 1947 on a research three-dimensional smoke tunnel which was operational at the University of Notre Dame in 1948.<sup>3,5</sup> As a result of the lessons learned earlier, this smoke tunnel had five 5.51 by 7.09 meshes per cm (14 by 18 per in.) bronze screens at the inlet of the 12:1 contraction section. The test section was maintained at 610 by 610 mm (24 by 24 in.) in cross-section and 914 mm (36 in.) long. Useful speeds of 10.7 m (35 ft) per second could be attained using a squirrel cage fan driven by a 5 hp motor. Coked wheat straw was used with a total of 12,000 watts of steady lighting to obtain photographs of the flow. This three-dimensional smoke tunnel evolved slowly into the one used today. In conjunction with his smoke tunnel develop-

ment, Brown developed a movable smoke rake and the first easy-to-use kerosene smoke generator which could produce large quantities of smoke. He was also the first to take three-dimensional and stereo photographs of smoke flows. In fact, most of the progress and refinement of smoke visualization techniques are credited to Brown.<sup>6</sup>

Expanding the techniques of Brown, V.P. Goddard (also at the University of Notre Dame) was able to produce the world's first and only supersonic smoke tunnel in 1959.<sup>7,8</sup> An indraft supersonic wind tunnel with seven screens and a large inlet contraction to the nozzle throat was designed and built. A modified Schlieren system permitted the simultaneous photographing of both smoke and shock-wave patterns. Using the same smoke generation and injection techniques as in the subsonic tunnels, smoke photographs were taken at speeds of up to 404 m (1320 ft) per second (i.e., a Mach number of 1.38). Most researchers in this field still do not believe this is possible until they actually see it. Figure 1 shows two photographs taken by Goddard, indicating the quality of the first supersonic smoke flow visualization data.

It was clear by 1959 that the smoke tunnel was an important research tool. From publications since 1959, it is evident that the state-of-the-art established by Brown, Goddard and Lippisch has not changed to the present day. As a result of unique data Brown obtained, especially in the area of boundary layer transition, there has been a renewed interest in using these established techniques.

#### Project Scope

The purpose of this project was to study the high speed flow visualization method developed by Goddard and to establish the requirements for a wind tunnel, smoke generating equipment and data acquisition methods so this technique could be used in other high speed flow facilities. The project was divided into two phases. The first phase was an evaluation of the present high speed flow capability at the University of Notre Dame. The second phase was the detailed study directed at the establishment of design criteria for a high speed smoke flow visualization facility at the Flight Dynamics Laboratory.

As mentioned, the only known transonic and supersonic smoke flow visualization research has been conducted at the University of Notre Dame. The goal

of the first phase was to develop a better understanding of the high speed visualization method as developed by Goddard. The preliminary work of Goddard has shown that it is possible to introduce and maintain well defined smoke streaklines in a supersonic flow field. Some applications of his work have shown that these streakline data can yield significant quantitative information.<sup>9</sup>

The initial work focused on the evaluation of the flow field within the high speed flow visualization tunnels and the optical and photographic techniques used in collecting smoke visualization data. The main requirement for any facility designed to conduct flow visualization research is a low turbulence level within the flow field. The low turbulence level will minimize the diffusion of the smoke particles and allow for greater definition of the smoke streaklines. The low turbulence levels are achieved in the University of Notre Dame's tunnels through the use of the high contraction ratio inlets and the use of anti-turbulence screens at the entrance to the inlet. In Goddard's original design, seven screens were used but, apparently, he did not determine the optimum number or relative placement of these screens. The influence of the anti-turbulence screens on the flow field is also of primary interest. A series of tests was performed using both photographic data for quantitative assessment and hot-wire anemometer measurements of turbulence levels to assess the influence of the anti-turbulence screens. These data were used to establish the flow field requirements for smoke flow visualization in both high speed subsonic and supersonic flow fields.

Goddard developed an opaque stop Schlieren system for use with the high speed flow visualization; it was used to take simultaneous smoke/Schlieren photographs. Since it allowed for this unique method of simultaneous flow visualization analysis, one goal of the research program was to reconstruct this system and evaluate its potential as a data acquisition technique.

The evaluation of the best methods for lighting and photographing the test section for direct smoke flow photography is another critical aspect of the project. When dealing with such high speeds, thick tunnel wall glass, relatively low smoke levels, size and structural restraints associated with high speed tunnels, the proper lighting of the smoke lines is a definite problem. Attempts were made to develop optional lighting and photographic



techniques which could be applied to different types of high speed test sections and flow conditions. These initial studies were conducted using some simple geometric shapes such as a sphere, a cone, a wedge, and a two-dimensional airfoil.

The results of the initial phase were used to provide a starting point for the development of design criteria for a much larger high speed flow visualization capability. The design criteria are for an indraft, high speed flow tunnel and to establish the requirements for inlet and test section design, smoke generation equipment and data acquisition techniques.

The characteristics of the flow in the test section are sensitive to the inlet design. The original supersonic tunnel inlets were designed using the same techniques as those used for Brown's subsonic tunnels. One goal was to improve the inlet design and, having established a better understanding of the influence of the anti-turbulence screens, arrive at an inlet/screen combination which would allow for the best application of the flow visualization technique. A new inlet was designed and tested using the same wind tunnel test section as in the preliminary phases of the study and it illustrated the importance of the inlet design on the quality of the flow visualization results.

Most of the work was conducted using the kerosene smoke developed by Brown. There was also an evaluation of the possibility of using alternate methods of smoke generation. Particular emphasis was placed on water-based systems. There exist a number of alternatives which produce a smoke that is non-toxic and that does not present the flammability problems of kerosene.<sup>10-12</sup> These methods were not found to be superior to the kerosene technique. This conclusion was based on a subjective evaluation of the quality of the smoke photographs and on the safety aspects of using each technique.

The transonic flow regime provides a situation in which the smoke flow visualization method could provide very valuable information. The non-intrusive nature of the technique is ideal in studying the complex interaction that can occur. For this reason, an important aspect of this study was to demonstrate the use of the method in a transonic wind tunnel. The design and fabrication of such a facility was a joint effort between the Flight Dynamics Laboratory and the University of Notre Dame. This tunnel was then used to collect the first transonic smoke visualization data on record.

The experience gained in the initial phases of the study were incorporated into a set of design criteria for a large scale, high speed flow visualization facility. It was initially anticipated that this facility would be an indraft tunnel with a 0.37 sq. m (4 sq. ft) test section. Since the size of the power requirements for such a tunnel would be very large and the design would require a significant extrapolation of results acquired in this study, alternative recommendations are presented.

## UNIVERSITY OF NOTRE DAME'S HIGH SPEED SMOKE VISUALIZATION FACILITIES

### Original Tunnel Design

The supersonic tunnel facilities at the University of Notre Dame are air indraft, continuous flow tunnels which were designed for high speed flow demonstrations and research. A planform view schematic of the facilities is shown in Figure 2. Three tunnel diffusers are connected to a common manifold which can be evacuated using one, two or three vacuum pumps. The pumps are each driven by 125 hp, AC motors, with a mass flow capability sufficient for continuous operation of the tunnels. For a typical test, only one test section is used and the other diffusers are sealed either with a valve at the downstream end of the diffuser or a plate placed over the upstream end.

Two different supersonic, fixed nozzle block test sections were used for a majority of the tests conducted during this research program. Most of the testing was conducted using the pilot tunnel shown schematically in Figure 3. Table 1 lists certain geometric parameters for the original pilot tunnel as used by Goddard. The original pilot tunnel was composed of a series of anti-turbulence screens which were mounted upstream of the rigid inlet section. The inlet itself had a rectangular cross-section with an aspect ratio (height/width) of 3.25 at the entrance and an aspect ratio of 3.0 at the exit of the inlet. The inlet was connected to a fixed geometry converging-diverging nozzle that was designed using the Foelsch method.<sup>13</sup> One of the primary items of interest in this research program involved the area contraction ratio associated with the indraft tunnel design. For the discussions in this report, the term "contraction ratio" will be used for the ratio of the area at inlet or screen to the area of the test section, unless stated otherwise. This means that the pilot tunnel has a contraction ratio, with the original inlet and with anti-turbulence screens attached, of 164:1.

The pilot tunnel nozzle is a two-dimensional design with a constant width of 63.5 mm (2.5 in.) and a design Mach number of 1.42. The test section itself has a square cross-section approximately 50 mm (2 in.) long. Models are positioned in the test section using an aft sting mount. Both side walls of the test section are of optical quality glass. The top nozzle block is a sandwich construction in which a plexiglass sheet 13 mm (0.5 in.) wide is

placed between two metal blocks. The plexiglass is centered in the test section and allows for lighting of the test section in a plane perpendicular to the normal viewing direction.

The pilot tunnel inlet was designed using techniques which proved successful in the development of the large, three-dimensional subsonic tunnel at the University of Notre Dame. The two-dimensional method of Smith and Wang<sup>14</sup> was used, in which the inlet horizontal and vertical contraction shapes corresponded to streamlines in a simple, two-dimensional potential flow analogy. There was, apparently, no concern for the manner in which the inlet was mated to the fixed nozzle. There was a sharp discontinuity in the slope of the contraction geometry at the point where the inlet and nozzle met. There also existed a discontinuity in slope between the inlet extension on the upstream end due to the anti-turbulence screen frames and the inlet.

The inlet screens initially used on the pilot tunnel were made of two types of screen. Six screens were made of a multi-strand nylon mesh with a 0.05 mm (0.002 in.) diameter strand and a 10 per cm (26 per in.) grid; this represented a 9.3% blockage. The nylon was stretched on a rectangular frame but, due to the flexibility of the nylon strands, there was some sag in the screen. Any screens attached to the inlet upstream of the nylon screens were made of an aluminum mesh with a 0.23 mm (0.009 in.) diameter aluminum wire in a uniform 7.1 per cm (18 per in.). These screens had a 29.7% blockage based on area. The tunnel was originally operated using seven anti-turbulence screens. The outermost screen at the upstream end of the inlet was aluminum and the remaining screens were of nylon mesh.

For the pilot tunnel operating at choked nozzle conditions, the volume flow rate in the tunnel was  $0.696 \text{ m}^3$  ( $24.6 \text{ ft}^3$ ) per second of air at standard atmospheric conditions. At the entrance to the first (metal) screen when the tunnel was operated in the original configuration (seven screens - six nylon and one metal), the air speed was approximately 1.1 m (3.5 ft) per second and the  $Re_d$  (Reynolds number based on screen wire diameter) was 16. At the nylon screen located in the most downstream position, the approximate flow speed was 2.1 m (7 ft) per second and the  $Re_d$  for the nylon strand was 8. These two Reynolds numbers gave a representative range for the anti-turbulence screens. In this Reynolds number range, the flow about a two-dimensional circular cylinder

was characterized by an attached vortex pair and a laminar wake. If the  $Re$  exceeds approximately 40, the wake is characterized by periodic vortex shedding which could have an adverse effect on the smoke flow visualization. A detailed discussion of the influence of the screens is presented later in the report.

The second test section used in this research program was mounted on the largest of the three diffusers. It, too, was a fixed geometry converging-diverging nozzle design with a  $160 \text{ mm}^2$  ( $25 \text{ in.}^2$ ) test section and a design Mach number of 1.51. It also had a high contraction ratio inlet and anti-turbulence screens, as shown in Figure 4. Operating in the configuration shown in the figure, the contraction ratio for this tunnel was 83:1. This tunnel will be referred to as the "5 by 5" tunnel in this report.

The inlet for this tunnel was not designed for the purpose of smoke flow visualization. The inlet does match the slope of the fixed nozzle contour at the downstream end of the inlet. Apparently, the inlet was not designed to any specific criteria and there are manufacturing irregularities in the inlet geometry. Although several preliminary tests were conducted using this inlet, most of the effort was focused on the pilot tunnel.

#### Smoke Generation Techniques

Direct high speed flow visualization requires the production of large quantities of smoke. The word "smoke" is used in a very broad sense and includes a variety of smoke-like materials such as vapors, fumes and mists. The smoke used must be generated in a safe manner and must possess the necessary light-scattering qualities so that it can be readily photographed. It is also important that the smoke not adversely affect the wind tunnel into which it is introduced nor the model being studied. Another desirable but not absolutely necessary qualification is that the smoke be non-toxic in the unlikely event that the experimenters are exposed to it. Finding a smoke-like substance which meets all these criteria is not an easy task.

A large number of materials have been used to generate smoke; examples are, the combustion of tobacco,<sup>1</sup> rotten wood,<sup>2</sup> and wheat straw,<sup>3</sup> the products of reaction of various chemical substances such as titanium tetrachloride and water vapor, and the vaporization of hydrocarbon oils, to name just a few.<sup>15</sup> The smoke-like materials used may be referred to as aerosols since aerosols

are composed of colloided particles suspended in a gas. A great deal of interest has been focused on aerosol properties and generation because of their close relationship to meteorology, air pollution, cloud chambers, smokes, combustion of fuels, colloid chemistry, etc.<sup>15</sup> The common methods for aerosol generation are shown in Table II which was taken from Reference 15.

Two very practical items must be carefully examined before the choice of smoke-like material is made for flow visualization. The smoke or aerosol particles must be as small as possible so they will closely follow the flow pattern being studied. These smoke particles must be large enough to scatter a sufficient amount of light so that photographs of the smoke pattern can be obtained. An approximate range of particle size for various materials and organisms is shown in Figure 5. Although many of these materials and substances have particle sizes below one micron, the most practical ones for flow visualization are the tobacco smoke, rosin smoke, carbon black, and oil smoke. There is no doubt that all these particles are small enough to follow the flow. Note that the flow particles in water vapor (fog) are generally much larger than one micron. If one now considers the light scattering ability of the particles used, another constraint becomes apparent. According to the laboratory methods of measuring particle sizes, particles should be larger than about 0.15 micron to scatter a sufficient amount of light to be readily seen (Figure 6). This light scattering criterion indicates that tobacco smoke and carbon black particles are mostly lower than 0.15 micron and, therefore, would be more difficult to photograph.

Resin is a semi-solid, organic substance exuded from various plants and trees or prepared synthetically, whereas rosin is the hard, brittle resin remaining after oil of turpentine has been distilled. Maltby and Keating<sup>16</sup> describe an electrically fused, pyrotechnic resin smoke generator which was developed for wind tunnel use up to speeds of 16 m per second. This smoke generator was manufactured by Brocks Fireworks Company, Ltd., in England and was based on the vaporization of resin. Maltby and Keating<sup>16</sup> also mention that some ammonium chlorate is present in the resin canisters, which must be stored away from heat since this substance is unstable. The device is simply a smoke bomb adapted for wind tunnel use. This appears to be the only mention of a resin or rosin smoke generator used for wind tunnel flow visualization.

There are, of course, a large number of possible hydrocarbon mixtures,

i.e., oils, which undoubtedly could be used to produce smoke by combustion or vaporization. From the point of view of laboratory safety, it would be desirable to use vaporization rather than the combustion technique. Properties of interest for three common hydrocarbon mixtures are shown in Table III. Furthermore, it would also be safer to use an oil which would vaporize at the lowest possible temperature and be the least flammable. Figure 7 presents data for the temperature versus per cent distilled (vaporized) for six oils. Mineral oil requires the highest temperature for vaporization, while charcoal lighter fluid requires the lowest. The second lowest temperature for vaporization is for kerosene. Since kerosene is less flammable than charcoal lighter fluid, it is the obvious choice. Kerosene seems to offer the best compromise when particle size, light scattering ability, low vaporization temperature, and low flammability are considered.

#### Kerosene Smoke

Although the first oil smoke generator was developed by Preston and Sweeting,<sup>17</sup> one of the most successful oil smoke generators was designed by F.N.M. Brown in 1961. Large quantities of dense kerosene smoke were produced quickly and safely with this generator. This four-tube kerosene generator is shown schematically in Figure 8.

A flat electric strip heater is located inside a 51 mm (2 in.) square thin wall conduit tube. The entire unit is set at a convenient angle (about 60°) and a sight-feed oiler is mounted on the unit at the upper end of each tube so the oil drips on the upper end of the strip heater. It has been determined that a drip rate of approximately two drops per second is more than sufficient to produce the desired amount of smoke. Faster rates result in inefficient and wasteful operation. Furthermore, an extremely fast drip rate can result in back-firing of the unit. A squirrel cage blower mounted at the low end of the unit is used to force the smoke through the system. The squirrel cage blower is more or less mandatory - in the event of back-firing the sudden increase in pressure is easily transmitted through the rotor.

Before entering the smoke rack, the smoke is allowed to pass through a heat exchanger made of 42 mm (1.65 in.) diameter pipe, as shown in Figure 9. The prime function of this heat exchanger is to cool the smoke down to room

temperature. The entire system has drain cocks conveniently located, one at the bottom of each tube of the generator itself to remove excess oil not converted to smoke, and others at the bottom of the heat exchanger to remove whatever oil might have been condensed. After passing through the heat exchanger condenser system, the smoke flows into a 97 mm (3.82 in.) manifold and is passed through an absorbent cloth filter. This filter serves a dual purpose: it removes most of the remaining lighter tars and aids in distributing the smoke uniformly into the evenly spaced tubes that extend from the manifold. As will be mentioned later in the report, a number of differently sized tubes were used during this study. These evenly spaced tubes determine the initial smoke line spacing. Such an array of tubes with the manifold has a rake-like appearance and, thus, is referred to as a smoke rake.

Appropriate measures should be taken to guard against leaks in the system and to provide an outside exhaust from the tunnel, for the excessive and prolonged inhalation of oil smoke would be a health hazard.

Various types of oil have been tried. It has been found that kerosene produces the best quality smoke. Kerosene may be obtained from Thompson-Hayward Chemical Company in Kansas City, Kansas, under the name of Deodorized APCO #467.

Oil smoke generators of this type have been constructed in single, double, and quadruple units. This grouping arrangement of units is basically a method of increasing the volumetric output of smoke.

#### Alternative Methods

The only reason for trying to replace the kerosene smoke generation technique of Brown would be to produce a non-toxic and non-flammable smoke-like substance. All products of combustion, reactions of chemical substances, oil and paraffin, vapors, and aerosols are toxic to some degree.<sup>18-20</sup> Many of these substances are flammable and some are corrosive or chemically active. The only technique available which does not have one or more of these undesirable properties appears to be the steam-liquid nitrogen method.<sup>10-12</sup> However, generating large quantities of steam in some type of boiler presents a different safety hazard. After generation, the steam is mixed with liquid nitrogen and introduced into the wind tunnel. Although the apparatus used to generate the steam is somewhat different in References 10 and 12, the end product is the



same. Both the M.I.T. and Iowa State University laboratories have used pure steam with reasonable success. The steam or steam-liquid nitrogen mixtures have been used in both open and closed circuit subsonic wind tunnels.

Although the use of steam for flow visualization has the advantage of being clean and non-toxic, it does have disadvantages. For example, the system temperature must be controlled carefully if a neutrally buoyant fog is to be obtained. As pointed out earlier, water vapor is composed of much larger particles on the average than oil smoke. It also has the disadvantage that the steam condenses to water on cold model surfaces, walls, and other protrusions in the test section. The steam photographs reasonably well and can produce useable visualization records. To determine whether or not steam was useable for flow visualization in Notre Dame's indraft, supersonic wind tunnels, a simple experiment was performed. Pure steam from an industrial, portable steam generator was injected upstream of the first screen of the pilot tunnel. Although the steam velocity was considerably higher than the air entering the tunnel, the steam persisted through the test section and the streakline formed by the steam was photographed. The diameter of the steam stream from this point is rather large for detailed investigation; nevertheless, it does demonstrate the possible use of this method. Also, the steam was pumped into the tunnel through a small orifice. Low speed streams of the steam could be introduced into the tunnel and flow for proper positioning of the steam stream. The steam was photographed at the pilot tunnel test section during this test. In the photograph, there was considerable condensation of the steam in the test section. As is shown in this picture, the steam diffuses quite rapidly and the streaklines are not present.

Griffin and others developed a nebulizer generation system for low speed wind tunnel flow visualization. This system used a polydisperse liquid aerosol of different sized droplets, referred to as BOP. This flow visualization method was developed for the relatively low speeds used (maximum tunnel speed was 8 m/sec). One of the reasons this aerosol system was developed was to avoid the problems associated with oil smoke. Although BOP was originally thought to be non-toxic, later it was found to be toxic which limits its use.

Tests were conducted using a general oil smoke generator made by Festing Industries, Inc., of New York. The particular generator

used was the Cloud Maker, Model No. fl-48. Initially, an attempt was made to pump the smoke from the generator into the usual smoke rake before introducing it into the tunnel. The smoke generator could not provide adequate pressure nor smoke volume to do this so the smoke was taken directly from the generator in a flexible hose which was then mounted in front of the screens. The generator was unable to produce large quantities of smoke but a single smoke filament was visible, although faint. One of the photographs in Figure 11 shows the comparison between the two types of smoke at the same time. The kerosene smoke is more dense simply because there is more of it; also, being closer to the light, it appears to be brighter. The more unfortunate aspect of the mineral oil is that it condenses on the model. This fouling of the model would most likely be considered a major drawback of the mineral oil smoke.

Although many substances have been used to produce smoke for flow visualization in wind tunnels, kerosene smoke appears to have a significant advantage over all other substances studied. With a properly designed and maintained generation and distribution system, kerosene smoke should not present any significant fire hazard or toxicity problem. The remainder of the results presented in this report were achieved using the kerosene smoke generation system.

#### Smoke Flow Photography

One of the most critical aspects of flow visualization photography is in obtaining sufficient light on the subject of interest. In wind tunnel applications this problem is often the most difficult to overcome because of space limitations. The main problem is the large quantity of light required for proper illumination of the smoke streaklines, as well as in maintaining high contrast between the smoke and the background. As most high speed wind tunnels have very limited viewing areas, one is generally forced to use less light than desirable to minimize unwanted reflections or adverse heating problems. Space limitations often restrict the placement of lights and cameras.

Figure 12 illustrates the three most commonly used lighting arrangements. When the lights are positioned on the opposite side of the tunnel and out of the direct field of view of the camera, the arrangement is called "back

lighting." Glare from the model can be minimized using the back lighting arrangement. If the lights are positioned on the same side of the tunnel as the camera, the arrangement is called "front lighting." Major difficulties with front lighting are in the reflections and glare from the model and tunnel windows. These problems can be minimized by proper positioning of the lights and camera. However, when there is a limited viewing area and space is restricted, it may not be possible to position the lights properly. The final lighting arrangement is called "top" or "bottom lighting." This arrangement can be used in any test section where the flow can be illuminated in a plane perpendicular to the normal viewing direction. It is accomplished in the Notre Dame pilot tunnel by using a test section nozzle block which has a transparent plastic insert in the top portion of the block. The test section can be illuminated through this transparent slit. An advantage of top and bottom lighting is that the light source is normal to the field of view and interference such as reflection and glare from the model is minimized.

The type of light source required for smoke visualization tests depends upon the particular test being conducted. The two most widely used light sources are stroboscopic and high intensity continuous lamps. Short duration flash lamps such as the General Radio 1532-B strobolumes or their equivalent have been found to produce satisfactory results. These lamps operate from an electrical source of 120 volts and 60 cycles. The power consumed varies up to 500 watts, depending upon the flash rate. The output of an individual lamp is rated at 10 megacandlepower when the flashing rate is set at 60 flashes per minute. The rated duration of the flash is approximately 30 micro-seconds. For still photographs, the strobolumes are synchronized with the camera shutter and operate similarly to any camera using an electronic flash. With movies, the flash rate is adjusted to the framing speed. The number of lamps required depends on the nature of the test being conducted. For continuous lighting, high intensity spot lamps are required. A summary of the photographic equipment needed for smoke flow photography is included in Table IV.

#### Photographic Procedures

In the later sections of this report much will be said regarding the tunnel design requirements for producing quality smoke filaments in the test section. Over the years, many universities and research laboratories (both

government and private) have attempted to obtain flow visualization data at low speeds. Most of these efforts have ended in failure for a variety of reasons. Even in tunnels where quality smoke is available, only poor smoke flow photographs were obtained. One can only speculate on the reasons for such failure. However, one of the difficulties is probably due to the fact that the experimentalist could see the flow pattern with his eye but was unable to obtain good photographic plates. This is usually because, in such installations, the photographic work is left to a photographic technician. To achieve quality smoke photographs, the experimental aerodynamicist should also be the photographer. An experimental aerodynamicist is familiar with the phenomena and their influences on the smoke pattern in the flow field. This is not to say that a photographic technician cannot be used; however, the aerodynamicist must be willing to spend enough time with the photographer so the technician knows what is required. Some of the difficulties in obtaining quality smoke flow photographs are included in Table V.

Processing the photographic data presents another challenge. Due to the difficulties in lighting, the photographic plates are usually underexposed and the exposure is generally uneven. Therefore, to produce a quality print, an uneven exposure of the negative is required. This procedure is referred to as "photographic dodging." It enables one to enhance the photographic image, i.e., to capture all the data on the print. Again, the person processing the film must know what he or she is looking for in the print, otherwise much, if not all, useful data will be lost. Table VI summarizes the photographic procedures needed to obtain good photographs.

One final point: the use of flow visualization techniques in the study of complicated flow patterns is as much an art as it is a science. Obtaining good flow visualization data requires a great deal of patience and time. Each new application will present the experimental aerodynamicist with new photographic difficulties. However, with patience and some effort, meaningful flow visualization data can be acquired.

#### Preliminary Visualization Studies

To establish some experience with collecting high speed flow visualization data, one of the first tasks involved photographing a number of different models at various flow speeds in the two original supersonic wind tunnels

(5" by 5" and pilot tunnel). These data provided a baseline for future studies and helped indicate areas in which improvements could be realized. Through the use of the pilot tunnel, Goddard showed the potential of the smoke visualization technique. These preliminary tests were intended to determine what factors could influence the quality of the visualization data that Goddard collected using the pilot tunnel and whether or not the technique could be extended to the "5 by 5" tunnel, a larger but apparently comparable design.

The first set of experiments to be discussed here were conducted in the 0.127 by 0.127 m (5 by 5 in.) test section. The tests were conducted using a full tunnel span right circular cylinder model with a 16 mm (5/8 in.) diameter. The camera was mounted on the side of the tunnel section, with the camera axis normal to the window. Lights were positioned on the opposite side of the tunnel and out of the direct field of view of the camera (back lighting). They were also positioned to eliminate reflections off the tunnel walls and model. Both still and high speed motion picture photographs were attempted. Some sample photographs at free stream Mach numbers of approximately 0.2 and 0.6 are shown in Figures 13 and 14.

The still photographs were taken using stroboscopic flash illumination, synchronized with the camera shutter. The high speed motion pictures were taken at 125 frames per second using synchronized strobe lighting, and at 500 frames per second with continuous lighting.

Additional tests were conducted using the "5 by 5" tunnel to evaluate the suitability of back lighting for a number of different models in supersonic flow. Figures 15 and 16 include some of the results from these tests. It is quite noticeable that, as the Mach number increased, there was a reduced smoke density and it was more difficult to achieve photographs of the same quality as Goddard's originals. There was adequate light on the smoke streaklines with the camera set in an f:22 to f:32 range with a 210 mm lens. The large f stop allowed for good focal field depth. The exchange between focal depth and light intensity is critical. Unfortunately, although it was adequate at the lowest speed ( $M = 0.2$ ), at higher speeds the smoke quality was rather poor.

The other models used in this study included at 16 mm (5/8 in.) diameter

spherical model and an  $AR = 0.59$ ,  $7^\circ$  double wedge airfoil, wing model. Figures 15 and 16 highlight some of the problems associated with the "5 by 5" tunnel/inlet design. There is considerable breakdown of some of the streaklines, particularly at the supersonic condition, while some of the streaklines remain quite well defined. Two different smoke rakes were used to introduce the smoke upstream of the screens. For the "5 by 5" tunnel, the best results seem to be achieved using the rake with the largest (19 mm, 0.75 in.) smoke tube inner diameter. This simply allows for the introduction of larger quantities of smoke and reduces the effect of the diffusion problems.

Although the quality of the visualization data in the "5 by 5" tunnel was less than desirable, it did provide much valuable information. This tunnel appeared to have all the criteria which had been associated with successful visualization facilities (high contraction ratio, anti-turbulence screening); it became apparent that these would have to be defined in greater detail before general design criteria could be established.

The next phase of the preliminary visualization study involved an investigation of the influence of the anti-turbulence screens on the quality of the flow in the pilot tunnel. The smoke was introduced into the test section in the normal manner, upstream of the set of anti-turbulence screens. The tests were conducted with various numbers of anti-turbulence screens present. Four additional metal mesh (7 per cm, 18 per in.) screens were fabricated and used with the original seven screens. Tests were conducted using combinations of one, three, five, seven, nine and eleven screens, and with both a medium (15.1 mm, 0.594 in.) inner diameter smoke rake and a small (9.5 mm, 0.375 in.) inner diameter rake. Some of the results of these tests are shown in Figures 17-19. It was of great interest to note that the additional screens, over the seven used by Goddard, resulted in an improvement in the quality of the smoke streaklines.

An additional difficulty associated with the operation of an indraft, high speed tunnel was encountered. As the air from the atmosphere is accelerated into the test section, the static temperature drops. As it drops below the dew point, condensation begins; this condensation can both alter flow characteristics and degrade the quality of the visualization data. So long as the ambient (outside) temperature was below  $70^\circ$  F, there were never any problems

with condensation in either the pilot or the "5 by 5" tunnel. Condensation was not apparent to the eye nor evident on the photographic records. In these cases, even though the static temperature in the test section may have been below the dew point, the air was not supercooled; the acceleration was so rapid between inlet and test section that there was not adequate time for vapor formation. There were instances, when the outside temperature exceeded 80° F with high relative humidity, when the condensation was a significant problem and severe enough to preclude operation of the tunnel. The high humidity causes both a condensation shock and severe clouding of the test section with water vapor. It is apparent that, unless the air in the plenum from which the air is drawn is dried, there will be some limitations on the operation of such an indraft facility. At the University of Notre Dame, this means that during two months (July and August), the use of the visualization facility is questionable and dependent upon daily weather conditions.

#### Inlet Flow Field Study

The experience with the original tunnel designs indicated, and not surprisingly so, that the inlet design and associated turbulence management devices were critical to the success of the smoke flow visualization method. The preliminary visualization studies conducted in the pilot tunnel showed a direct correlation between the number of screens and the quality of the smoke visualization results, and indicated that improvements were possible. It was felt that a more complete understanding of the inlet flow field required having quantitative data as well as the qualitative smoke photographs. A series of detailed hot-wire anemometry measurements of the inlet flow field was then conducted.

The tests were made using a DISA Type 55M01 CTA hot-wire system with a DISA Type 55D10 linearizer unit. Both single wire and X-wire probes were used for both turbulence and mean velocity measurements. The turbulence data were processed using a TSI rms digital voltmeter (Model 1076). The output signal from the linearizer unit was filtered to eliminate all signals above 10 kHz and both the mean and rms voltage measurements were made with the digital voltmeter. The geometry of the original inlet, the Smith and Wang design, is shown in Figures 20 and 21; it will be referred to as the Smith/Wang inlet in this report. The inlet was modified so the hot-wire probe could

be positioned at locations 1, 2 and 3, as shown in Figure 22. The hot-wire probe was initially supported on the inlet itself but preliminary data indicated that the wire output was significantly influenced by mechanical vibrations of the inlet. The hot-wire assembly was then supported from the floor of the laboratory and no significant vibrations were apparent in the hot-wire signals.

The first series of tests involved measurements of the mean velocity and turbulence intensity along the centerline of the original inlet. At port location #1, the probe was located 38 mm (1.5 in.) behind the entrance to the inlet, i.e., behind the most downstream screen. The mean velocity was 3.05 m/s (10 ft/s) at this location on the tunnel centerline. The rms velocity fluctuations are given in Figures 23, 24 and 25. At port #1, the velocity fluctuations ranged from 0.043 to 0.012 m/s (0.14 to 0.4 ft/s). All the turbulence level measurements were conducted using the same sequence of screens. The first measurements were conducted with no screens in the inlet and then one, three and five fabric screens were added. Once the five fabric screens were in place, metal screens were added until a total of thirteen were mounted upstream of the inlet. The screens were removed in pairs and the results checked for repeatability. With only a few screens present, the fluctuations in the rms signal were significant and Figures 23-25 give the extent of these fluctuations. The results for port #1 show, very dramatically, the influence of the screens on the fluctuations in the rms signal. There is a rapid decrease in the range of the fluctuations and in the mean velocity fluctuations with the addition of the first five screens. The disturbances which are drawn into the tunnel and those created by the screen should not be directionally dependent, so that, although the turbulence measurements are for the axial component of velocity, they should reflect similar trends in the other, normal, components of the velocity fluctuations.

Port #2 was located so the probe was 0.34 m (13.5 in.) behind the entrance to the inlet. The mean velocity was 26.3 m/s (88 ft/s). The magnitude of the rms signal increased over the value from port #1 as would be expected due to the rapid increase in the mean speed. The same trends which were present in port #1, with respect to the number of screens, were shown at port #2. Again, the largest improvement in the turbulence levels took place with the addition



of the first seven screens, with a more gradual decrease after that. Port #3, located 0.48 m (19.4 in.) downstream of the entrance to the inlet, demonstrated a behavior comparable to ports #1 and #2. The mean velocity at port #3 was 49.4 m/s (162 ft/s) and this increase in mean speed was also reflected in an increase in the magnitude of the rms velocity fluctuations. The third port was located in the section of the inlet in which the area was nearly constant but still upstream of the fixed nozzle block. Surface oil flow studies in this region of the inlet did show a separation region ahead of the forward facing "step" created by the discontinuity in slope between the nozzle block and the inlet. Although the surface oil flow results were highly qualitative and difficult to record with any detail due to the small size and inaccessibility of the downstream end of the inlet, there was quite obviously a separation region. The presence of such a region, even though it was confined to the near wall region in the constant area section of the inlet, could account for the somewhat larger range in the velocity fluctuations with even a large number of screens present.

The centerline axial turbulence level measurements are summarized in the form of turbulence intensity measurements for all three ports in Figure 26. These results correlate quite well with the preliminary smoke flow visualization data described in the previous section of this report. The visualization data showed a marked improvement in the quality of the smoke streaklines during the addition of the first seven screens. This agrees directly with the turbulence level measurements. Additional screens (from seven to eleven) do indicate a slight improvement at each of the ports studied. Since the streakline carries with it a "history" of the turbulence, this somewhat slight decrease in turbulence is reflected as a continued improvement in smoke streakline quality. This is particularly noted as an increased steadiness of the streaklines when the eleven anti-turbulence screens were used.

It is particularly significant to note that as more screens were added to the original inlet, the geometry of the inlet was actually significantly altered. With eleven screens in position, the inlet is 32% longer than without them. The screens actually form a constant area section upstream of the converging inlet. It then becomes difficult to separate the influence of the screens from the influence of the modified inlet geometry.

As a result of these preliminary tests, it was decided to design and fabricate another inlet for the pilot tunnel. There is a detailed discussion of inlet design methodology presented later in this report but it was apparent early in the project that there was no "best" method available for three-dimensional inlet designs. It was decided to try to arrive at the simplest design available which appeared to overcome the problems with the Smith/Wang inlet design. The new pilot tunnel inlet which will be referred to as the Modified Pilot Tunnel inlet or MPT inlet in this report is shown in detail in Figures 27-29; a photograph of the inlet installed on the pilot tunnel is shown in Figure 30. The criteria used to design this inlet were:

1. Eliminate the wall slope discontinuity at the junction between the inlet and the fixed nozzle block.
2. Eliminate the wall slope discontinuity at the upstream end of the inlet and attempt to have the flow normal to the screens across the entire inlet.
3. Use the same screens as used with the Smith/Wang inlet on the pilot tunnel. The new tunnel would then have the same contraction ratio, and upstream and downstream inlet height to width ratio.
4. Simplify design and fabrication requirements by having the inlet geometry composed of straight lines and circular arc sections.

Both hot-wire and smoke flow data were collected using the new inlet design. The hot-wire anemometry data were collected in a manner similar to that for the Smith/Wang inlet and the results are shown in Figures 31-35. The hot-wire probes were located at the following positions relative to the upstream end of the inlet.

<u>MPT Inlet</u>	<u>Distance from Inlet Lip</u>	<u>Centerline Velocity</u>
Port #1	0.054 m (2.13 in.)	1.59 m/s (5.2 ft/s)
Port #2	0.384 m (15.13 in.)	3.84 m/s (12.6 ft/s)
Port #3	0.613 m (24.13 in.)	19.9 m/s (65.3 ft/s)

The axial velocity fluctuations vary with the number of anti-turbulence screens for each of the three ports. Figures 31-33 indicate the same type of behavior as observed in the Smith/Wang inlet. It is important to note that

the three ports used for the MPT inlet do not correspond to the same cross-sectional areas or mean velocities as the port locations for the original inlet. At port #1, Figure 31, there has been a decrease in the axial component of the velocity fluctuations with the addition of screens but this has not been a particularly large reduction. Port 1 is located in the extreme upstream end of the inlet, in an almost constant area section. As indicated in References 21 and 22, the screens have a greater influence on the velocity fluctuations in the plane of the screen (i.e., those normal to the mean flow direction). This is supported with the results of a series of X-wire anemometry measurements in which both axial ( $u'$ ) and transverse ( $v'$ ) velocity fluctuations were measured. Figure 35 shows the results for ports #1 and #2 of the MPT inlet of the transverse turbulence intensity; the marked reduction is very evident until about seven screens are added. The axial turbulence intensity measured with the X-wire probe was also compared with the single wire measurements in Figure 34 (solid symbols). This figure also indicates the importance of the contraction on the turbulence intensity level which drops by an order of magnitude between ports #1 and #3.

A series of smoke flow visualization studies was also conducted using the MPT inlet with the pilot tunnel, Figure 36. The sequence of photographs illustrate both top and back lighting techniques using one, three, seven and eleven screens. The model shown in these photographs is a  $20^\circ$  half angle cone with a  $10^\circ$  boattail afterbody. These data show much more dramatically than the hot-wire results the improvements realized with the new inlet design. With only one screen the smoke streaklines are discernible, though diffused, unlike the Smith/Wang inlet; with as few as three screens, the smoke quality is reasonably good. There is still a mild unsteadiness with seven screens but using eleven screens results in very good quality, high contrast smoke streaklines. These visual results correspond well with the hot-wire data and, although they do not provide definitive, quantitative criteria for the design of a smoke tunnel, they do indicate the influence of two important aspects, the inlet design and the use of anti-turbulence screens.

It is worth noting a couple of additional tests which were conducted during the evaluation of the inlet and screens. Since honeycomb has been considered an effective turbulence management device and has been used in a

number of wind tunnel applications, a honeycomb insert was fabricated and evaluated with the pilot tunnel. The honeycomb used was a six-sided cell, with a 12.7 mm (0.5 in.) cell width and an 88 mm (3.5 in.) depth, made of paper. Some smoke streakline data using the honeycomb section, both alone and in conjunction with the screens, are shown in Figure 37. The cell size of the honeycomb tested was smaller than the inner diameter of the smoke rake tubes. The smoke streaklines were then split as they passed through the honeycomb, bringing about a "stringy" character to the smoke. Even the addition of screens downstream of the honeycomb does not completely eliminate this effect. The hot-wire data associated with the honeycomb are shown in Figure 38. The honeycomb is effective in reducing the turbulence intensity but an examination of the hot-wire signal shows that the honeycomb produces a very definite wake structure. Although it may effectively eliminate much of the large-scale turbulence, the small-scale disturbances caused by the honeycomb itself remain. They are not effectively damped by the short contraction section, and the disturbance of the smoke at the honeycomb is carried along into the test section and degrades the streakline data.

Difficulties associated with the use of any anti-turbulence devices such as screens or honeycomb are the losses associated with the flow through these devices and the increased power required to run the tunnel. Since most facilities use only a few anti-turbulence screens, tests were conducted to determine the total pressure losses associated with the use of a large number of screens. Figure 39 gives the results of such a test in which the sequence of the screens (whether fabric or metal first) was varied. The total pressure was measured using a pitot-static tube located at the tunnel centerline in the MPT inlet. As would be expected, there may well be a variation in losses across the face of the inlet but these data were not acquired. As can be seen in Figure 39, the first few screens account for a majority of the losses and the effect of additional screens is not so great. This is most likely due to modification of the velocity distribution over the inlet face. With the addition of more screens, the flow at the inlet is most likely more uniform and the speed near the centerline is reduced, accounting for the smaller losses in this region. Since heating of the air is not a factor in the indraft tunnel and the losses associated with the screens are rather small, it is felt that the use of the large number of screens is not a detrimental factor when considering overall tunnel performance.

## Optical Data Acquisition Techniques

There are a variety of optical techniques that can be used to analyze the flow patterns around aerodynamic shapes in a supersonic flow. Only those techniques which can be readily used in conjunction with the smoke streaklines will be discussed in this section.

Smoke photographs depend upon the scattering of light, while Schlieren and shadowgraph photography depend upon the deflection of light rays from their normal path. A combined smoke and Schlieren/shadowgraph picture can be produced by three separate procedures. The first procedure entails the exposure of two photographic plates. A shadowgraph can be produced by exposing a photographic plate with a point light source passing through the test section. The resulting negative reveals the shock patterns present in the flow field. Using the same camera, a second photographic plate is exposed using strobe lights synchronized to the camera shutter. The negative will yield the images of the smoke streaklines. If the alignment of the optical system is unchanged during the photographic process, the two negatives can be aligned and a composite picture printed. This procedure has been used successfully by Goddard<sup>2</sup> and later by Slovisky and Roberts.<sup>9</sup> For this technique to produce valid flow visualization data, the following two conditions must be satisfied:

1. The two photographed images must be identical in size and suitable photographic markings must be present in both negatives so that the negatives can be properly aligned for the composite print.
2. Because of the time lag involved in taking two separate photographs, the resulting photographic composite is only valid if the flow field is a perfectly steady flow.

This procedure could also be used to obtain a composite Schlieren/smoke photograph.

Obviously, it would be desirable to obtain a simultaneous photographic image of the smoke and shock patterns. This would eliminate the difficulties inherent in the first technique. Two different optical arrangements were tested to obtain simultaneous photographs. The first arrangement consisted of modifying an existing conventional knife-edged Schlieren system. A sketch of the Schlieren system used in Notre Dame's Aerodynamics Laboratory is shown

in Figure 40. To convert this to an opaque Schlieren system, the slit source was replaced by a point source and the knife-edge replaced by a round opaque stop.

A Schlieren system configured in this way produces a relatively dark field with density deviations appearing as bright lines. The dark field is necessary to produce the required contrast between the background and smoke lines which are illuminated by another light source.

The modified Schlieren system is a single-pass system using two mirrors. Both point and slit light sources were used in conjunction with point and slit opaque stops. The combination of a slit light source and a 1.58 mm (0.0625 in.) opaque slit stop produced a picture that could not be focused. Three different point sources and stops were used. The diameters used were 0.889, 1.78 and 2.54 mm (0.035, 0.07 and 0.10 in.). Several tests were conducted using the modified Schlieren system. Very clear images of shock waves were obtained using this system. Figure 41 shows an attached oblique shock on a  $9^\circ$  half angle wedge at a Mach number of 1.42. The only light which passed by the opaque stop was that refracted in passing through the shock wave. The interaction of the shock with the test section wall and the reflected wave with the body and sting are shown in detail.

A test was also conducted using the same model but with smoke present. The smoke was illuminated using both back and top lighting methods, with only marginal results. Due to the size of the Schlieren system, the intensity of the light reflected from the smoke and collected by the camera used in the Schlieren system was quite low. Figure 42 shows a sample photograph of the simultaneous Schlieren/smoke system.

A new opaque stop Schlieren system was designed and evaluated. The system was essentially a reconstruction of Goddard's original set-up. A sketch of the system is shown in Figure 43. The mirror, beam splitter, mounting pins and benches were purchased from Edmund Scientific Corporation, Barrington, New Jersey. The mounting brackets were fabricated in the Aerospace Laboratory's machine shop. Although no satisfactory photographic results came from this investigation, several things were learned with regard to the experimental set-up. First, it is imperative that the system be mounted on optical benches so that accurate alignment and positioning of the optical equipment

can be achieved and maintained. Second, the size of the spherical mirror should be at least as large as the test section viewing area. The focal length of the mirror should be selected so that the camera could be located close to the test section. The closer the camera can be placed to the test section, the better the smoke images will be. The reason for using the opaque stop Schlieren is to create an image where the shock and expansion waves appear as light images on a black background. The smoke lines were illuminated by strobe lights controlled by the camera shutter; this allowed for the super-position of the smoke and Schlieren images. If the camera was positioned too far from the test section, the smoke images were too faint for photographic analysis. The primary reason for the failure of this particular procedure was due to the poor quality of the optical components. All the mirrors used in this investigation failed to focus the image to a point at the opaque stop. It is believed that this technique would work if high quality optical components were used in the system.

## NEW FACILITIES AND DESIGN CRITERIA

Although the primary goal of the project was to define criteria with which a large, high speed flow visualization facility could be designed, an important part of establishing this criteria was to demonstrate that these methods could be used in the transonic flow regime. This required the designing and fabrication of an indraft, transonic wind tunnel which would be compatible with the existing facilities at the University of Notre Dame. The design of this tunnel was strongly influenced by the experience gained in the studies documented earlier in this report.

### Inlet Design Methods

When considering the design of a wind tunnel contraction section, some or all of the following criteria were used:

1. A high degree of exit flow uniformity.
2. No flow separation or unsteadiness within the inlet.
3. Minimize boundary layer growth.
4. Reduction in upstream turbulence and intensity.
5. Shortest possible length to reduce overall facility size and cost.

As in most design problems, the criteria were not complementary. Reference 23 mentions that Prandtl considered the inlet design problem and realized almost any smooth, curved surface could be used for a contraction cone geometry if the flow were inviscid. Different geometries would yield different degrees of velocity nonuniformity at the exit section and, for most geometries, a relatively gradual transition is required to achieve "good" uniformity. However, the more gradual the transition, the greater the length for boundary layer development. Figures 44 and 45 from Reference 24 highlight some of the practical problems associated with flow in a simple axisymmetric contraction geometry. Figure 44 shows that, even if the upstream flow were uniform, there exist nonuniformities in the velocity distribution at both the upstream and downstream ends of the contraction section. As in all subsonic flows, the presence of the inlet is felt upstream and distorts the flow at the entrance to the inlet. Figure 45 shows the wall velocity distribution for a  $CR = 4$  inlet in comparison with an ideal one-dimensional distribution based on area ratio. This figure shows one of the most critical aspects of the



inlet design problem. For any finite length inlet, there exist regions of adverse pressure gradient (i.e.,  $dv/dx < 0$ ) at both the entrance and exit of the inlet near the wall. Both of these regions could interact adversely with the developing boundary layer, causing intermittent or continuous separation. The one-dimensional flow solution does not predict these regions of possible separation and it is for this reason that one must be cautious when considering various design methods.

There has been considerable interest in the prediction of the flow in wind tunnel contractions. When the problem is posed in either two-dimensional planar or axisymmetric geometries, the solutions are attractive from a mathematical point of view. A number of earlier works in the area were potential flow solutions to the inviscid flow problem.<sup>14,25-31</sup> These involved various geometry transformations which allow for closed form analytic solutions or the use of the hodograph (velocity) plane. Although, in most cases, the solutions lacked any practical physical basis, the results of many of these methods were used to design wind tunnel contractions. The low turbulence smoke visualization tunnels developed by F.N.M. Brown at the University of Notre Dame, and the inlet for the pilot tunnel, were designed using the method developed by Smith and Wang.<sup>14</sup> At the time the tunnels were designed it was the newest technique available and, although it lacked any experimental correlation, it provided reasonable results. These inlets have proven very successful on the subsonic tunnels but, as shown in the earlier section, this was not the best method available for the high speed application. This was primarily due to the fact that the Smith and Wang method did not account for the presence of the screens in the upstream end of the wind tunnel inlet. It was felt that this rapid change of slope between the screen section and the inlet was to be avoided.

A number of more current works have attempted to overcome some of the deficiencies of the earlier work by adding more practical constraints to the inlet flow solutions.<sup>24,32-37</sup> These have included more reasonable requirements on exit velocity uniformity and, most importantly, the influence of the boundary layer and its interaction with the inlet flow field. The most significant of these later works is that of Morel. More than simply solving for the contraction cone flow fields for a specific class of inlet geometries, he established a series of design charts which could be used in actual design studies.

For these reasons, Morel's method was adopted for the design of the inlets for the transonic demonstration tunnel.

The initial design decision was a selection of contraction ratios. It was decided to use two different contraction ratios and to evaluate their influence on the quality of the flow visualization data. Since overall facility size is a primary concern for any new wind tunnel, there was interest in determining the smallest contraction ratio which would still allow for good quality data. The contraction ratio is governed by a maximum allowable flow speed at the anti-turbulence screens. Reference 21 shows that each type of turbulence damping screen has a characteristic critical screen Reynolds number, based on screen wire diameter, below which the screen helps damp out turbulence and above which the screen is actually detrimental. This new transonic tunnel design was limited to using screen materials similar to those used with the pilot tunnel. The closest comparison in Reference 21 is screen type B which had a solidity of 33% and a wire diameter of 0.19 mm (0.0075 in.) The critical Reynolds number for this screen under the condition of Reference 10 was 55 which corresponded to a free stream speed of 4.0 m/s (13.2 ft/s). To maintain a somewhat conservative design approach, a maximum acceptable speed at the screen was set at 3 m/s (10 ft/s). For an indraft tunnel, this sets a minimum contraction ratio to approximately 75 to 1 for a design Mach number of 1.0. Another larger inlet with a 150 to 1 contraction was also designed to provide comparison. This larger contraction ratio had proven successful when used on the pilot tunnel.

Of the two methods developed by Morel, the data available for the axisymmetric method is limited to a contraction ratio (CR) of 25. Therefore, the two-dimensional planar was applied for values of  $m = 2-10$ , where  $m$  was an inlet entrance to inlet exit height ratio. The transonic tunnel required a three-dimensional, square cross-section inlet with an area contraction ratio of 75:1 and 150:1. If one assumes that the two-dimensional planar method provides adequate results and the same contraction geometry is used in the horizontal and vertical planes of the inlet, then the  $m = 10$  based on inlet heights is a CR = 100 based on inlet area for a square cross-section.

The method is based on the results of numerical solutions which were incorporated into a series of design charts. The wall geometry is expressed

as two matched cubic polynomials, see Figure 46. The user has a choice of the contraction ratio (i.e., a height ratio between inlet and exit) and two wall pressure coefficients,  $C_{pe}$  and  $C_{pi}$ . These two parameters are used to help avoid wall boundary layer separation. The theory then provides the location of the match point (the common point between the two cubic curves) and the length of the inlet. The two parameters, when combined with the width of the inlet at the entrance and exit, completely define the inlet geometry.

The transonic inlets were designed using two particularly conservative values of the wall pressure coefficients,  $C_{pe} = 0.05$  and  $C_{pi} = 0.2$ . These were used to determine the non-dimensional match point,  $X$ , for the height ratio,  $m$ , of 8, 9 and 10. The design procedure yielded the results shown in Figures 47 and 48.

For a value of  $m = 8.66$ , the resulting square three-dimensional inlet has a  $CR = 75$ . The values of  $X$  and  $L/H_1$  were interpolated from Figures 47 and 48. For  $H_2 = 102$  mm (4 in.), the resulting inlet is 984 mm (38.75 in.) long. The inlet geometry is shown in Figure 49. The  $CR = 150$  inlet was designed in much the same way except the results on Figures 47 and 48 were linearly extrapolated to  $m = 12.25$ . The resulting inlet was 1.39 mm (54.9 in.) long. It is shown in Figure 50. Due to the very conservative choice of  $C_{pe}$  and  $C_{pi}$ , the inlet has rather long sections with very small slopes, both near the inlet and exit. The inlets were then shortened to the length shown in Figures 49 and 50. This shortening was done to improve the quality of the smoke streaklines (shorten the distance for the smoke to diffuse). The inlets were fabricated using inexpensive sheet metal techniques and appear to be true to the design contour to  $\pm 5$  mm.

Although the design procedure used for these inlets was one of a number of methods which could have been used, it was a very straightforward method and allowed for a number of design studies resulting in inlets with "reasonable" contours.

#### Transonic Flow Visualization

The transonic flow regime may provide one of the most important regions for application of the high speed flow techniques. The unique non-linear

analytic problems and the complex physical interactions which occur in the transonic regime have long hampered design and developments in this area. The opportunity of visualizing the transonic flow fields with the smoke should provide another tool to complement other existing optical techniques and analytic methods.

To demonstrate the applicability of the method to transonic flows, a transonic, slotted wall test section was designed and fabricated by the Air Force Flight Dynamics Laboratory. The section was designed to be compatible with the University of Notre Dame's high speed wind tunnel facility and was installed on the diffuser used for the "5 by 5" tunnel. The test section was a slotted wall, 6% open area on the top and bottom walls and solid, easily removable glass side walls with a square cross-section and area  $104.0 \text{ cm}^2$  ( $16 \text{ in.}^2$ ). The flow in the tunnel is controlled using a second throat downstream of the test section. The second throat is composed of a series of cylindrical rods normal to the flow. Rods of various diameters can be used to provide different throat areas. The plenum pressure can be controlled by two valves connected into the diffuser downstream of the second throat. A schematic of the test section is shown in Figure 51.

The test section could be attached to either the 75:1 or the 150:1 contraction ratio inlets described in the previous section. A series of anti-turbulence screens were fabricated for each tunnel. The screens were stretched on frames 17 mm (0.67 in.) thick. The screens were set into an extension on the front end of the inlet so the inside screen dimension corresponded to the inlet entrance area. There were five fabric and six metal screens, of the same specifications as the pilot tunnel, fabricated for each inlet.

A demonstration of the high speed smoke visualization was conducted using both inlets and a number of tunnel operating conditions. In all cases, the back lighting technique was used due to the solid top and bottom walls of the tunnel and plenum chamber. Due to the limited number of cases actually considered, these tests were simply to demonstrate the feasibility of the technique and not to provide a comprehensive application throughout the transonic regime.

The model shown in each of the transonic smoke photographs is a 12%

thick, symmetrical airfoil supported on circular disks between the two glass side walls. The disks could be rotated to change the angle of attack of the section. The glass side walls were constructed of a clear acrylic plastic. There were slight scratches in the plastic, which can be seen in the photographs. In the photographs in Figures 52-57, the flow is from left to right. Since the calibration of the transonic section was not complete when this report was written, the Mach numbers indicated in the photographs are approximate and do not account for model interference. Figure 52 shows the influence of the number of anti-turbulence screens for the  $CR = 75$  inlet. In both cases, the quality of the smoke streaklines is not particularly good but there is a marked improvement using the eleven fabric screens in comparison to just five. Figures 53 and 54 show the influence of modifying the plenum pressure and also changes in angle of attack, again for the  $CR = 75$  inlet. In each of these photographs, the smoke streaklines are not as sharp as they were in the pilot tunnel but they are still rather good considering the flow speeds are still an order of magnitude larger than those which can be achieved in most flow visualization facilities.

Figures 55-58 show the results using the  $CR = 150$  inlet. The quality of the streaklines is very good in comparison with the smaller inlet. The lines are well defined and little diffusion is evident throughout the test section. The plenum pressure influence is quite apparent and it illustrates a potential application of the smoke data, that is, a tailoring of the free stream conditions by evaluation of the smoke flow away from the body. The separation of the flow for the  $\alpha = 15^\circ$  case is quite obvious and, although the details of the flow in the separated region are not as sharp as smoke data taken at much slower speeds, the ability to locate and define regions of separation may well be another important contribution of the method.

Although this study using the transonic section reflects only a preliminary demonstration, it does show the potential for using smoke flow visualization in transonic flows. Future work is anticipated in this tunnel and, as with all the flow visualization studies conducted to date, as more experience is gained in collecting the smoke data, the quality of the photographs will improve. Figure 59 indicates that the visual data need not be constrained to viewing normal to the flow direction. In these photographs, the camera

is located approximately  $45^\circ$  to the flow direction and additional details of the flow over the airfoil is observed. It is just this type of variation in the data acquisition procedure which, when tailored to a particular test, will allow for the acquisition of the most useful visualization data.

#### Facility Design Criteria

Establishing definitive criteria for design of a high speed smoke visualization facility is indeed a difficult task. The ideas presented in the following section are the results of experience gained during this research program as well as from other flow visualization studies. The criteria will be discussed in three general areas: (1) Facility Design, (2) Tunnel Design and (3) Data Acquisition Requirements. There is an obvious overlap between these areas but they do reflect those items of primary consideration to both the facility designer and user.

The basic facility considered is an indraft, continuous run, high speed wind tunnel. The tunnel should be located in a building which provides an adequate supply of air under reasonably controlled conditions. Once the mass flow requirements of the tunnel itself are determined, the building size can be established. As has been discussed, the quality of the smoke visualization data can be influenced by disturbances occurring in the air before it enters the wind tunnel inlet and are thus carried into the tunnel. It was determined that disturbances caused by movements of a technician in the laboratory were evident in the hot-wire anemometer signals taken in the tunnel inlet. Although the smoke itself is not as sensitive as the hot-wire, care must be taken to eliminate disturbances near the tunnel inlet. A "plenum" region must be provided about the tunnel inlet and this region should be large enough so that flows induced due to operation of the tunnel are less than 0.3 m/s. There should be no objects such as beams or columns in the region immediately upstream of the tunnel inlet.

Since smoke is introduced into the airstream immediately upstream of the tunnel inlet, the exhaust from the tunnel must be exited outside of the tunnel building; regardless of the type of smoke used, the air should not be recirculated through the building and again introduced into the tunnel. The diffuser and tunnel power supply should also be isolated from the test section area to reduce the noise associated with high speed tunnel operation. The

area surrounding the test section must be capable of being completely darkened so that photographic data can be collected. There should also be adequate room in the area of the test section for other optical or data acquisition equipment such as Schlieren systems or LDV's.

The tunnel itself should be of the indraft type and be composed of the following basic sections:

#### Inlet/Screens

The inlet should be of a high area contraction ratio; for the speed range capability of a facility where  $M \leq 1.5$ , this would most likely mean a  $CR = 150$ . Although other design considerations may indicate an inlet slightly larger or smaller, this does indicate an acceptable value. The contraction ratio is primarily decided by the flow speeds at the anti-turbulence screens. The speed of the flow at the screens must everywhere be below the critical Reynolds number for the screen material used (Reference 21). Although the critical Reynolds number is a function of screen solidity, a value of  $Re_c = 40$  for screens with a solidity of less than 30% appears to be reasonable for initial design considerations.

Studies documented in this report indicate that at least seven, and preferably eleven, anti-turbulence screens be incorporated into the inlet design. The screens should be mounted taut on individual frames so they can be removed from the tunnel and cleaned on a regular basis. The frames should be as thin as possible ( $\approx 2.5$  cm) to minimize the length of the screen section on the upstream end of the inlet. The screen material should be single filament, or a very tightly wound fiber in the case of fabric, with a good quality regular mesh, made of cleanable material which will not be harmed by the smoke. If seams are required in the screen material they should be staggered so that seam wake influence can be minimized.

The design of the inlet presents a particular problem. The following should be considerations in the inlet design:

1. Screening located in low speed end of inlet.
2. Flow velocity normal to screens and speed below critical screen speed.
3. Reasonably uniform velocity at low speed end of inlet.

4. Contraction ratio large enough to allow for low speed at inlet mouth over entire operating range of test section.
5. As short as possible to minimize the time for smoke diffusion as well as to reduce cost.
6. No slope discontinuities at the downstream end of the inlet where it joins the test section.
7. Maintain an attached boundary layer with minimum growth along the inlet wall.
8. Near uniform velocity distribution at the inlet exit.

As in most design problems, these criteria are not complementary and there exist no proven methods which allow all these to be satisfied when applied to real, three-dimensional inlet geometries. The preferred method at this time is the matched cubic approach of Morel which was used to design the inlets for the transonic tunnel. Whether or not those inlets can be improved upon will require additional study. The two-dimensional planar method presented in Reference 32 can be extended to provide a design geometry for rectangular or square cross-sectional, three-dimensional inlets by using the approach described earlier in this report. The critical decisions in such a design involve selecting the pressure coefficient criteria for a separation at the inlet entrance and exit.

As a very practical consideration, the inlet must be accessible for screen inspection and removal, and should be instrumented so that during facility check-out the presence of separated flow regions or unsteadiness can be determined.

#### Test Section

The test section design will be strongly dictated by the type (speed range) of the tunnel being considered. There are three types of test sections which could operate in the "high" speed regime (where the "high" is relative to most smoke flow visualization facilities). These are:

1. Constant area subsonic section  $M \lesssim 0.5$ .
2. Transonic test section (porous wall)  $0.5 \lesssim M \lesssim 1.2$ .
3. Solid wall, fixed or variable geometry supersonic nozzle section  $1.2 \lesssim M \lesssim 1.5$ .



The upper limit on use of the indraft, high speed tunnel for flow visualization appears to be near  $M = 1.5$  under ideal conditions. This is due to the condensation problems mentioned earlier and, unless great effort is made to dry (reduce the dew point) all the air entering the tunnel, the condensation will be a problem and severely degrade the flow visualization capability. As mentioned earlier, the test section must mate smoothly with the inlet. For the subsonic or transonic test section, this would normally mean that the wall slope at the exit of the inlet would be zero. For a converging-diverging supersonic section, it would require an inlet wall slope which matched the upstream nozzle geometry. This illustrates a problem associated with design of a single tunnel capable of using all three types of test sections. Such a tunnel would require multiple contractions and would only complicate the design problem.

The test section area should be based on the test section design Mach number and the area of the inlet entrance. In this way, the "best" speed can be maintained at the inlet screens in all operating speed regimes. This implies that a subsonic and supersonic test section with the same inlet could not have the same cross-sectional area.

The test section design is also very critical with regard to collecting the photographic smoke data. As minimum criteria, both front and rear walls of the section (or top and bottom) must be of optical quality glass or equivalent. This will permit the use of the back lighting technique. If it were also possible to provide a transparent section in a plane normal to the viewing direction for top lighting, this would allow additional flexibility in data collection. The tunnel windows must be readily accessible, both inside and out, for cleaning between test runs. Residue collects on the inside glass windows due to atmospheric impurities (dirt), condensation and smoke; after the tunnel has run for approximately twenty minutes, the residue will significantly degrade the quality of the visualization data. Other data acquisition systems such as Schlieren or LDV may also influence the test section window design.

One other aspect of the test section design also involves collection of the visualization data. Due to the large amount of high intensity light required to photograph the smoke streaklines, highly reflective surfaces

within the test section should be avoided. This may require anodizing metal surfaces and painting other materials to provide for "flat" black interior and to eliminate extraneous reflections. The area around the test section must also be designed so that lights and cameras can be easily moved and positioned for various tests.

The photographic requirements for obtaining smoke flow visualization data in a tunnel possessing coherent smoke lines includes the need for adequate lighting, precision optical equipment (Schlieren or shadowgraph) and an onsite photographic processing capability. If the criteria cited earlier in this report are incorporated in a tunnel design, coherent smoke filaments can be expected. Qualitative data on the flow field surrounding test models can be obtained by using still and high speed motion picture photography. The quality of the smoke photographs will be very dependent upon the lighting and camera arrangements. The optimum arrangement of the lights and camera will, in general, have to be obtained by a trial and error procedure, and depend upon the particular experiment. However, due to the space restrictions around the tunnel viewing areas, only a few possible arrangements are likely; therefore, only several trials need be attempted before the best arrangement is found. To facilitate the collection of smoke flow data an onsite photographic processing capability is essential. This allows for the rapid processing of the photographic results. The results of a particular test must be available to the test engineer before future tests can be conducted, models or conditions changed, etc. As noted earlier in this report, photographic plates of smoke flow patterns are usually underexposed and, therefore, require non-standard photographic procedures to acquire good photographic data. The data must be processed in close coordination with the aerodynamic test engineer.

Some of the most important visualization data available are combined Schlieren or shadowgraph and smoke flow photographs. These can be acquired by superimposing two separate photographic negatives or by using the opaque stop Schlieren system to obtain a simultaneous smoke Schlieren image. By measuring the shock inclination and smoke line deflections, the properties of the flow field can be determined without the use of intrusive probes.

Other types of data acquisition can be used in conjunction with the smoke flow visualization, such as the LDV, pressure and force measurements

or dynamic testing. The additional insight into the physics of a given flow field can be achieved by evaluating the visualization data in light of the experimental results acquired using the other techniques. It appears as though two of the most critical criteria for the successful operation of a smoke flow visualization facility are experience and patience.

## CONCLUSIONS AND RECOMMENDATIONS

The results of this research program show that the high speed smoke flow visualization method, first demonstrated by Goddard, can provide valuable aerodynamic data. It has been shown that it is possible to introduce and maintain coherent smoke streaklines in transonic and supersonic flow fields and to collect good quality photographic data. There is a reasonable amount of flexibility as to how the method can be applied to a particular aerodynamic problem as well as to the type of visualization data which can be acquired.

It appears that the methods developed at the University of Notre Dame can be extended to a larger facility. Design criteria for such a facility have been outlined in this report. These criteria are based on an evaluation of the present tunnels at Notre Dame. However, some care must be taken in extrapolating to a significantly larger facility. The wind tunnel proposed by the Air Force and considered during this study was intended to have a 0.61 by 0.61 m (2 ft by 2 ft) test section for either a transonic or supersonic flow. It is felt that the present study provides many criteria which could be used for designing such a tunnel. Unfortunately, there are other areas to be considered for a tunnel that size, such as boundary layer development, smoke persistence and the much greater distances over which the smoke lines must maintain their structures. The influence of these phenomena on a very large tunnel would most likely be adverse and there has been no opportunity in the present study to evaluate them. For this reason, it is recommended that the Air Force consider the design and fabrication of a smaller facility with a test section on the order of 0.25 by 0.25 m (10 in. by 10 in.) as a prototype for a larger smoke visualization tunnel. The design and eventual use of such a tunnel would provide valuable additional data on the application of smoke visualization to the high speed regime, as well as avoid the need for a significant extrapolation of the results of the present study.

This recommendation also highlights an important aspect of smoke flow visualization. As many researchers who have ventured into this area have discovered, there is a large amount of "art" involved in collecting quality visualization data. Although the art aspect of the problem will never be

completely eliminated, it can be significantly reduced through experience. It is felt that if a prototype tunnel were to be used by the Flight Dynamics Laboratory personnel, the experience gained in such a facility would be vital to the success of a larger research establishment.

There is no doubt that smoke flow visualization can provide a valuable tool for the high speed aerodynamicist. It will only be through the use of these methods in the study of important aerodynamic problems that this potential will be realized.

## REFERENCES

- <sup>1</sup>Mach, L., "Über die Sichtbarmachung von Luftstromlinien," Zeitschrift für Luftschiffahrt und Physik der Atmosphäre, Vol. 15, Heft 6, pp. 129-139, 1896.
- <sup>2</sup>Marey, E.J., "Des mouvements de l'air lorsqu'il rencontre des surfaces de différentes formes," Comptes Rendus des Seances de l'Académie des Sciences, Vol. 131, pp. 160-163, July 16, 1900.
- <sup>3</sup>Mueller, T.J., "On the Historical Development of Apparatus and Techniques for Smoke Visualization of Subsonic and Supersonic Flows," AIAA Paper No. 80-0420, presented at the AIAA 11th Aerodynamics Testing Conference, Colorado Springs, Colorado, March 18-20, 1980.
- <sup>4</sup>Lippisch, A.M., "Results from the Deutsche Forschungsanstalt für Segelflug Smoke Tunnel," Royal Aeronautical Society Journal, 43, pp. 653-672, September 1939.
- <sup>5</sup>Brown, F.N.M., See the Wind Blow, 1971.
- <sup>6</sup>Merzkirch, W., Flow Visualization, Academic Press, New York and London, 1974.
- <sup>7</sup>Goddard, V.P., McLaughlin, J.A., and Brown, F.N.M., "Visual Supersonic Flow Patterns by Means of Smoke Lines," Journal of the Aero/Space Sciences 26, No. 11, pp. 761-762, November 1959.
- <sup>8</sup>Goddard, V.P., "Development of Supersonic Streamline Visualization," Report to the National Science Foundation on Grant 12488, March 1962.
- <sup>9</sup>Slovisky, J.A., Roberts, W.B., and Crouse, J.E., "High Speed Flow Visualization for the Determination of Cascade Shock Losses," AIAA Paper No. 79-0042, AIAA 17th Aerospace Sciences Meeting, New Orleans, January 1979.
- <sup>10</sup>Bisplinghoff, R.L., Coffin, J.B., and Haldeman, C.W., "Water Fog Generation System for Subsonic Flow Visualization," AIAA Journal, Vol. 14, No. 8, pp. 1133-1135, August 1976.
- <sup>11</sup>Haldeman, C.W., Private Communication, 1980.
- <sup>12</sup>Brandt, S.A., and Iversen, J.D., "Merging of Aircraft Trailing Vortices," AIAA Journal of Aircraft, Vol. 14, No. 12, pp. 1212-1220, December 1977.
- <sup>13</sup>Foelsch, K., "The Analytical Design of an Axially Symmetric Laval Nozzle for a Parallel and Uniform Jet," Journal of Aeronautical Sciences, Vol. 16, No. 13, p. 161, 1949.
- <sup>14</sup>Smith, R.H., and Wang, C., "Contracting Cones Giving Uniform Throat Speeds," Journal of Aeronautical Sciences, pp. 356-360, October 1944.
- <sup>15</sup>Cornell, D., "Smoke Generating for Flow Visualization," Research Report No. 54, The Aerophysics Dept., Mississippi State University, November 1964.

<sup>16</sup>Maltby, R.L. and Keating, R.F.A., "Smoke Techniques for Use in Low Speed Wind Tunnels," AGARD-ograph 70, pp. 87-109, 1962.

<sup>17</sup>Preston, J.H., and Sweeting, N.E., "An Improved Smoke Generator for Use in the Visualization of Airflow, Particularly Boundary Layer Flow at High Reynolds Numbers," ARC R & M 2023, ARC 7111, October 1943.

<sup>18</sup>Griffin, O.M., and Votaw, C.W., "The Use of Aerosols for the Visualization of Flow Phenomena," International Journal of Heat Mass Transfer, Vol. 16, pp. 217-219, 1973.

<sup>19</sup>Griffin, O.M., and Ramberg, S.E., "Wind Tunnel Flow Visualization with Liquid Particle Aerosols," Flow Visualization, edited by T. Asanuma, Hemisphere Publishing Corporation, Washington, D.C., pp. 65-73, 1979.

<sup>20</sup>Sellberg, L.D., "Smoke Generator Type Lorinder for Flow Visualization in Low Speed Wind Tunnels," KTH AERO TN 55, Dept. of Aeronautical Engineering, Royal Institute of Technology, Stockholm, Sweden, 1966.

<sup>21</sup>Schubauer, G.B., Spangenberg, W.G., and Klebanoff, P.S., "Aerodynamic Characteristics of Damping Screens," NACA TN 2001, National Bureau of Standard, Washington, D.C., January 1950.

<sup>22</sup>Carrothers, P.J.G., and Baines, W.D., "Forces on Screens of Small Solidity Inclined to a Fluid Flow," presented at the Fluids Engineering Division of ASME at Winter Annual Meeting, Detroit, Michigan, November 11-15, 1973.

<sup>23</sup>Batchelor, G.K., and Shaw, F.S., "A Consideration of the Design of Wind Tunnel Contractions, Report ACA-4, March 1944.

<sup>24</sup>Morel, T., "Comprehensive Design of Axisymmetric Wind Tunnel Contractions," Journal of Fluids Engineering, ASME Transactions, pp. 225-233, June 1975.

<sup>25</sup>Lau, W.T.F., "An Analytical Method for the Design of Two-Dimensional Contractions," Journal of the Royal Aeronautical Society, Vol. 68, No. 639, p. 59, January 1964.

<sup>26</sup>Jordinsen, R., "Design of Wind Tunnel Contractions," Aircraft Engineering, pp. 294-297, October 1961.

<sup>27</sup>Whitehead, L.G., Wu, L.Y., and Waters, M.H.L., "Contraction Ducts of Finite Length," The Aeronautical Quarterly, Vol. II, pp. 254-271, February 1951.

<sup>28</sup>Libby, P.A., and Reiss, H.R., "The Design of Two-Dimensional Contraction Sections," Quarterly Journal of Applied Mathematics, Vol. IX, 1951.

<sup>29</sup>Gibbings, J.C., and Dixon, J.R., "Two-Dimensional Contracting Duct Flows," Quarterly Journal of Mechanics and Applied Mathematics, Vol. X, Pt. 1, pp. 24-41, 1957.

<sup>30</sup>Szczeniowski, B., "Contraction Cone for a Wind Tunnel," Journal of Aeronautical Sciences, pp. 311-312, October 1943.

<sup>31</sup>Thwaites, B., "On the Design of Contractions for Wind Tunnels," ARC, R & M No. 2278, March 1946.

<sup>32</sup>Morel, T., "Design of Two-Dimensional Wind Tunnel Contractions," ASME Paper No. 76-WA/FE-4, pp. 1-7, December 1976.

<sup>33</sup>Chmielewski, G.E., "Boundary Layer Considerations in the Design of Aerodynamic Contractions," Journal of Aircraft, Vol. II, No. 8, August 1974.

<sup>34</sup>Mikhail, M.N., "Optimum Design of Internal Flow Passages with Specific Reference to Wind Tunnel Contractions," Ph.D. Thesis, Carleton University, Ottawa, Canada, October 1976.

<sup>35</sup>Cohen, M.J., and Ritchie, N.J.B., "Low Speed Three-Dimensional Contraction Design," Journal of Royal Aeronautical Society, Vol. 66, pp. 231-236, April 1962.

<sup>36</sup>Bossel, H.H., "Computation of Axisymmetric Contractions," AIAA Journal, Vol. 7, No. 10, pp. 2017-2020, October 1969.

<sup>37</sup>Borger, G.G., "The Optimization of Wind Tunnel Contractions for the Subsonic Range," NASA TTF-16899, March 1976.

<sup>38</sup>Jacobs, Morris B., The Chemical Analysis of Air Pollutants, Interscience Pub., Inc.



## APPENDIX:

### SYSTEM SAFETY HAZARD ANALYSIS

One aspect of the design and operation of a high speed smoke visualization facility, which was not addressed in the report, is system safety. Although the operation of a smoke visualization facility is not radically different from any other wind tunnels with comparable characteristics, there are some unique aspects which present certain safety hazards.

The system considered can be divided into two major components: 1) Wind Tunnel; 2) Smoke Generation Equipment. The wind tunnel, of the type described in the body of the report, is an indraft, continuous operation tunnel. Details concerning criteria for the design of such a tunnel for the purpose of flow visualization are outlined in the report. These criteria are not related to the construction of such a facility but are directed towards its operating characteristics and performance. For these reasons, the hazards outlined in this summary have been identified through the expertise gained in the operation of the flow visualization tunnels at the University of Notre Dame.

#### Wind Tunnel

The primary hazards associated with the operation of the wind tunnel facility involve the high flow velocities within the tunnel, low pressures in the test section and diffuser section and sound levels generated by operation of the tunnel. The velocity and pressure problems are related to the structural design of the facility as well as the wind tunnel models used during a specific test. Any danger to operators or observers can be significantly reduced by using accepted engineering design procedures in preliminary facility development and subsequent test planning.

The indraft design does create some particular problems related to noise generated by the tunnel operation. Since there is a direct path out of the tunnel, through the inlet, when operating in a subsonic or transonic mode, there exists the possibility of excessively high noise levels near the tunnel. These could be hazardous to operators or observers as well as to the surrounding facilities. Isolation of the operating station and overall facility location may be influenced by the acoustical hazard.

### Smoke Generation Equipment

The unique feature of the visualization tunnel is the requirement to produce large quantities of dense, white "smoke." The report addresses a number of the properties of such a "smoke" in detail. Regardless of the type of smoke used in the facility, whether it be steam, vaporized kerosene, products of combustion, etc., the smoke must be isolated from individuals operating the tunnel. The smoke should not be toxic in small quantities, such as those which might occur with small leaks in the system or after the smoke has been highly diffused after passing through the tunnel. The smoke need only be present in the tunnel while the visualization data is being collected. The smoke generation system must be designed so that smoke will be introduced into the smoke rake only when data is to be collected and while the tunnel is operating. The exhaust from the wind tunnel should be exited to the outside air, allowing the smoke to diffuse in the atmosphere.

As an example, the smoke generator of the type used at Notre Dame will continuously produce adequate quantities of smoke for an hour, and vaporize approximately one quart of kerosene. This results in a minute amount of air pollution outside the laboratory. The smoke has an added feature of being very visible so that any small leaks in the system can be seen easily. If such leaks occur, the system can be shut down and corrective action taken.

All of the items cited in the previous paragraphs must be addressed in facility design. The system should then be able to be operated with minimum influence from these hazards.

# PILOT TUNNEL

Throat Area:	-	35.74 cm <sup>2</sup>	(5.540 in <sup>2</sup> )
Test Section Area:	-	40.32 cm <sup>2</sup>	(6.250 in <sup>2</sup> )
Inlet Area (downstream):	-	132.30 cm <sup>2</sup>	(20.50 in <sup>2</sup> )
Inlet Area (upstream):	-	.330 m <sup>2</sup>	(513 in <sup>2</sup> )
Screen Area:	-	.659 m <sup>2</sup>	(1022 in <sup>2</sup> )

# 5 inch TUNNEL

Throat Area:	-	138.3 cm <sup>2</sup>	(21.44 in <sup>2</sup> )
Test Section Area:	-	163.9 cm <sup>2</sup>	(25.40 in <sup>2</sup> )
Inlet Area (downstream)	-	516.0 cm <sup>2</sup>	(80 in <sup>2</sup> )
Inlet Area (upstream)	-	1.355 m <sup>2</sup>	(2100 in <sup>2</sup> )
Screen Area:	-	1.355 m <sup>2</sup>	(2100 in <sup>2</sup> )

Table I. Wind Tunnel Geometric Properties

CLASSIFICATION	DESCRIPTION
A. Mechanical Dispersion	A high-velocity gas stream shears a liquid film into small droplets. This is sometimes called atomization.
	A high-velocity liquid stream disintegrates through its own instability or because of striking an object.
	<ol style="list-style-type: none"> <li>1. Simple liquid jet.</li> <li>2. Helical-orifice jet.</li> <li>3. Solution-gas jet.</li> <li>4. Jet directed against a surface.</li> </ol>
	A liquid stream is dispersed by a rotating disk. Shear forces acting on the sheet of liquid leaving the disk cause droplet formation.
	A liquid stream is dispersed by ultrasonic energy.
B. Vaporization and Condensation	Evaporation of solvent from droplets of a solution containing a solid or liquid to be dispersed.
	Condensation of a vapor in a cool gas stream in the presence of appropriate nuclei.
C. Combustion and Chemical Reactions	Volatilization of noble metals in an electric arc.
	Combustion of fuels with insufficient air.
	Reaction of mixtures of fuels and oxidizers to form a dispersed solid product.

Table II. Methods for Aerosol Generation  
(from Reference 15)

	Boiling Point (°F)	Flash Point (°F)	Auto Ignition (°F)
Mineral Oil	600	275-500	500-700
Kerosene	350-550	110-130	440-560
Coal Tar Oil	96	60-77	-

Table III. Physical Properties of Hydrocarbons  
Used for Smoke Generation  
(from Reference 38)

1. Cameras

- a) A 4" x 5" view camera with an f/4.5, 6" lens in a shutter provided with a synchronizing switch suited to a short interval flash lamp.
- b) A high speed motion camera capable of 800 frames per second with associated synchronizing equipment.

2. Lights

- a) High intensity stroboscopic lights; at least six lamps should be provided.
- b) High intensity steady light sources (1000 watt spot lights); four spots should be provided.

3. Darkroom

- a) Darkroom should be located near the wind tunnel laboratory.
- b) Tank processing for 4" x 5" and 16 mm film must be provided.
- c) A high quality enlarger and equipment for processing 8" x 10" glossy prints is required.
- d) It is essential that the technician in charge of the darkroom be under the direction of the smoke tunnel engineer.

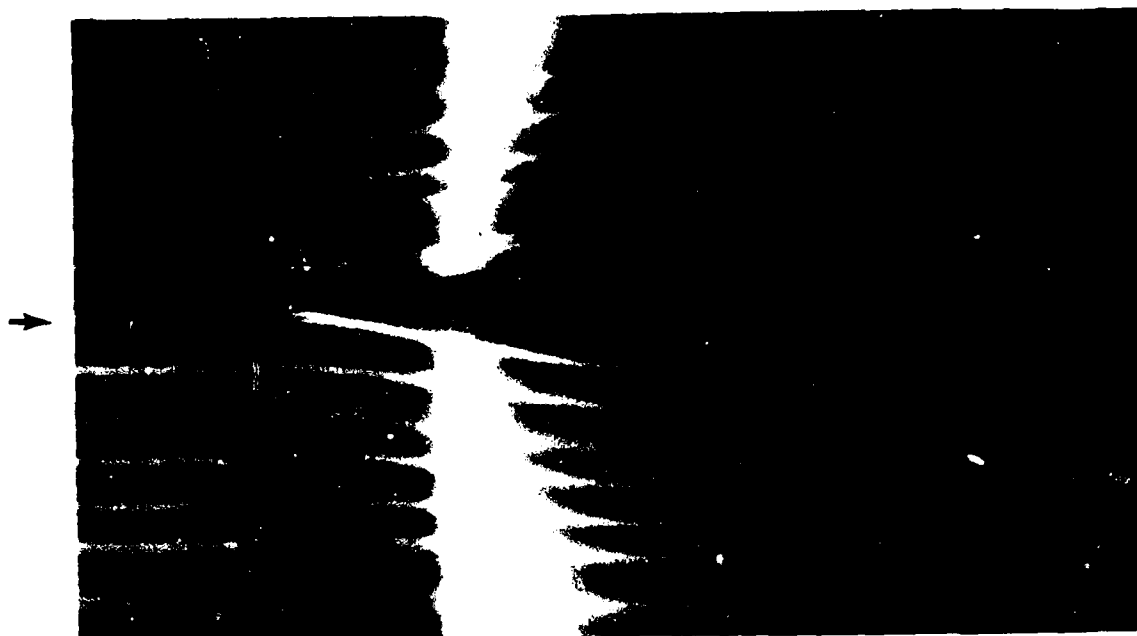
Table IV. Recommended Equipment for Smoke Flow  
Photography

1. Poor Smoke Quality
  - a) High turbulence level in the tunnel.
  - b) Inadequate smoke generation.
  - c) Smoke rake located inside the tunnel circuit.
  
2. Poor Photographic Procedures
  - a) Heavy reliance on photographic technicians.
  - b) Heavy reliance on commercial photographic processing.

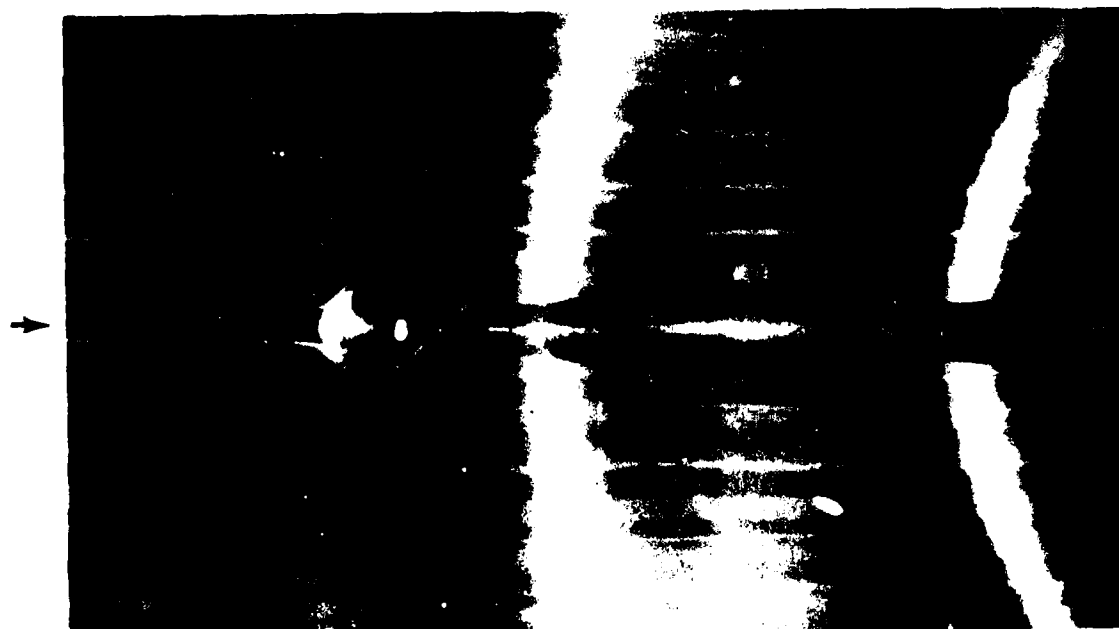
Table V. Sources of Problems in Flow Visualization Experiments

1. Negatives usually will require overdeveloping due to inadequate light.
2. Avoid batch processing of prints.
3. Prints will require photographic dodging.
  - a) Dodging is a technique to unevenly expose the print.
  - b) Dodging allows the maximum photographic data to be obtained on the print.

Table VI. Photographic Procedures



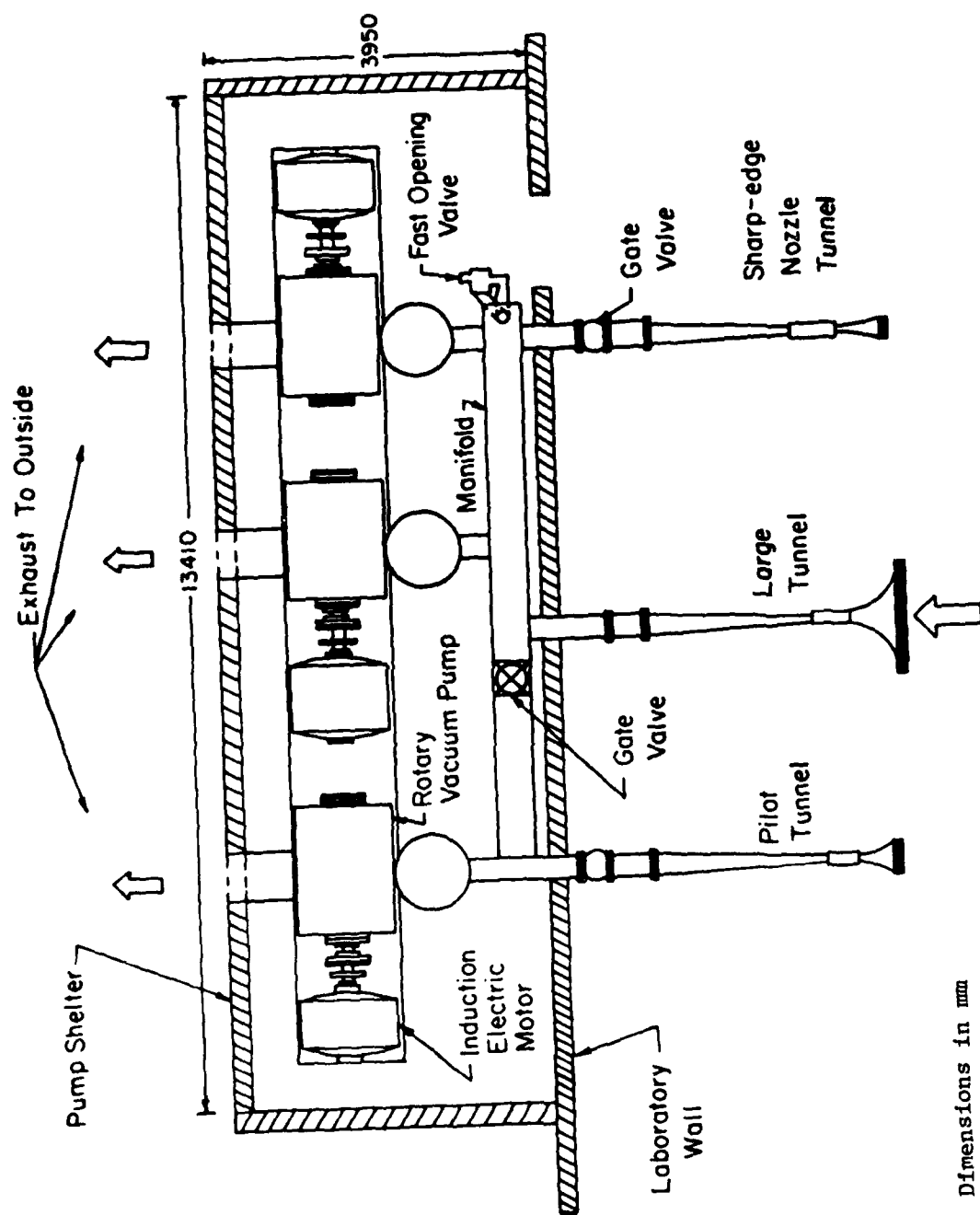
Two-Dimensional Wedge:  $M_{\infty} \approx 1.42$



Sphere:  $M_{\infty} \approx 1.42$

Figure 1. Original Photographs by V.P. Goddard





Dimensions in mm

Figure 2. Schematic of Notre Dame's High Speed Aerodynamics Facilities, Planform View.

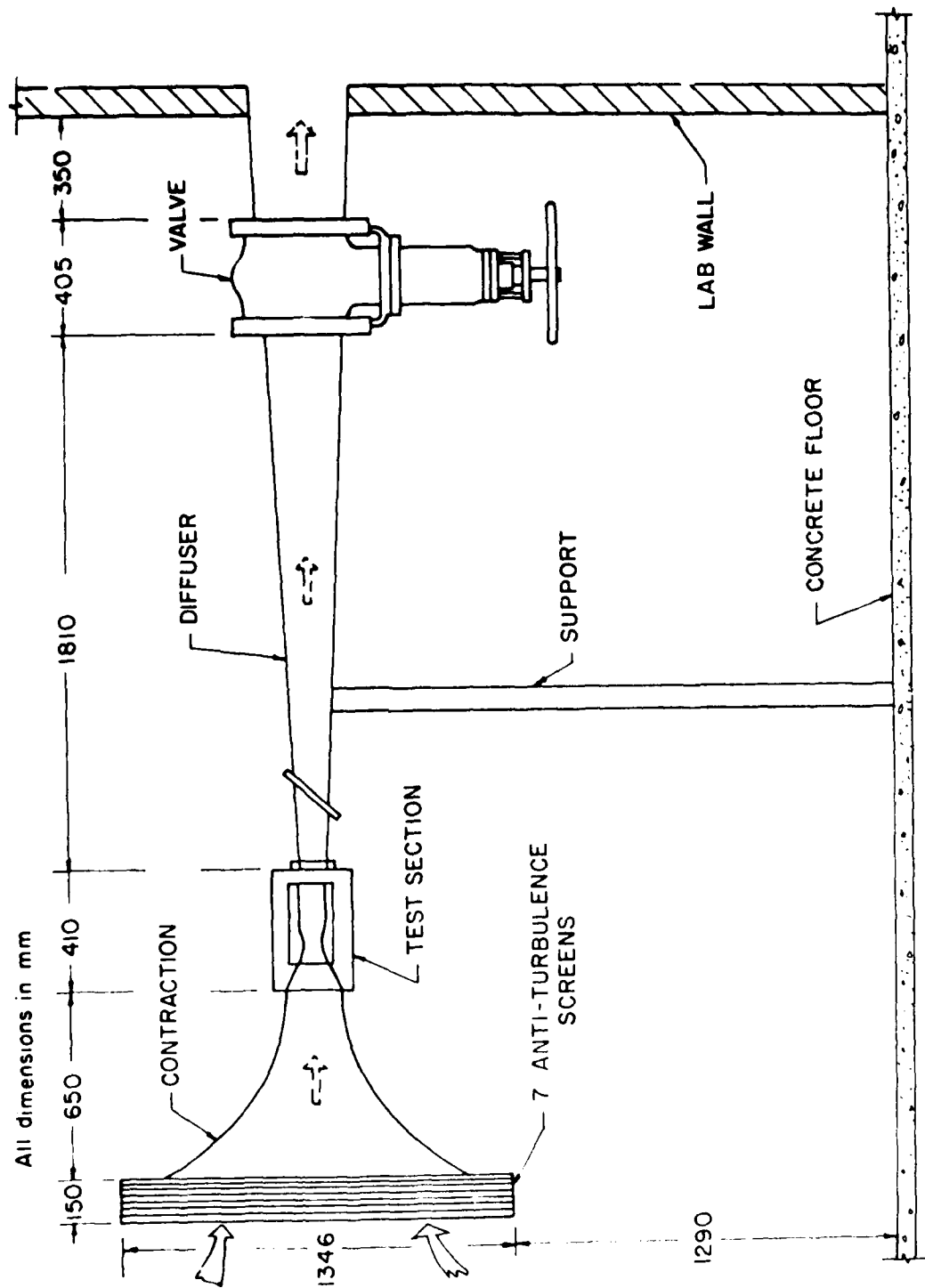


Figure 3. Schematic of Pilot Supersonic Tunnel, Original Inlet.

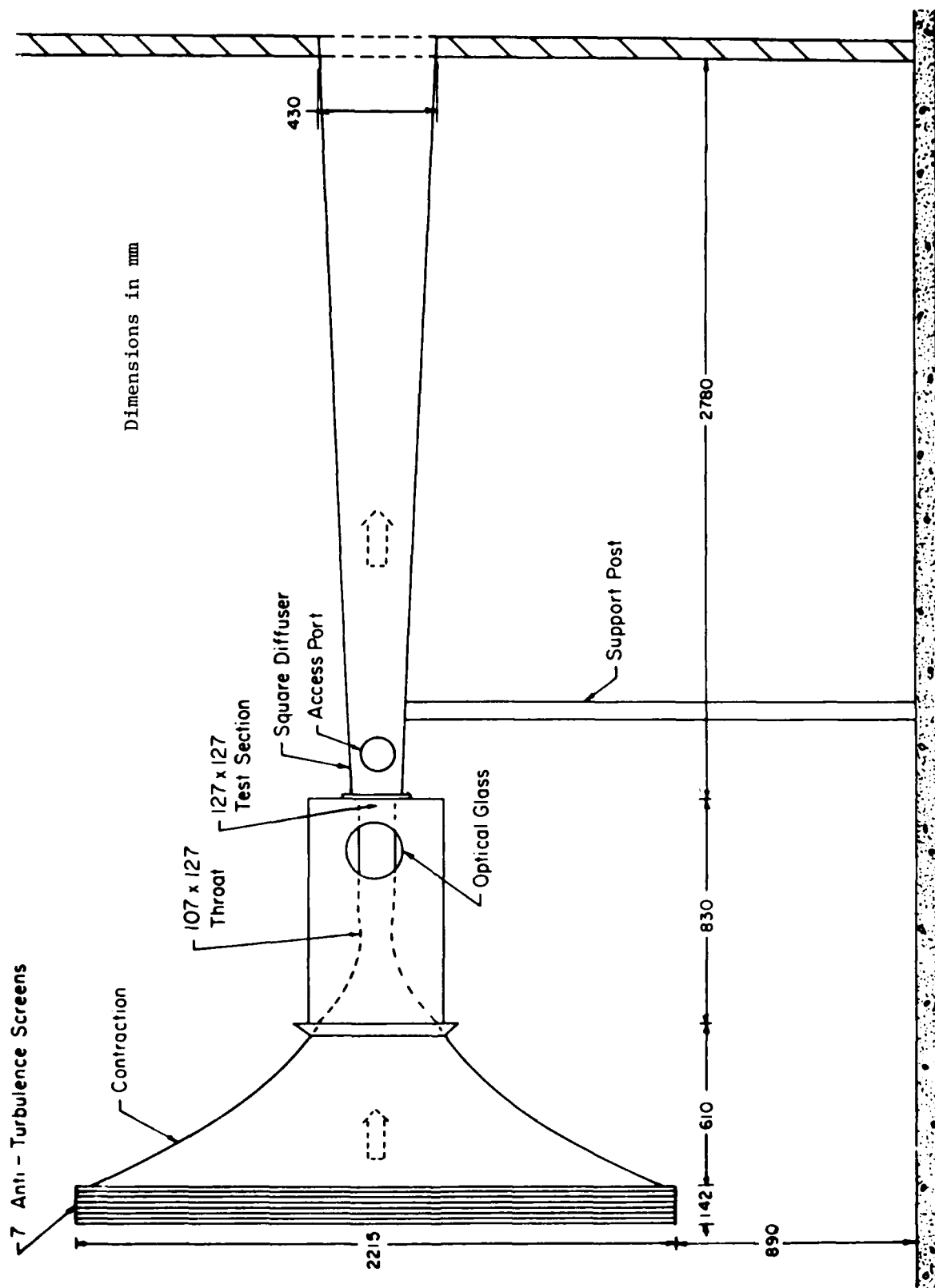


Figure 4. Schematic of 5" by 5" Supersonic Tunnel

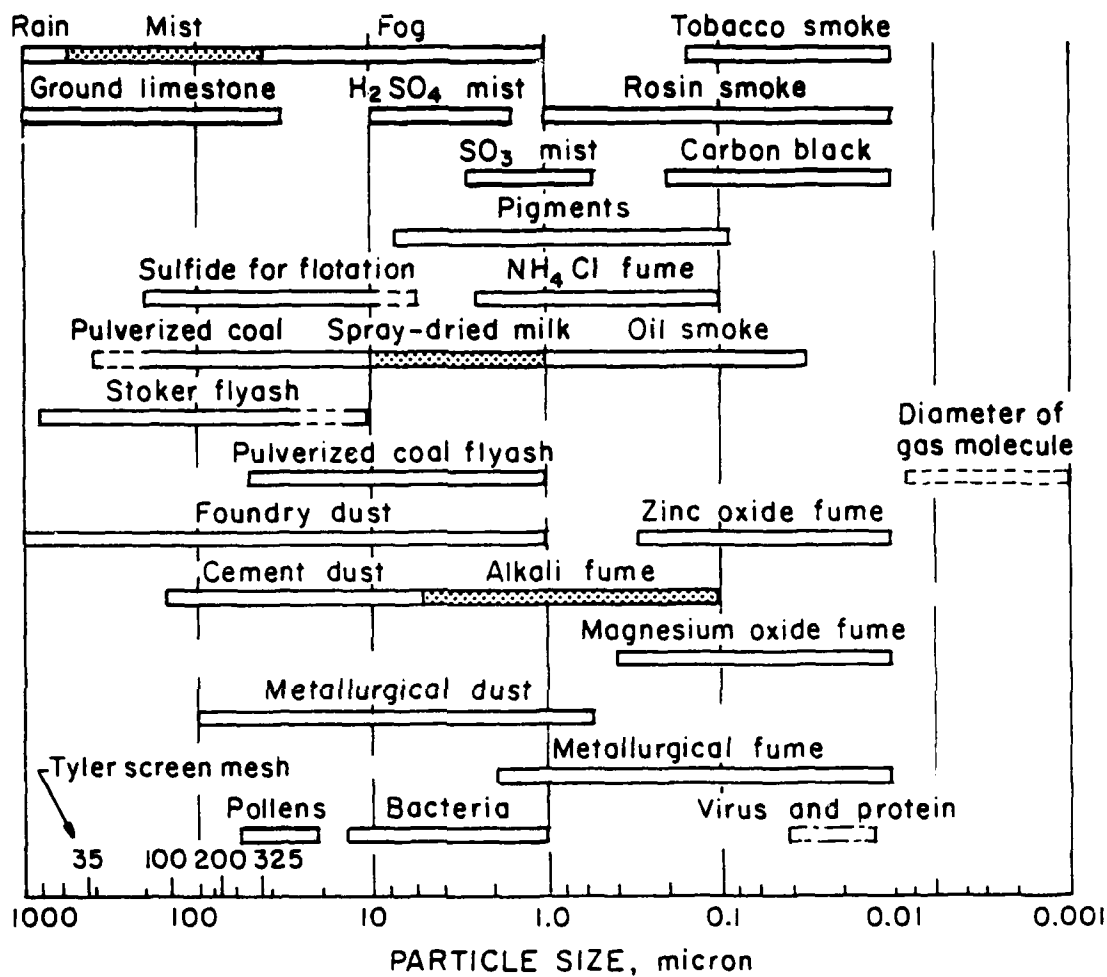


Figure 5. Range of Particle Size of Various Materials  
(from Ref. 38)

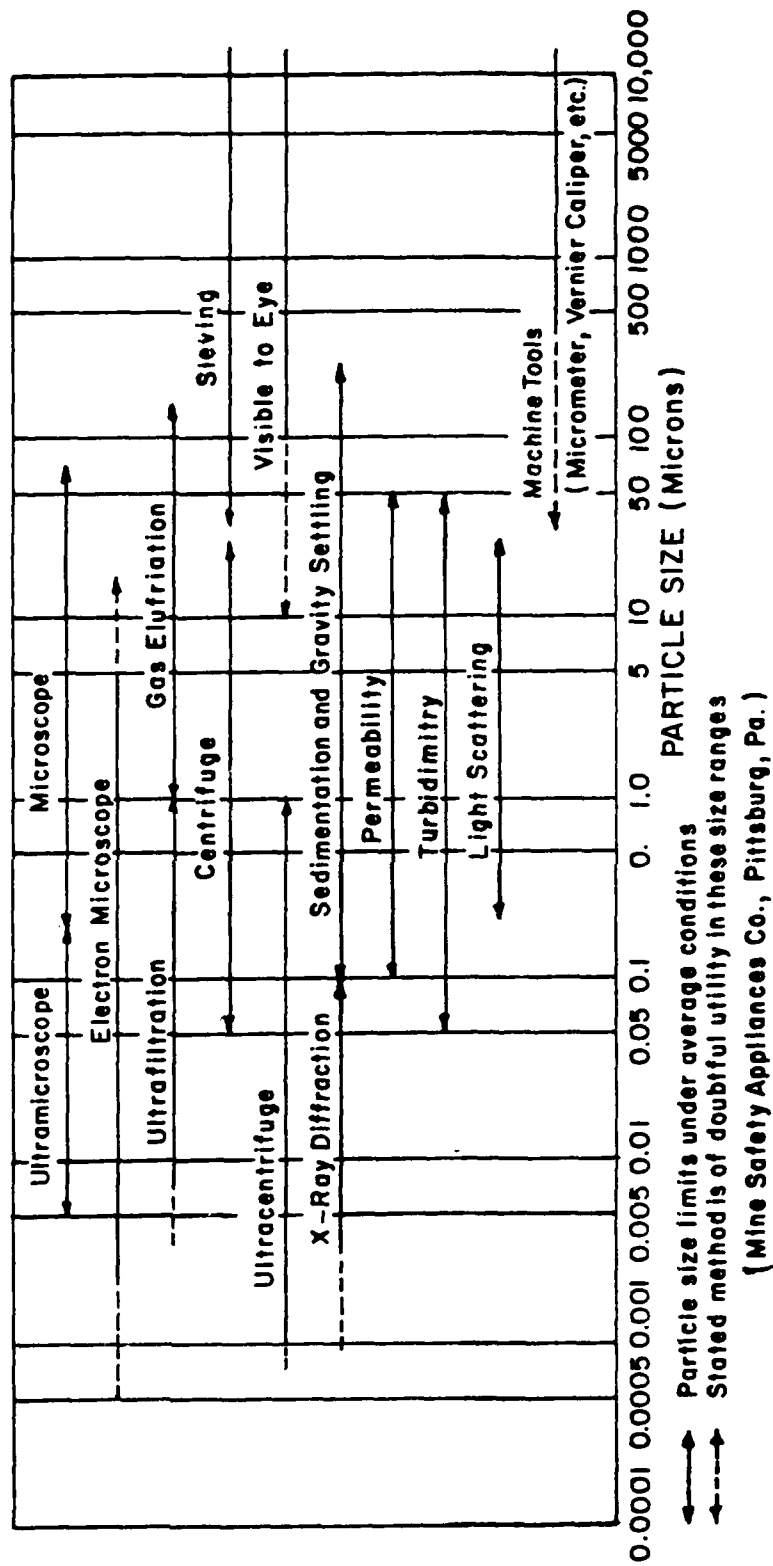
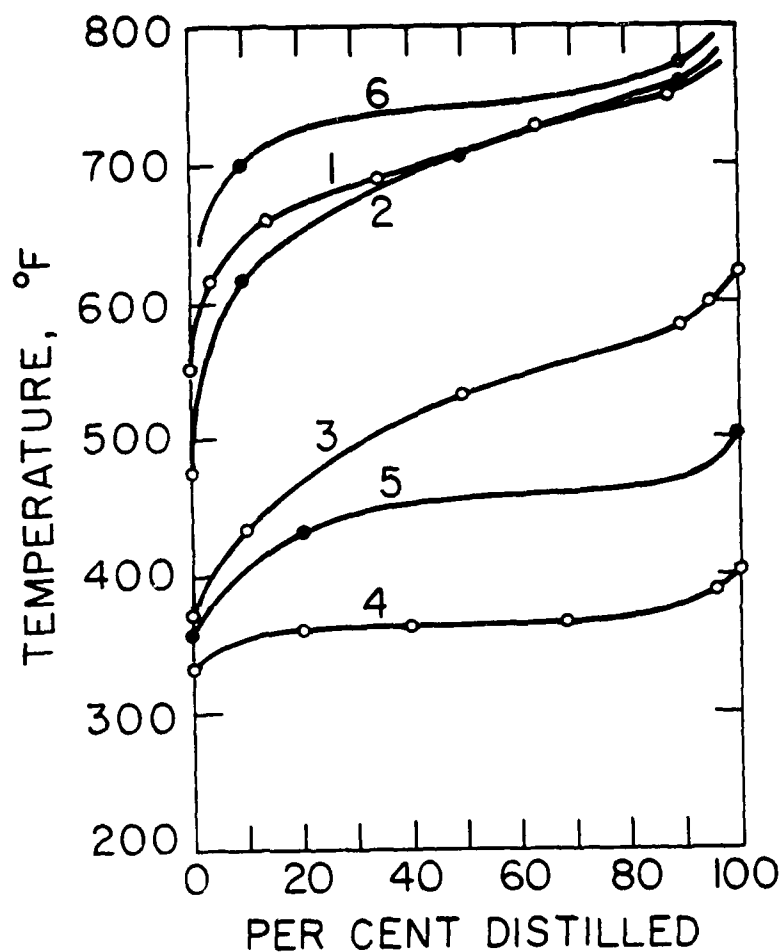


Figure 6. Methods of Particle Detection, Range for Light Scattering.



<u>CURVE NO.</u>	<u>LIQUID</u>
1	Life-like Products Model Railroad Smoke
2	Re-distilled No. 5 Fuel Oil
3	No. 2 Diesel Fuel
4	Charcoal Lighter Fluid
5	Kerosene
6	Mineral Oil

Figure 7. Distillation Curves for Hydrocarbon Mixtures  
(from Ref. 15)

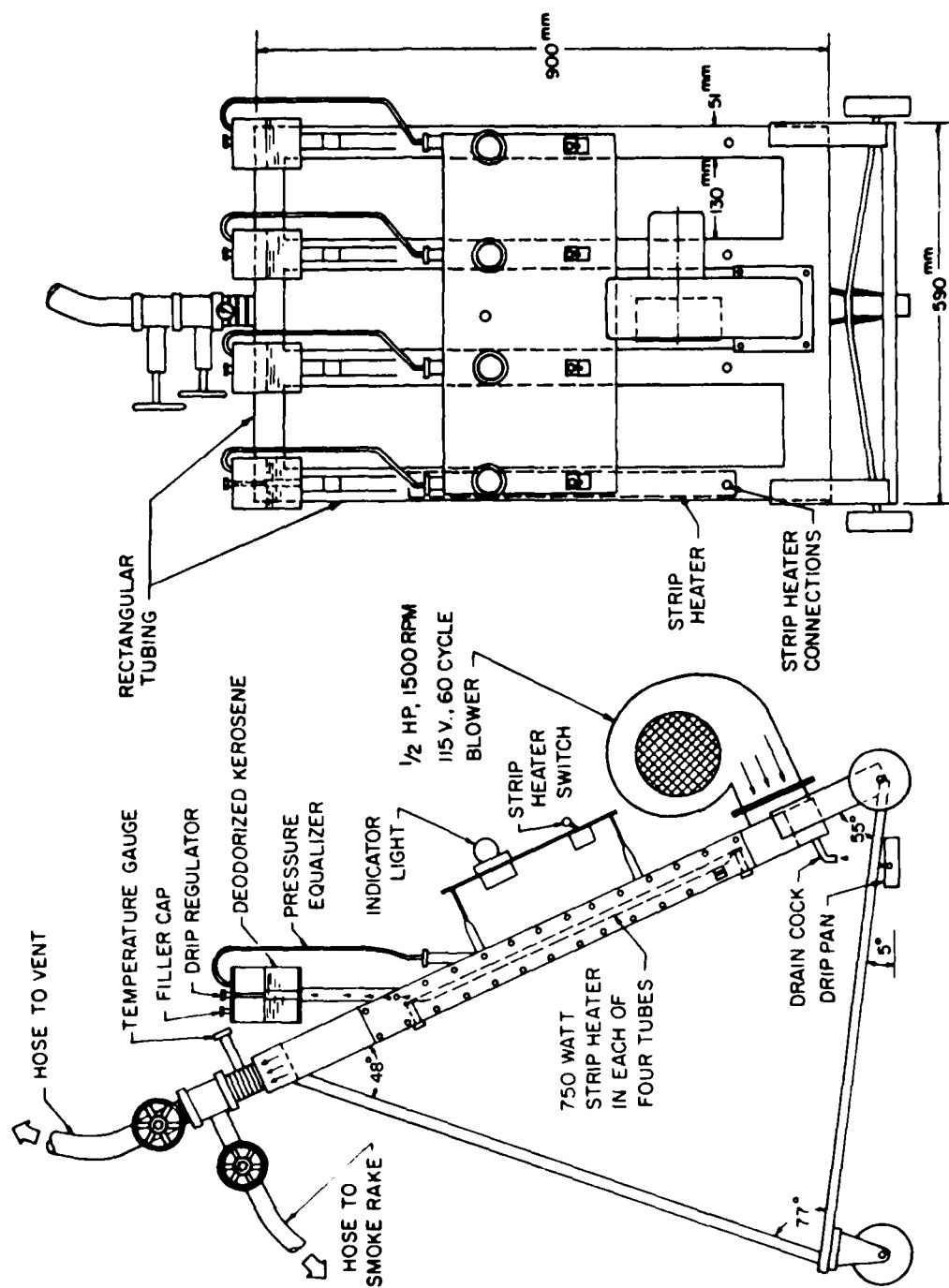


Figure 8. Kerosene Smoke Generator

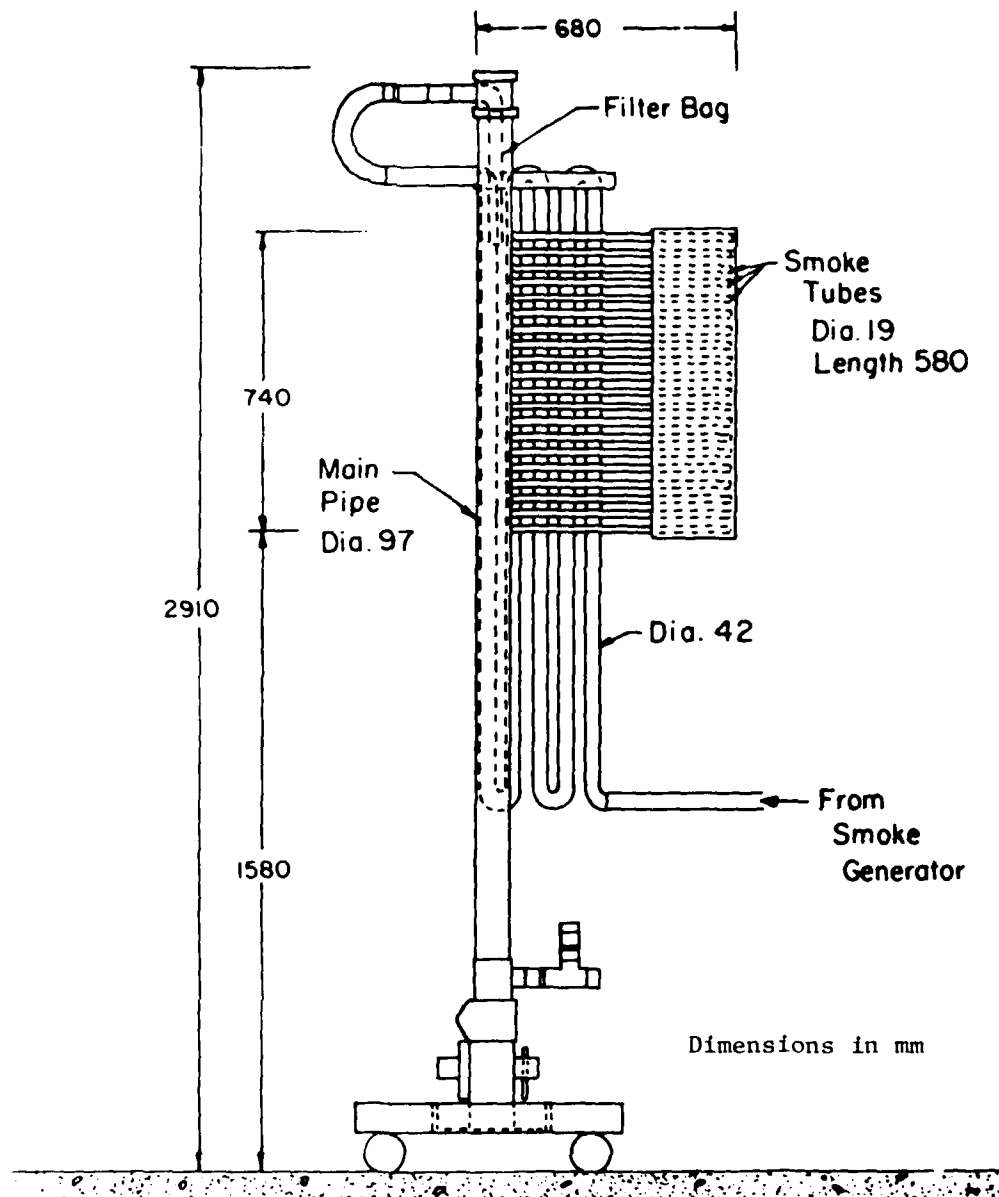


Figure 9. Schematic of Smoke Rake



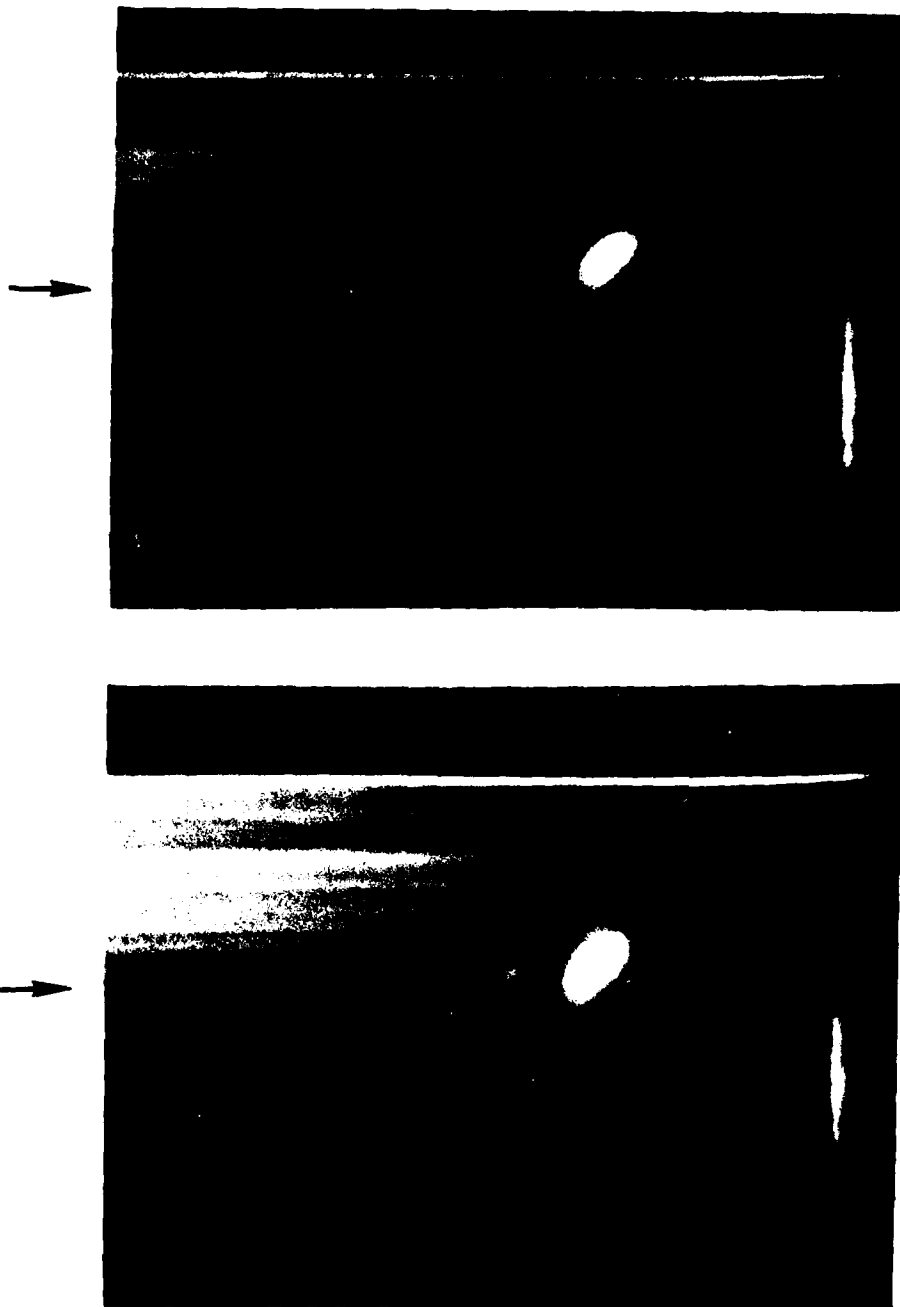


Figure 10. Photographs of Steam Visualization  
Experiment in Pilot Tunnel



Figure 11. Photographs of Mineral Oil Smoke  
Generator Demonstration

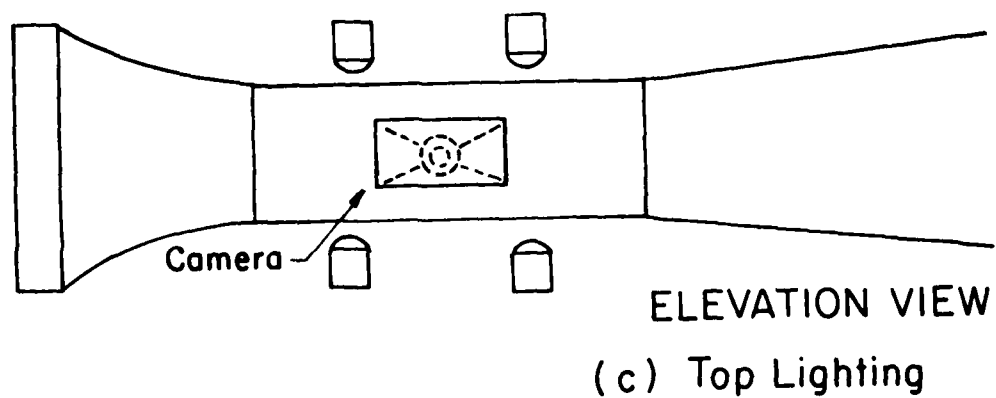
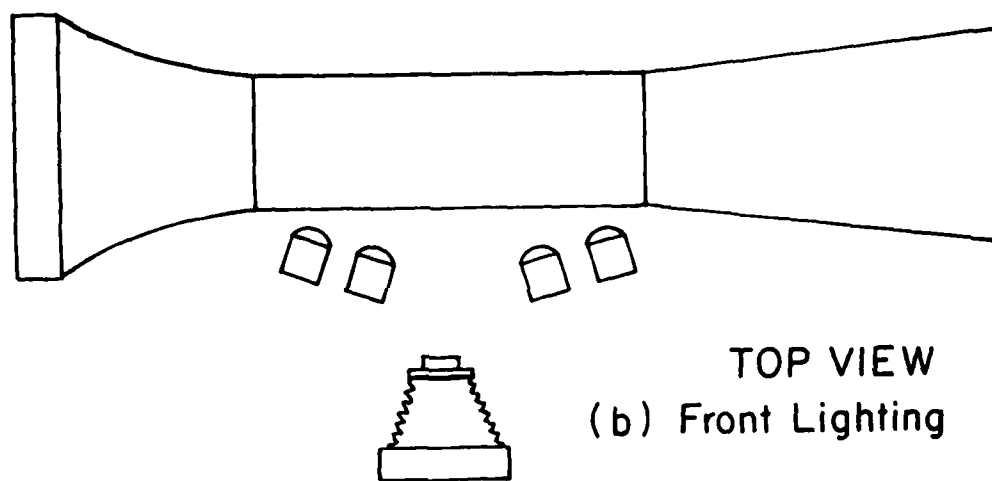
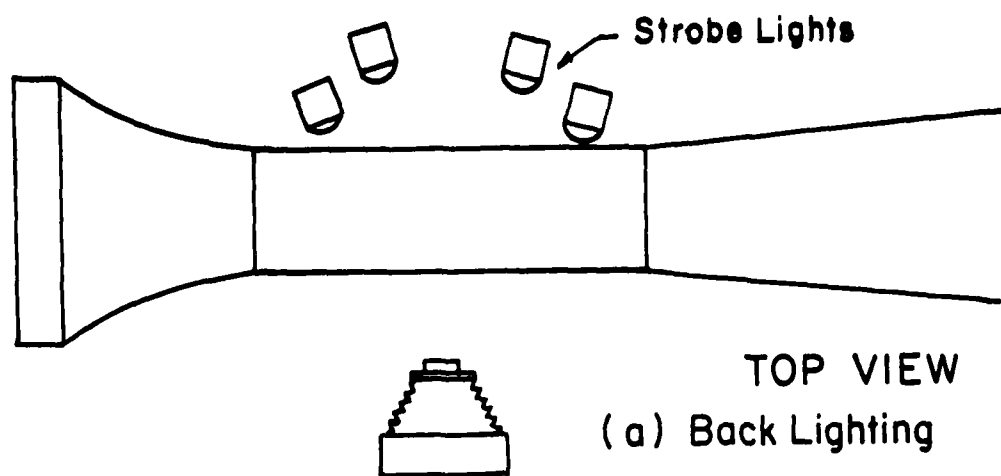


Figure 12. Lighting and Camera Arrangements

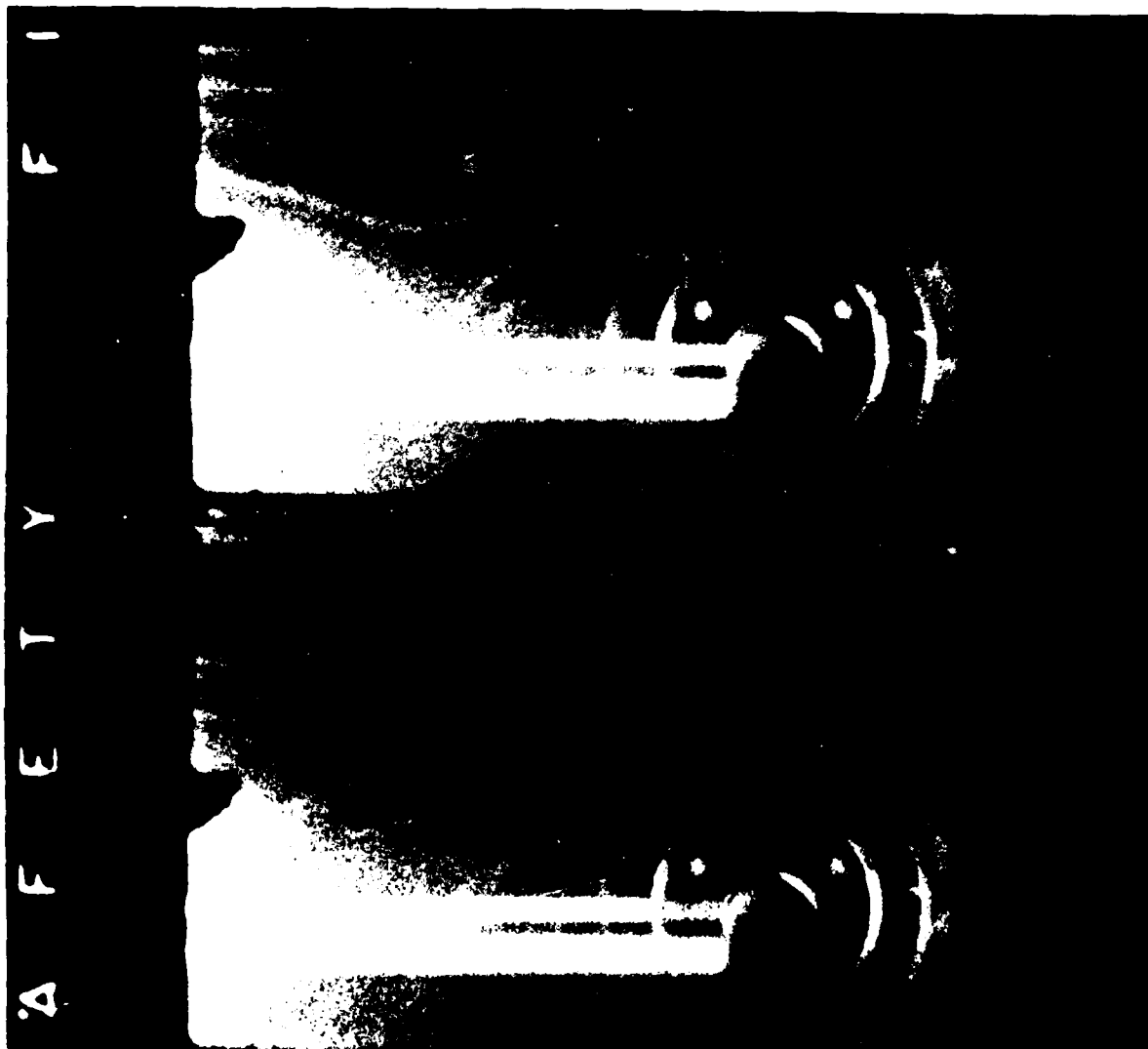
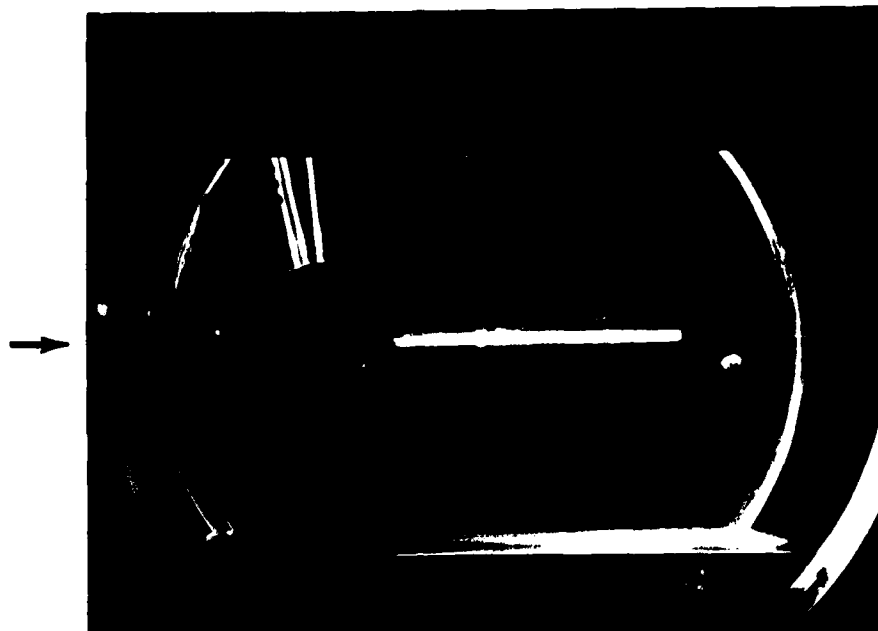
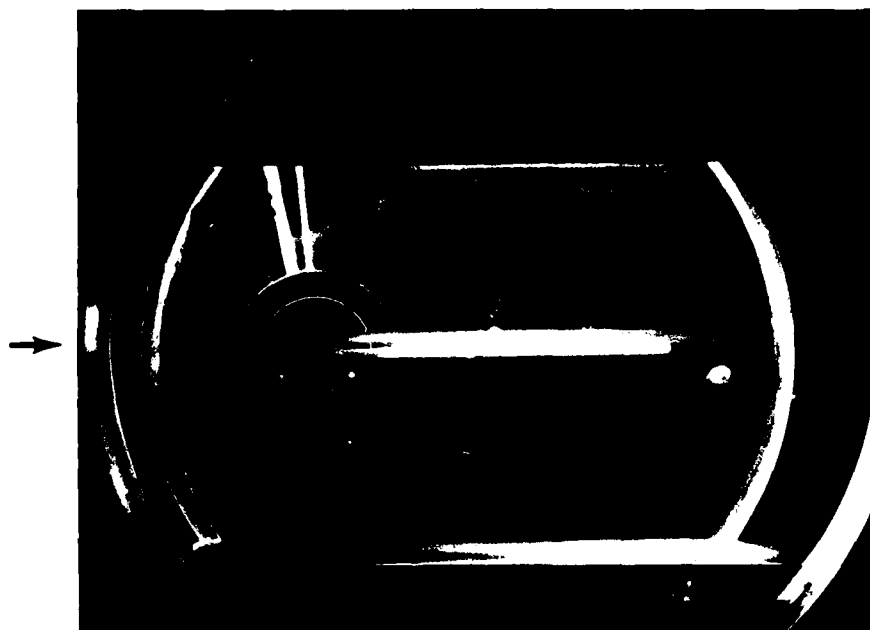


Figure 13. High Speed Motion Picture Photograph,  
Right Circular Cylinder Model,  
 $M_{\infty} = 0.55$ , 128 frames/second.



$M_{\infty} \approx 0.2$ , Back Lighting



$M_{\infty} \approx 0.60$ , Back Lighting

Figure 14. High Speed Still Photograph, Right Circular Cylinder Model, 5" by 5" Tunnel.

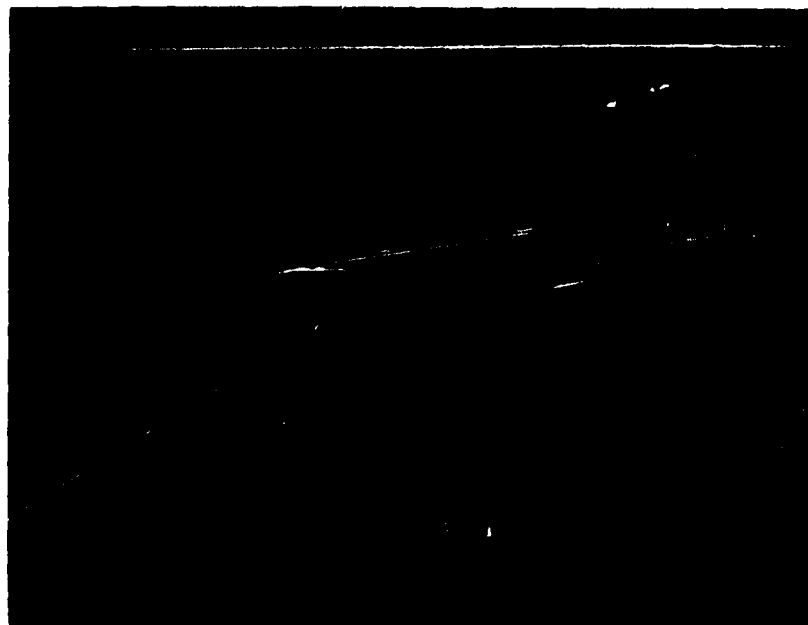


$M_\infty \approx 0.2$



$M_\infty \approx 1.2$

Figure 15. High Speed Still Photographs, Sphere Model.



$M_\infty \approx 0.2$



$M_\infty \approx 1.2$

Figure 16. High Speed Still Photographs, Double Wedge Airfoil.

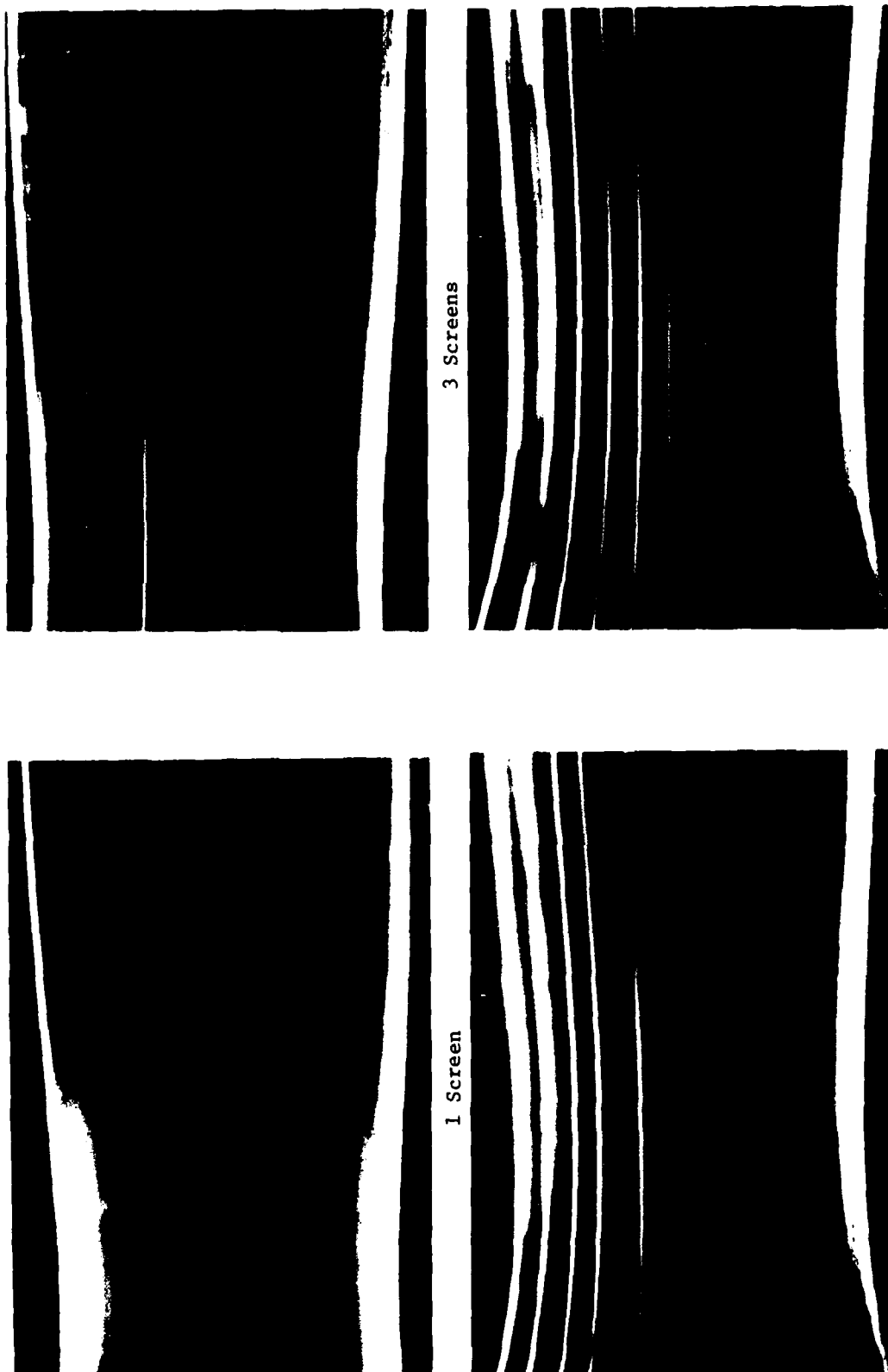
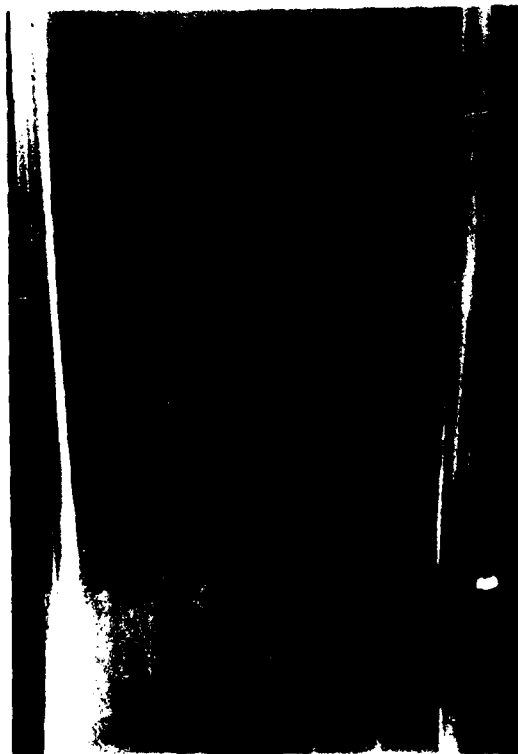
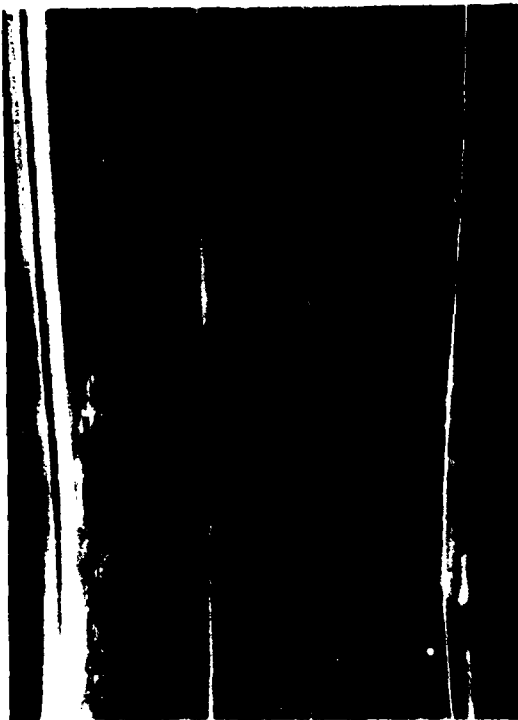


Figure 17. Screen Influence Study, Pilot Tunnel, Original Smith/Wang Inlet, Top Lighting.  
(15.1 mm ID Smoke Rake)





1 Screen



3 Screens



7 Screens



11 Screens

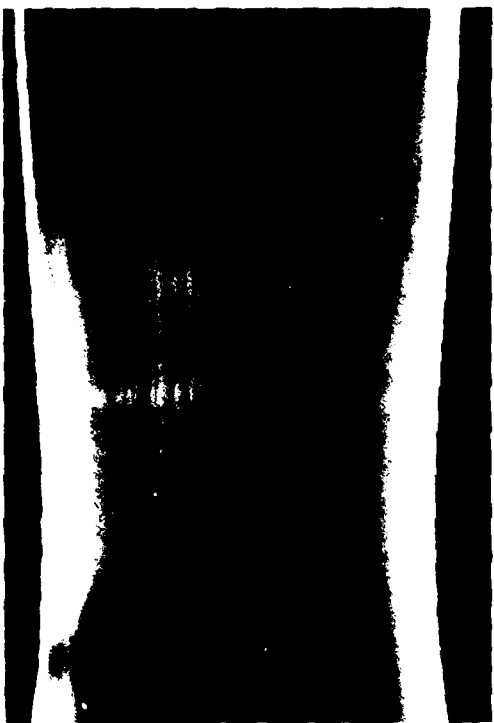
Figure 18. Screen Influence Study, Pilot Tunnel, Original Smith/Wang Inlet, Back Lighting.  
(15.1 mm ID Smoke Rake)



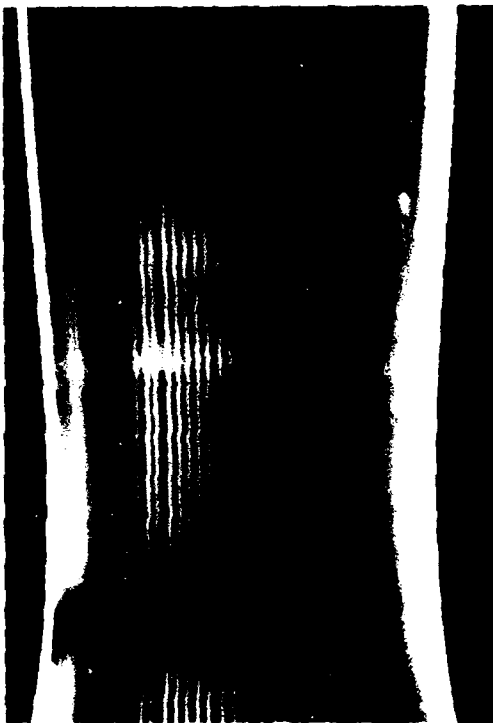
7 Screens - Back Lighting



11 Screens - Back Lighting



7 Screens - Top Lighting



11 Screens - Top Lighting

Figure 19. Screen Influence Study, Pilot Tunnel, Original Smith/Wang Inlet.  
(9.5 mm ID Smoke Rake)

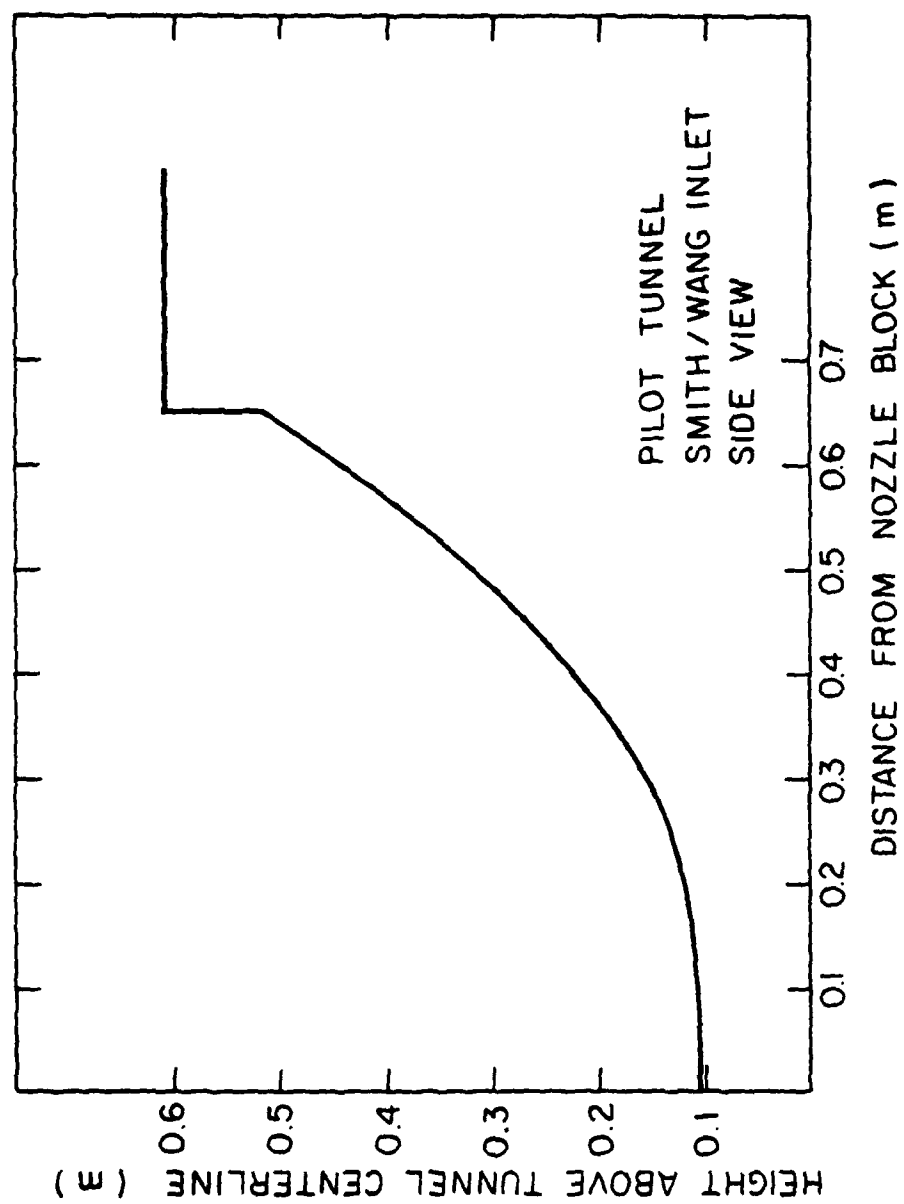


Figure 20. Inlet Geometry Profile, Smith/Wang Inlet, Side View.

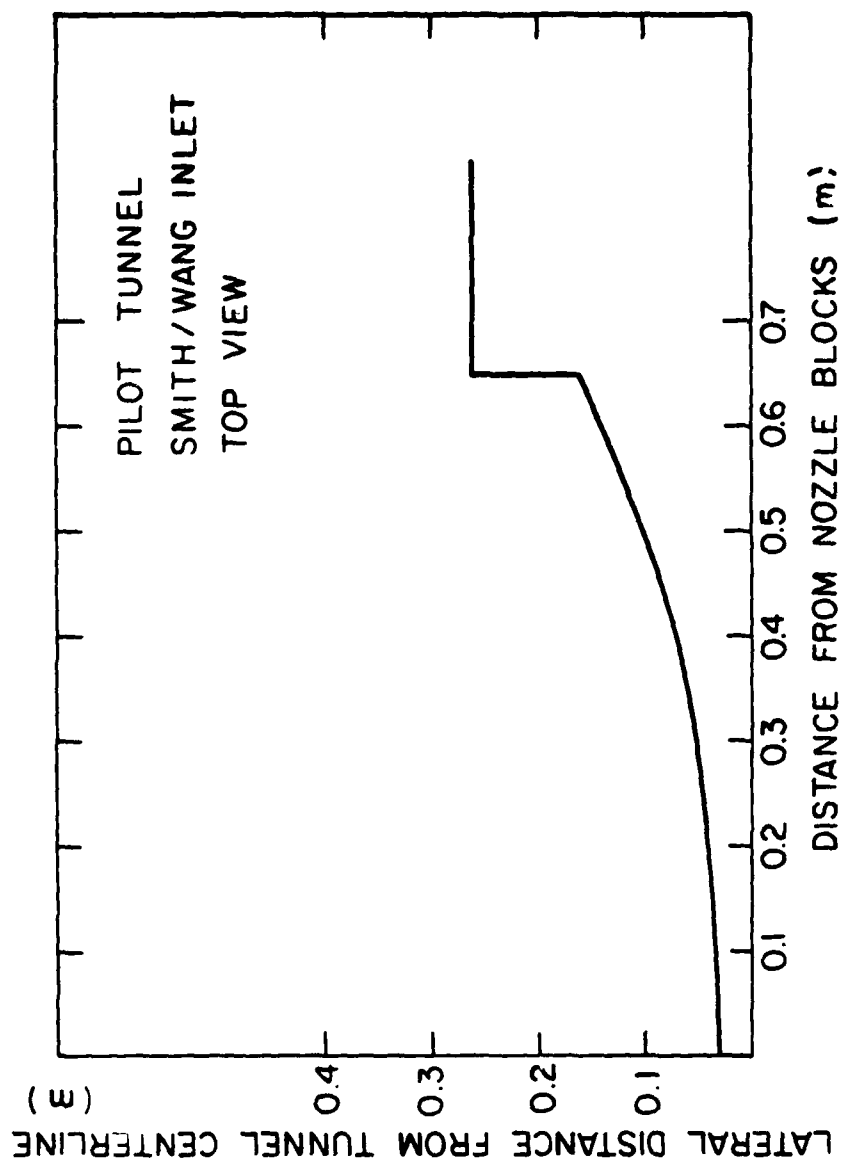


Figure 21. Inlet Geometry Profile, Smith/Wang Inlet, Top View.

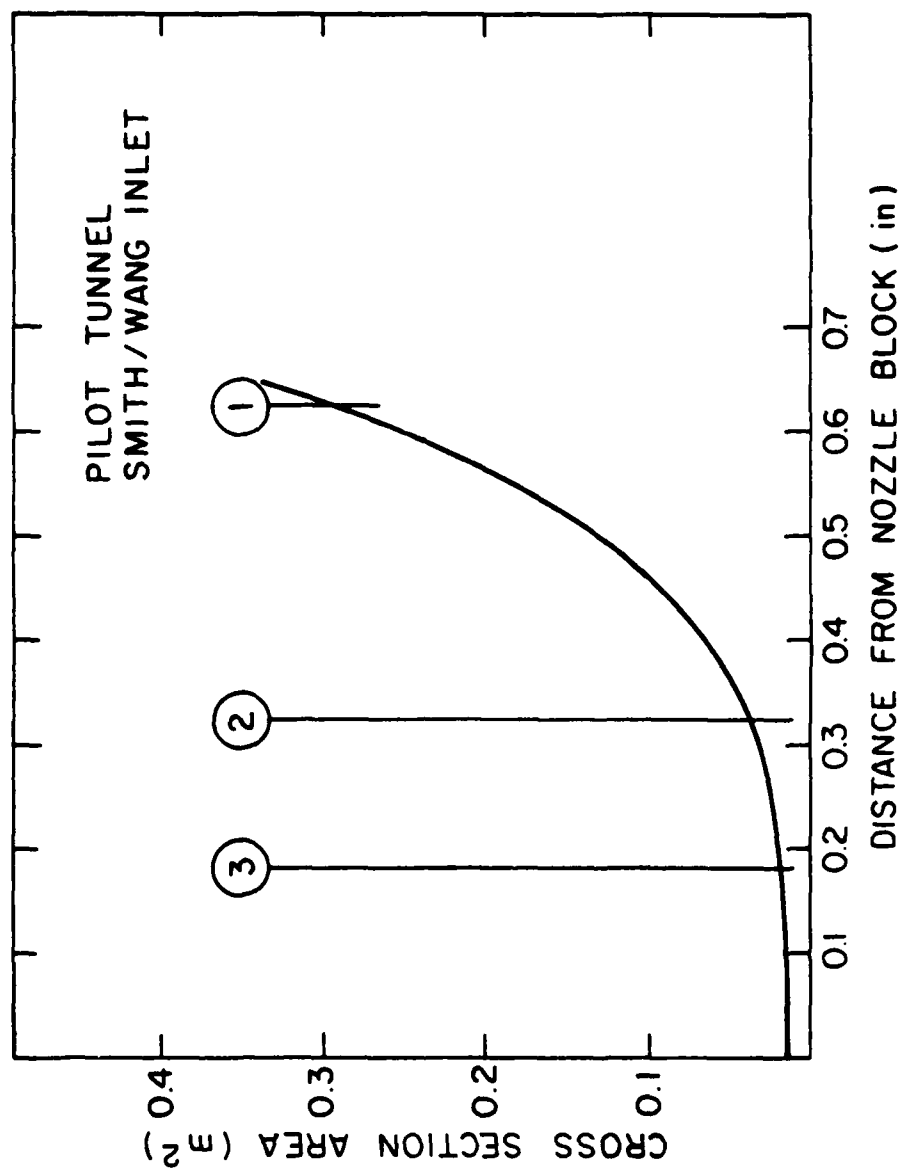


Figure 22. Axial Distribution of Cross-Section Area, Smith/Wang Inlet.

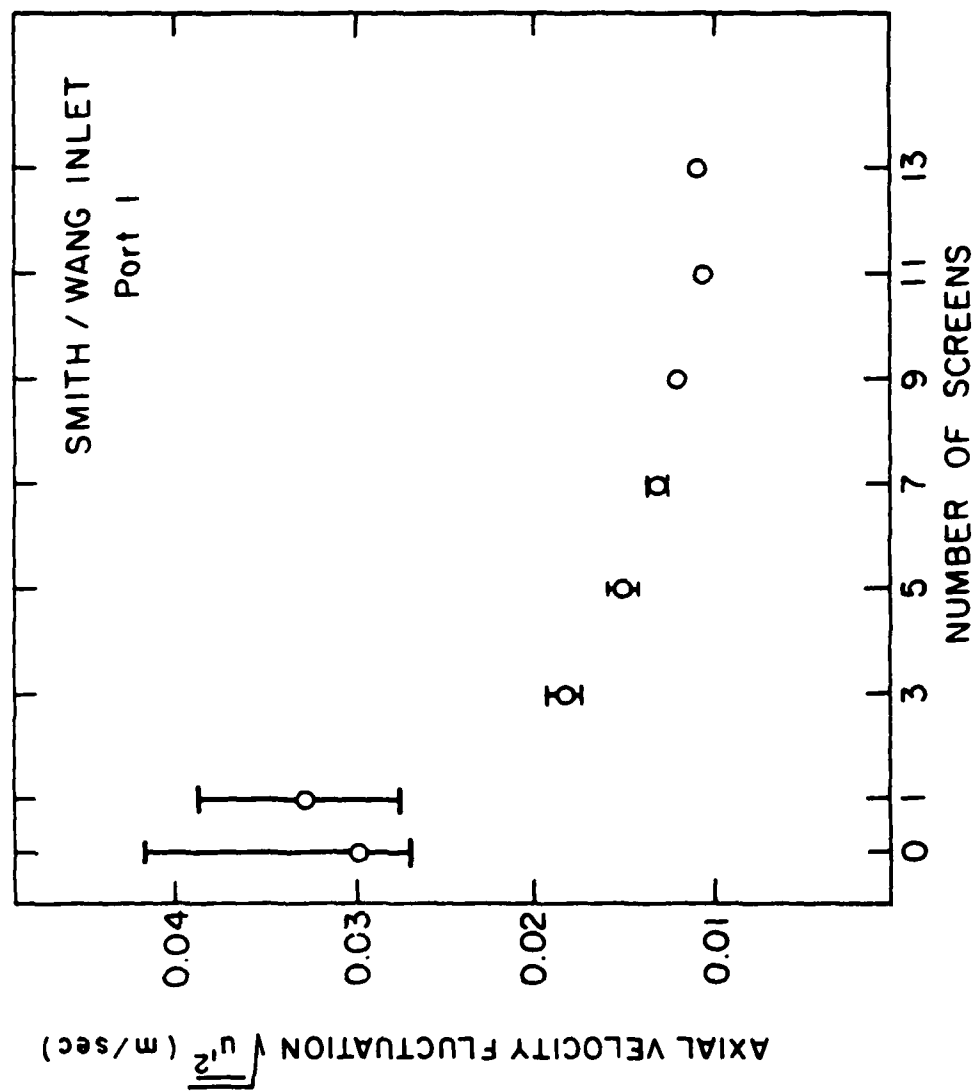


Figure 23. Axial Velocity Fluctuations, Smith/Wang Inlet, Port 1.

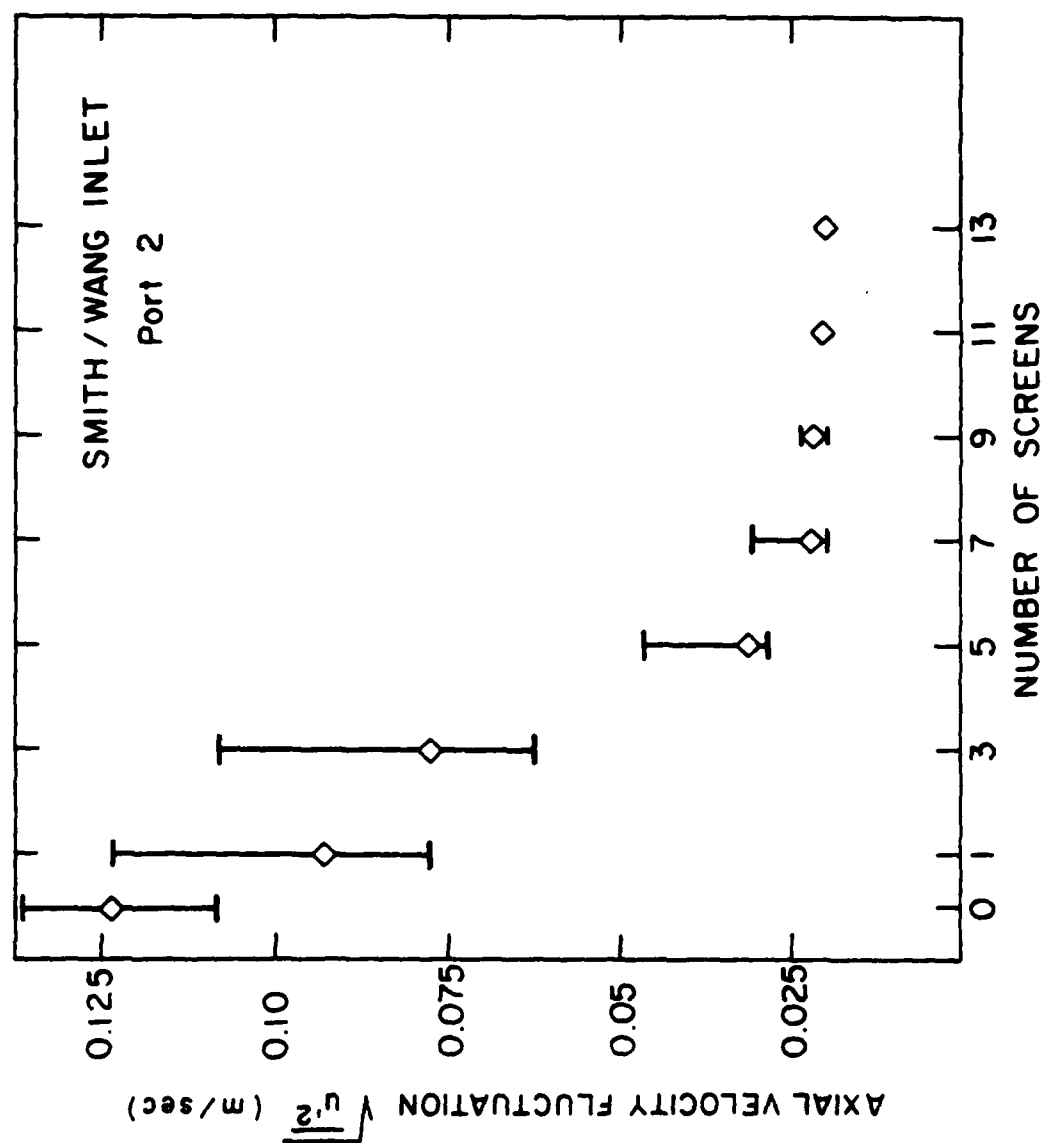


Figure 24. Axial Velocity Fluctuations, Smith/Wang Inlet, Port 2.

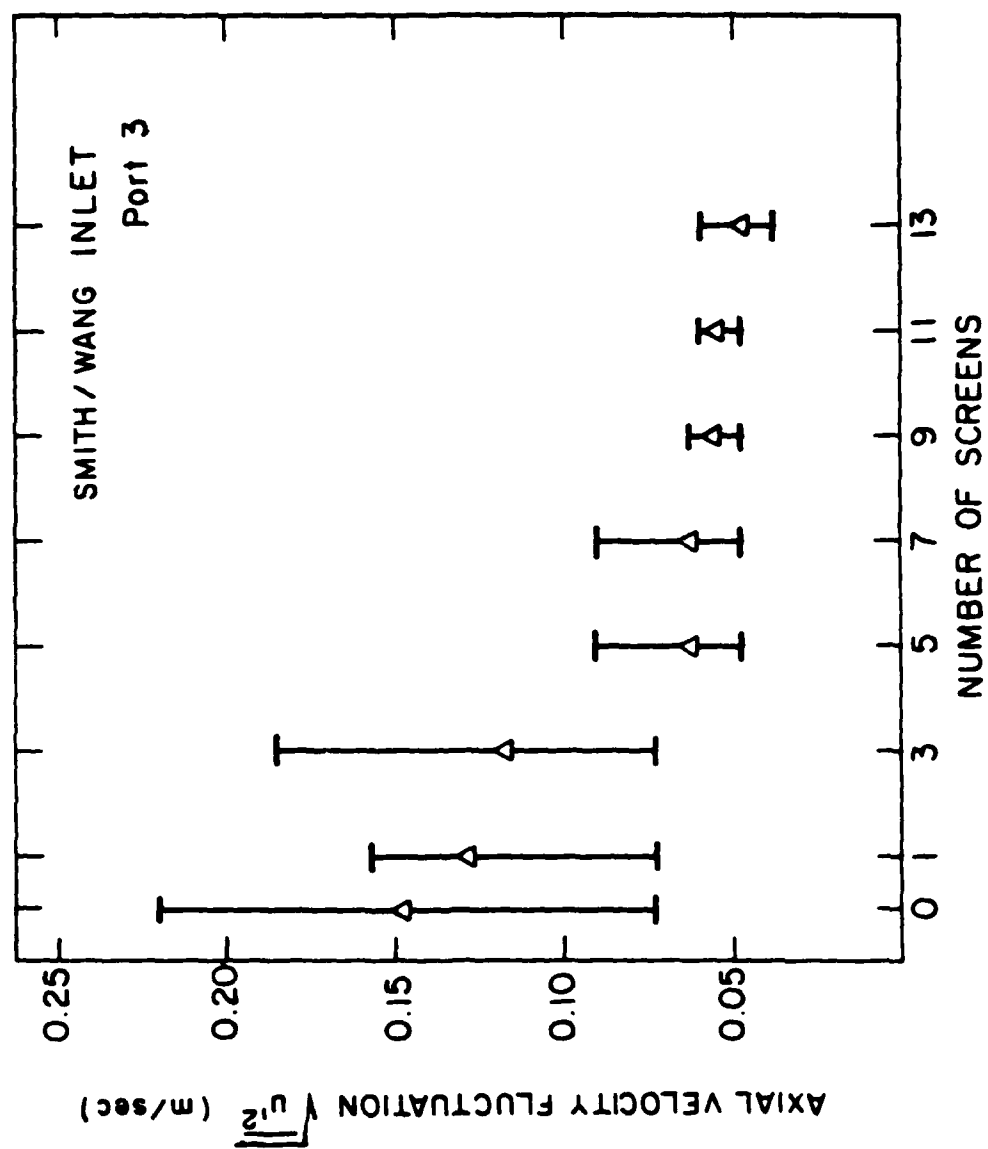


Figure 25. Axial Velocity Fluctuations, Smith/Wang Inlet, Port 3.



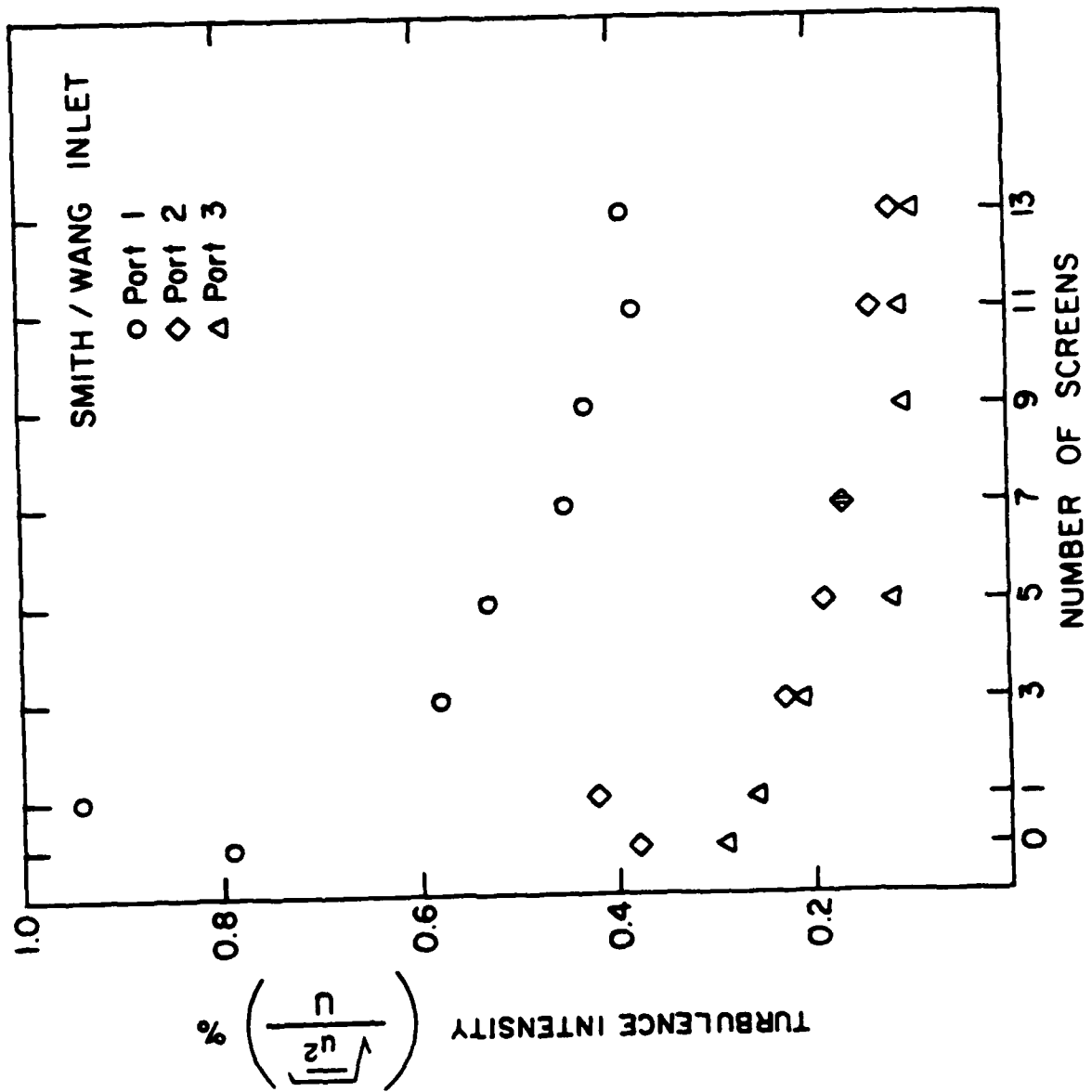


Figure 26. Axial Turbulence Intensity Summary, Smith/Wang Inlet.

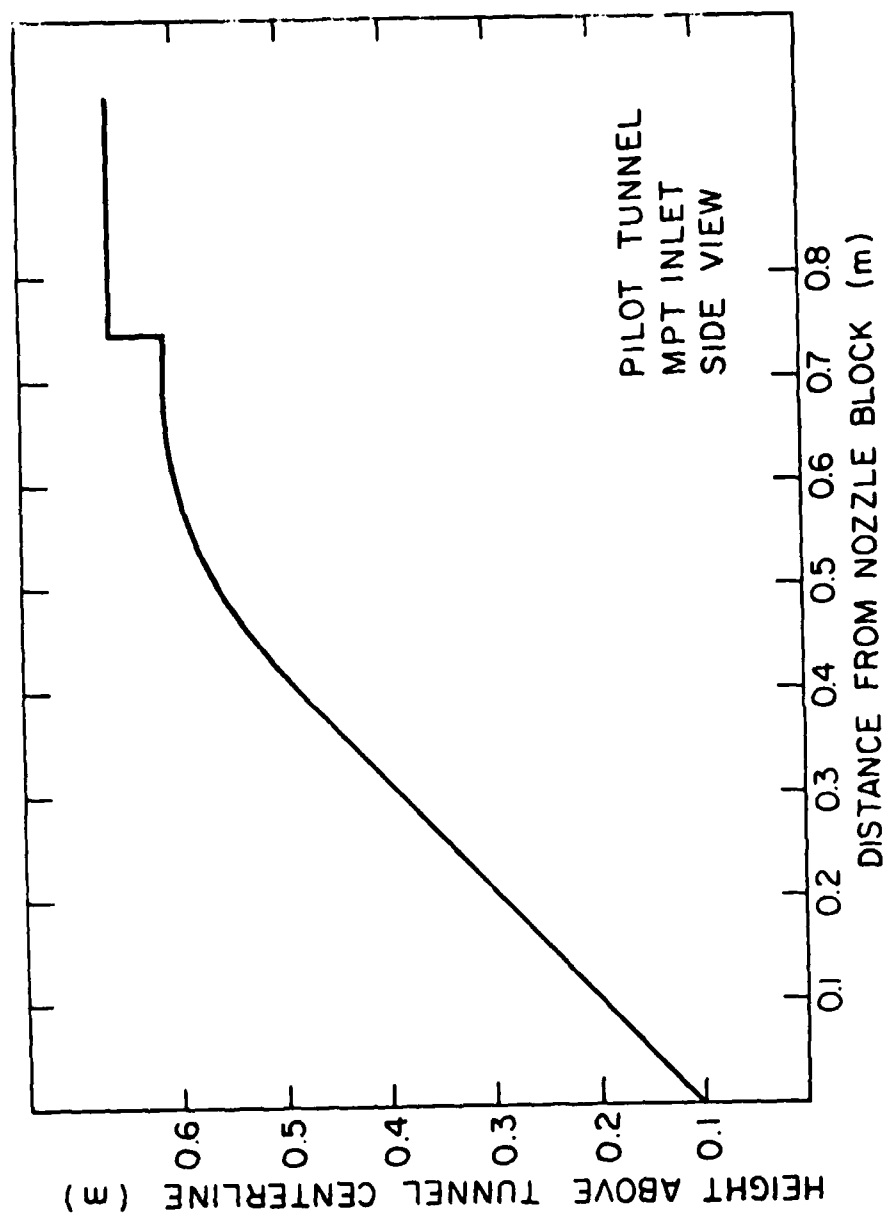


Figure 27. Inlet Geometry Profile, MPT Inlet, Side View.

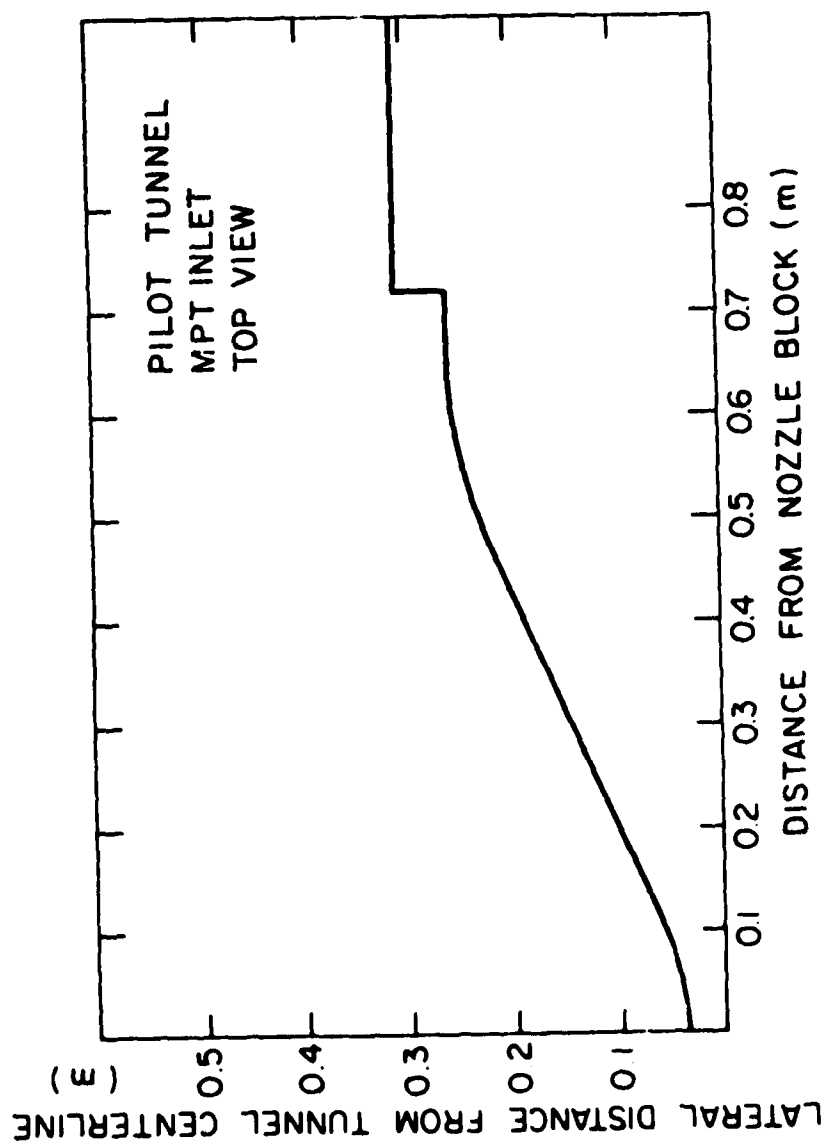


Figure 28. Inlet Geometry Profile, MPT Inlet, Top View.

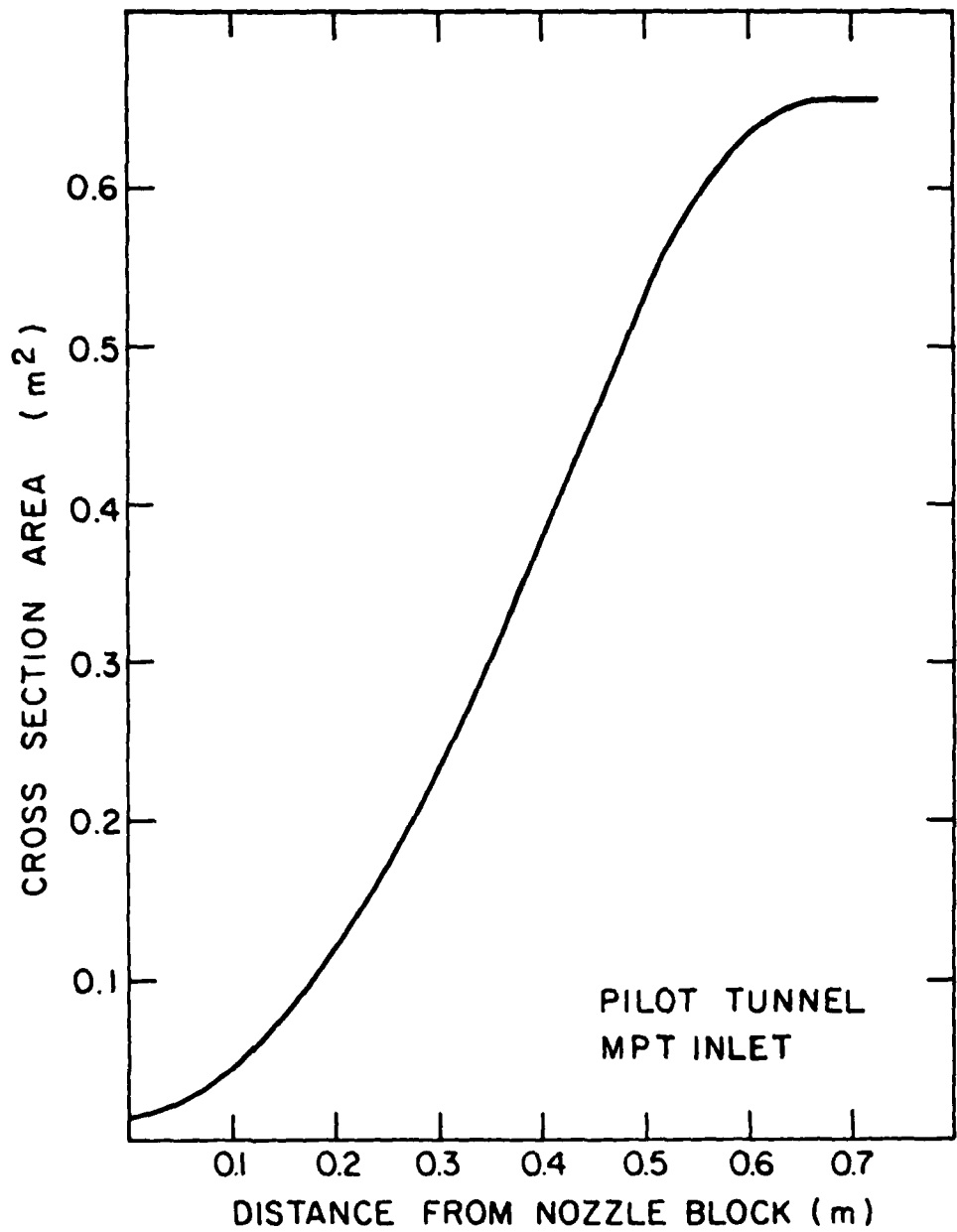


Figure 29. Axial Distribution of Cross-Section Area, MPT Inlet.

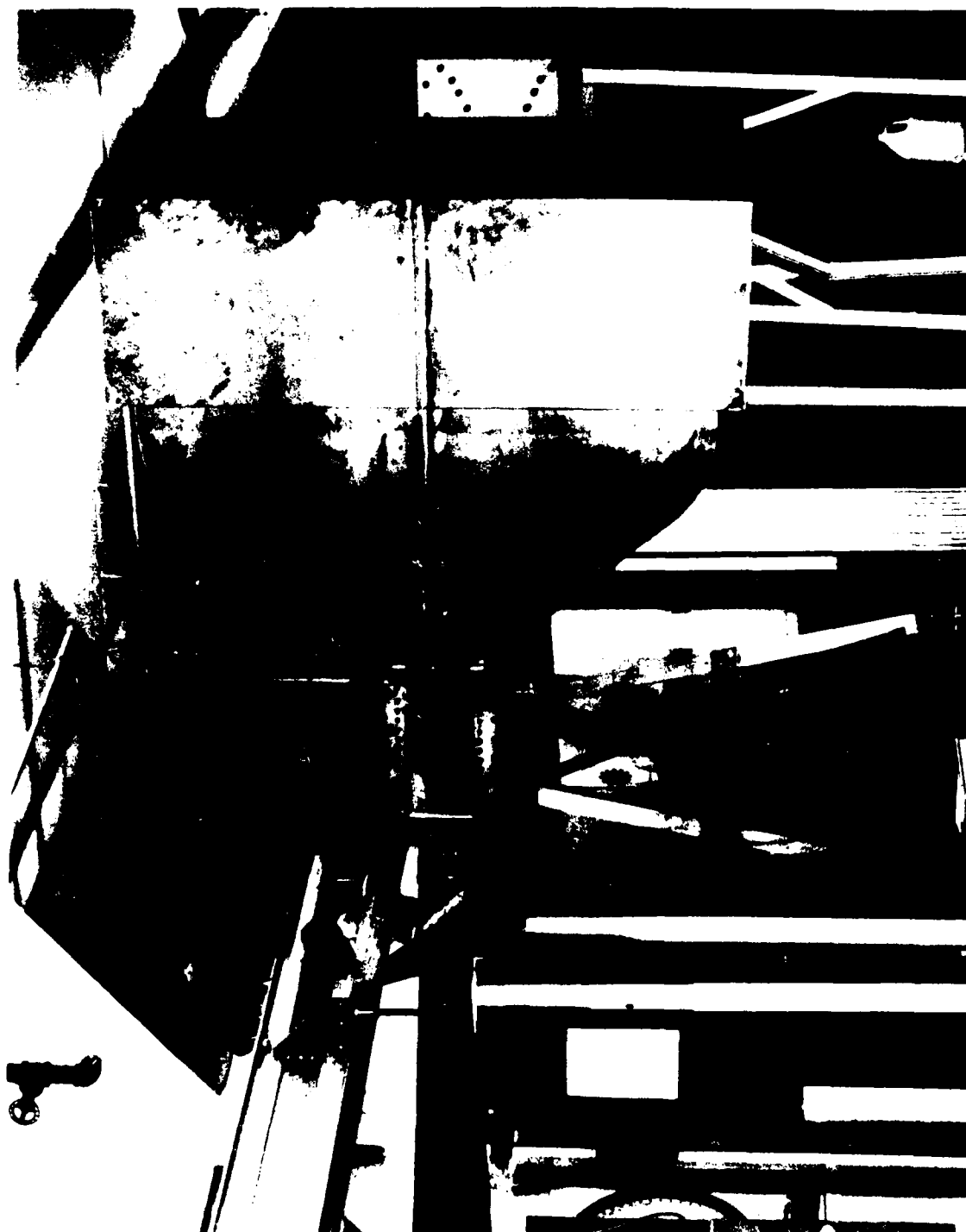


Figure 30. Photograph of MPT Inlet Installed on Pilot Tunnel

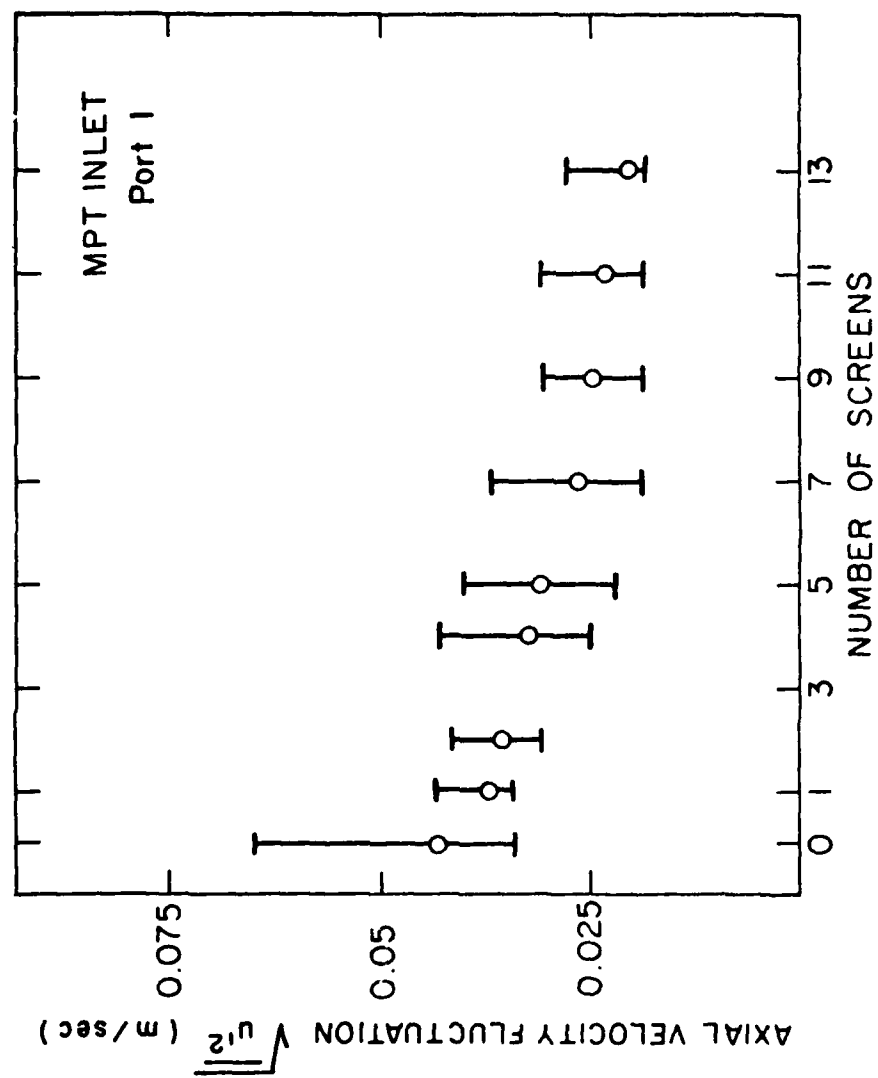


Figure 31. Axial Velocity Fluctuations, MPT Inlet, Port 1.

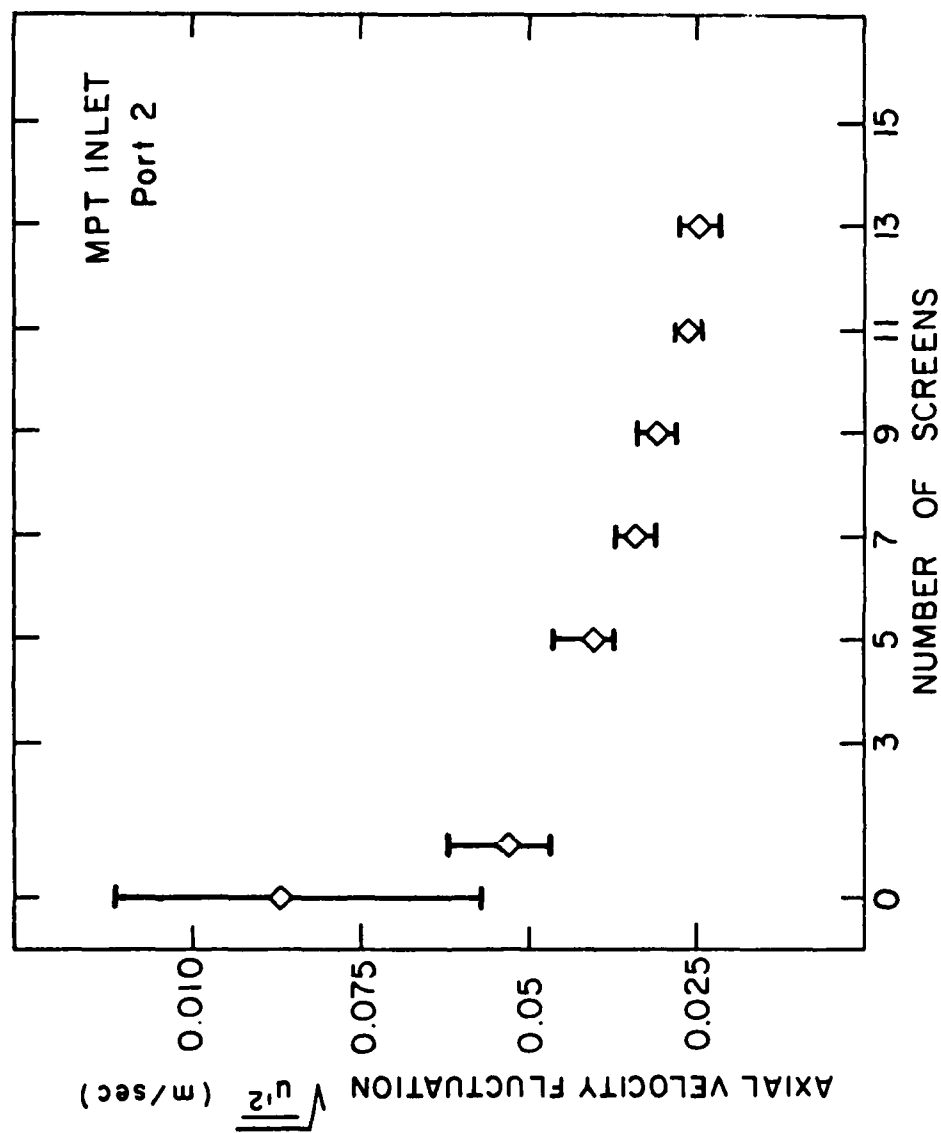


Figure 32. Axial Velocity Fluctuations, MPT Inlet, Port 2.

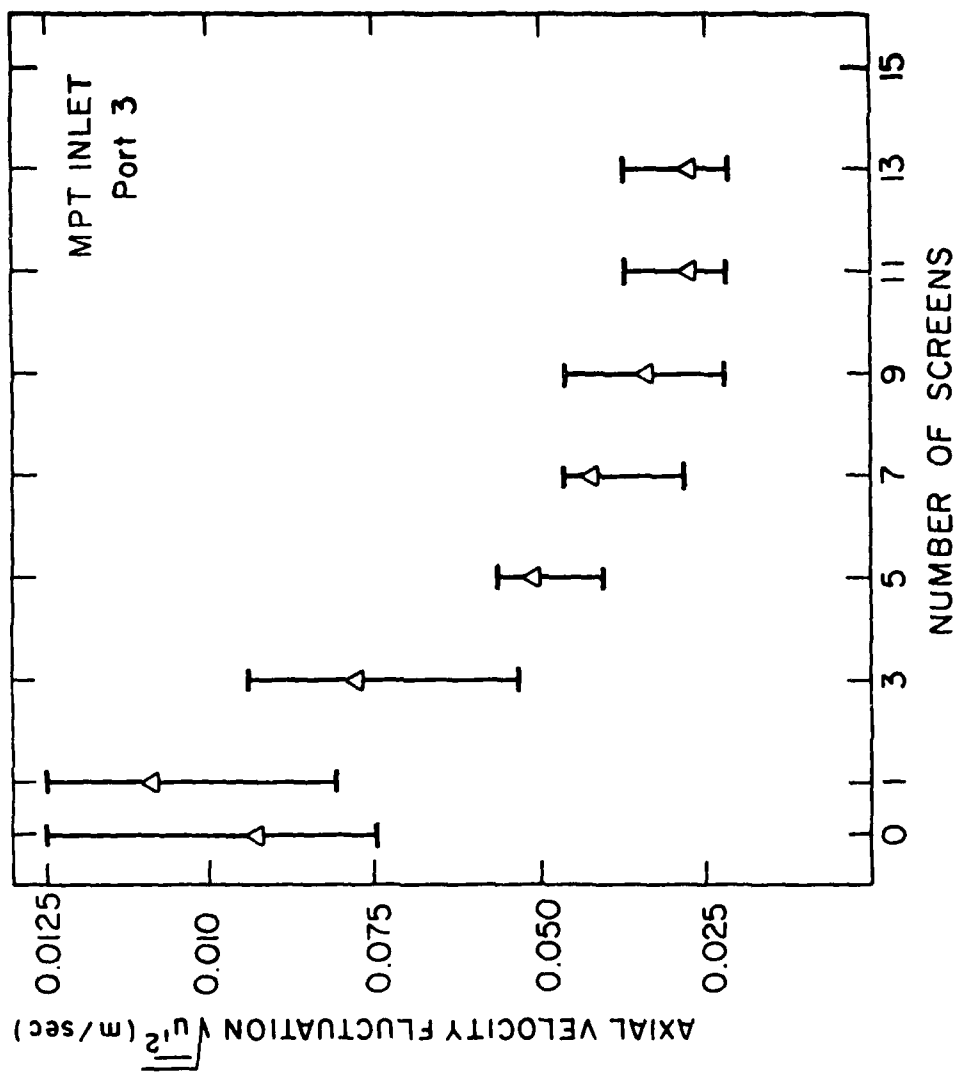


Figure 33. Axial Velocity Fluctuations, MPT Inlet, Port 3.



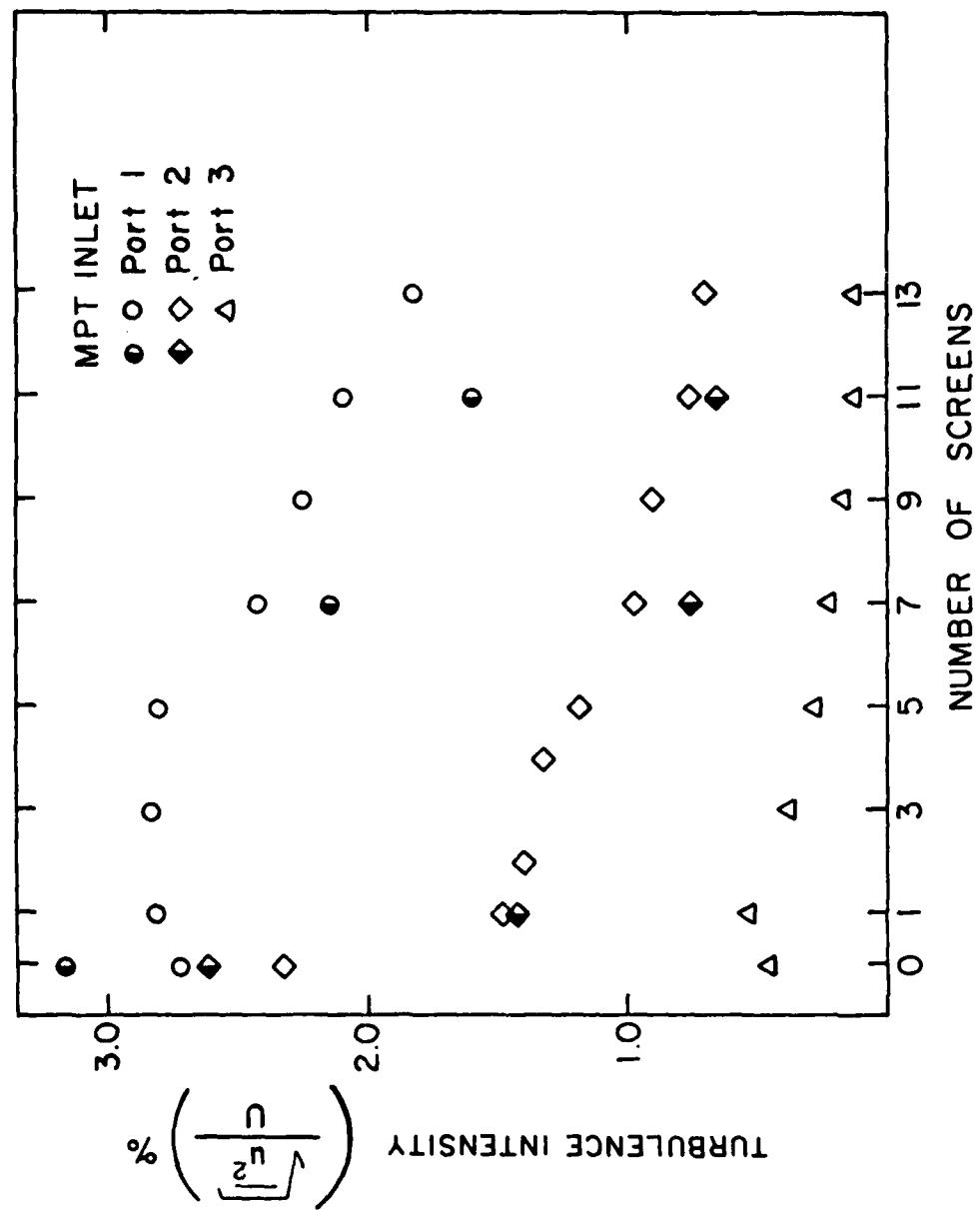


Figure 34. Axial Turbulence Intensity Summary, MPT Inlet  
(Solid Symbols are X-Wire Measurements).

ND-A100 333

NOTRE DAME UNIV IND DEPT OF AEROSPACE AND MECHANICA--ETC F/G 20/4  
HIGH SPEED SMOKE FLOW VISUALIZATION. (U)

MAR 81 S M BATILL, R C NELSON, T J MUELLER

F33615-79-C-3034

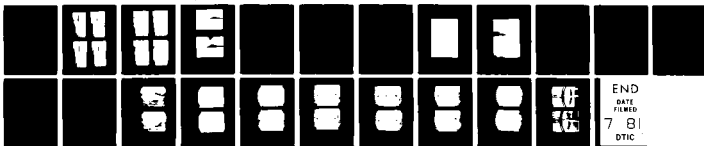
UNCLASSIFIED

AFWAL-TR-81-3002

NL

2.2

2.2



END  
DATE  
FILMED  
7 81  
DTIC

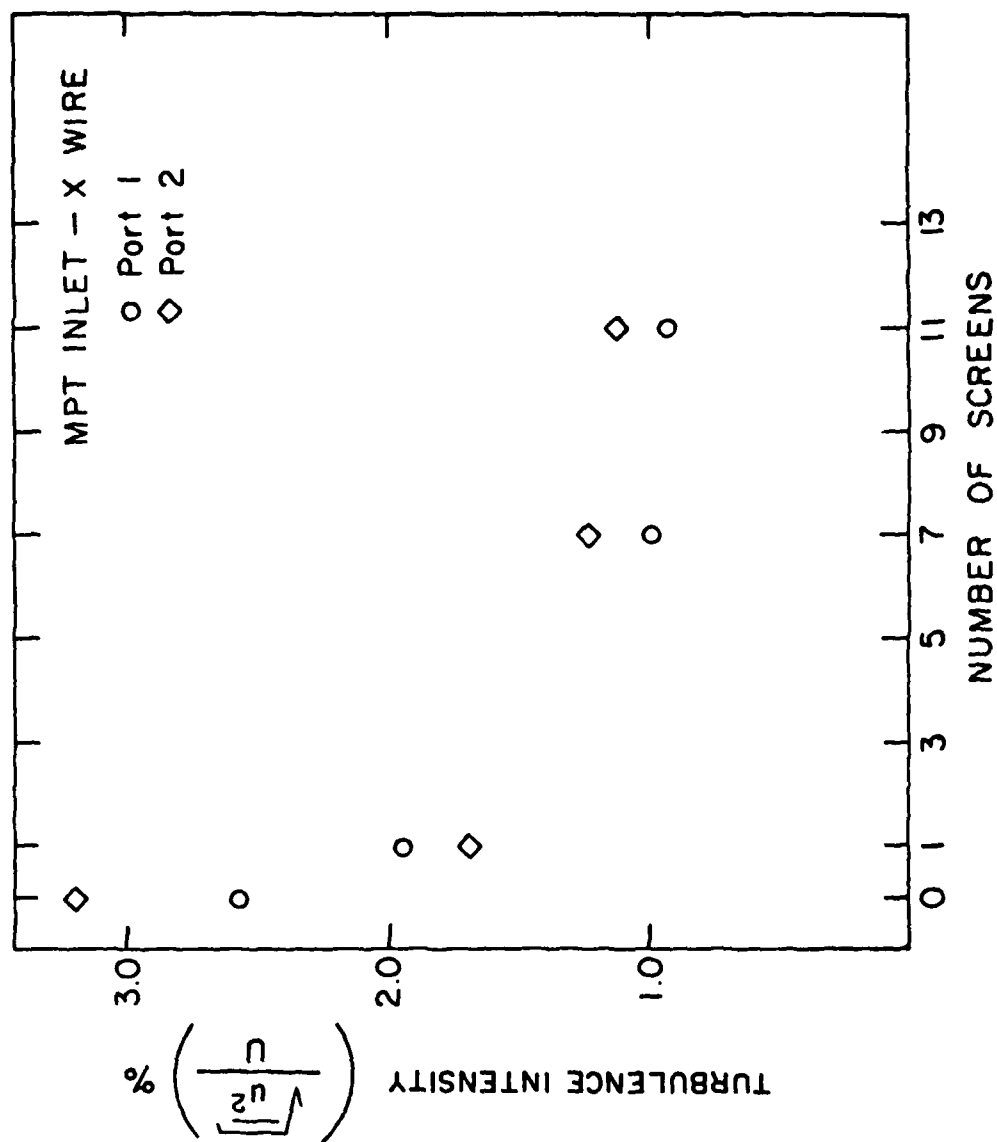


Figure 35. Turbulence Intensity Summary. Transverse Component, MPT Inlet.



3 Screens



11 Screens

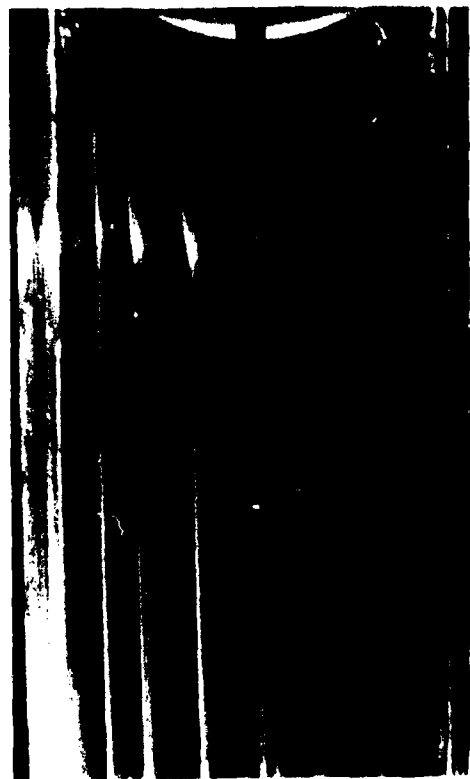


1 Screen

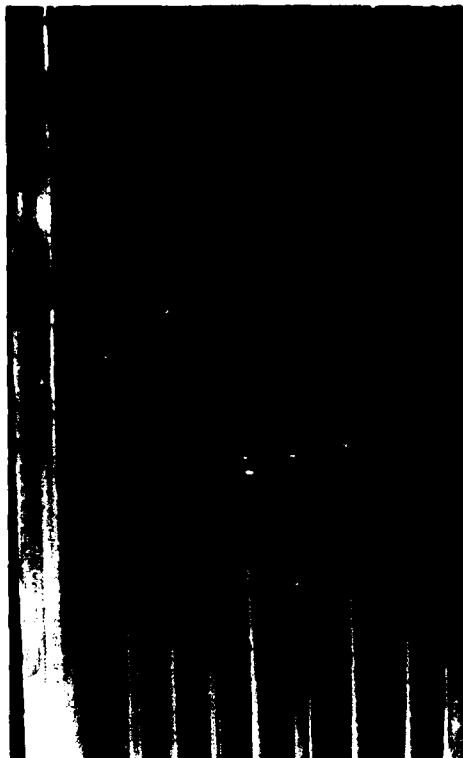


7 Screens

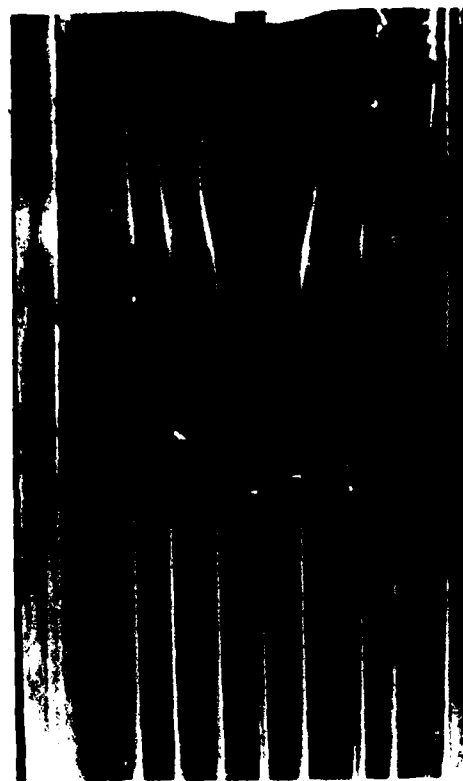
Figure 36. Screen Influence Study, Pilot Tunnel MPT Inlet. Top Lighting.  
(19.1 mm ID Smoke Rake)



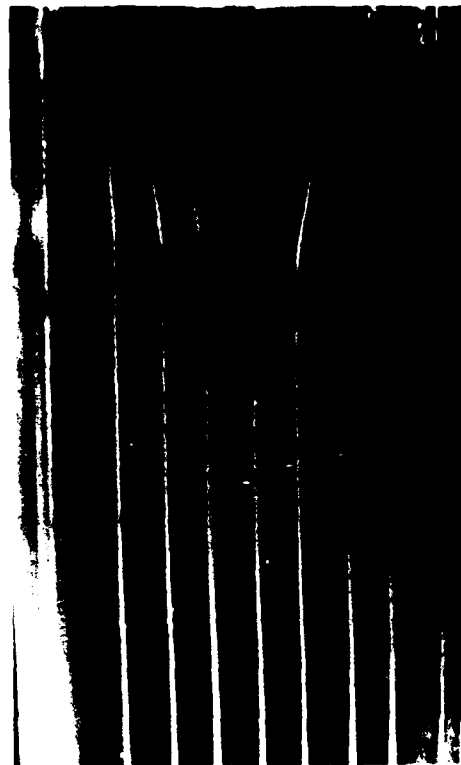
1 Screen



3 Screens



7 Screens

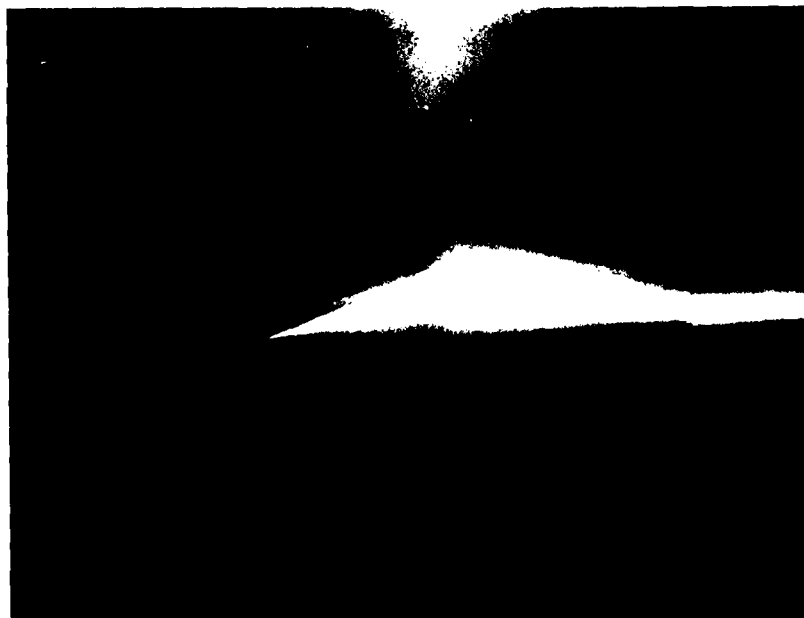


11 Screens

Figure 36 (Continued). Screen Influence Study, Pilot Tunnel MPT Inlet, Back Lighting.  
(19.1 mm ID Smoke Rake)



Honeycomb Upstream of 10 Screens



Honeycomb Downstream of 10 Screens

Figure 37. Influence of Honeycomb Insert on Smoke Visualization Data

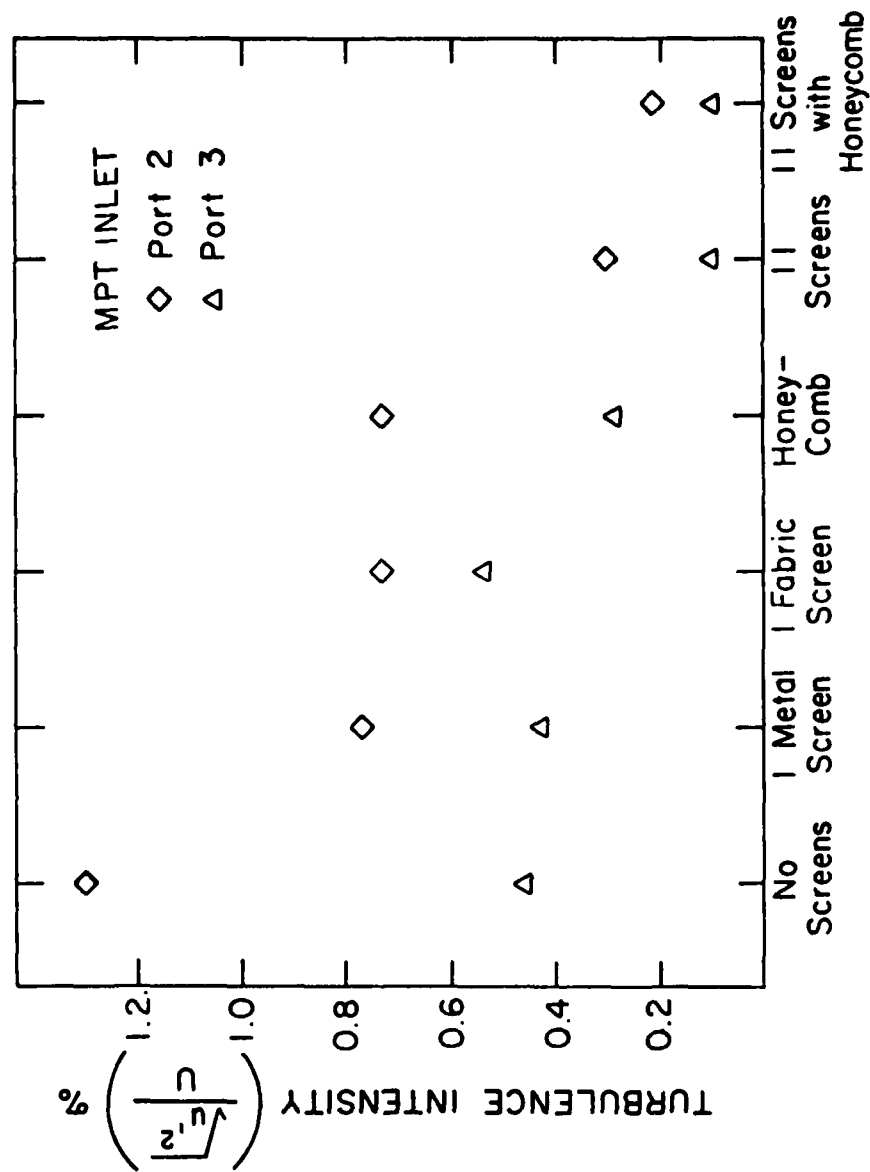


Figure 38. Axial Turbulence Intensity Summary, MPT Inlet with Honeycomb.

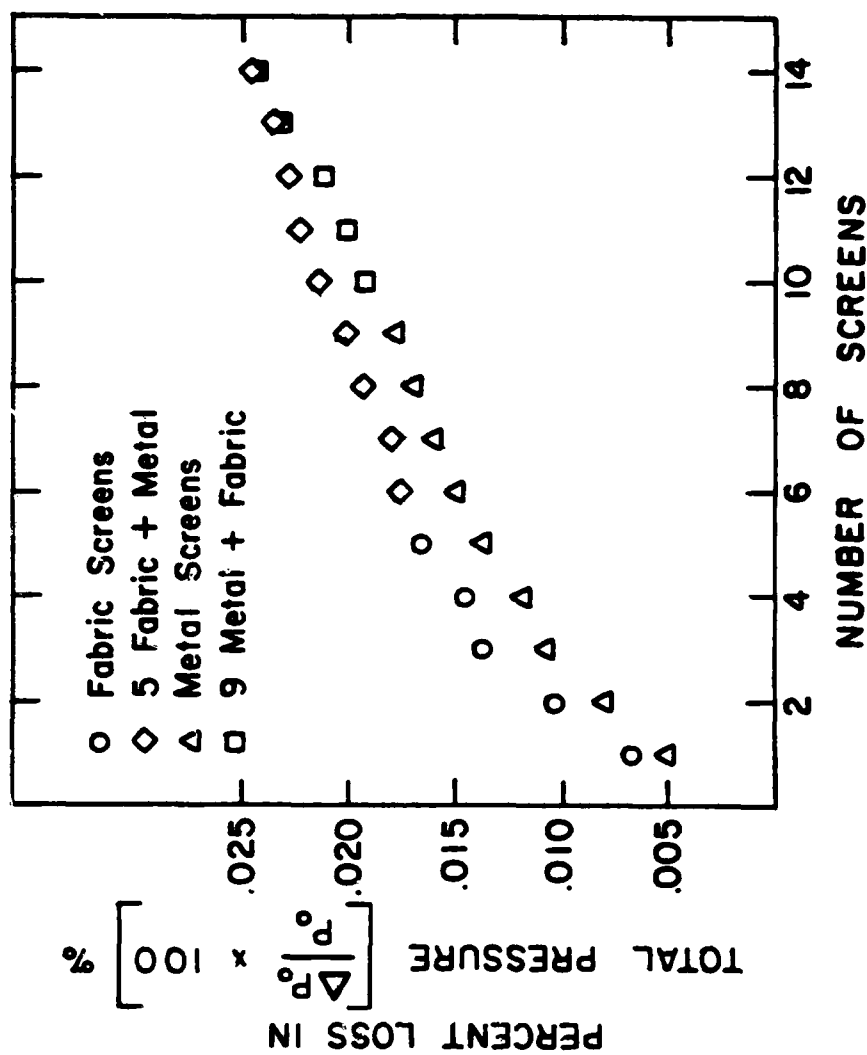


Figure 39. Total Pressure Loss through Anti-Turbulence Screens



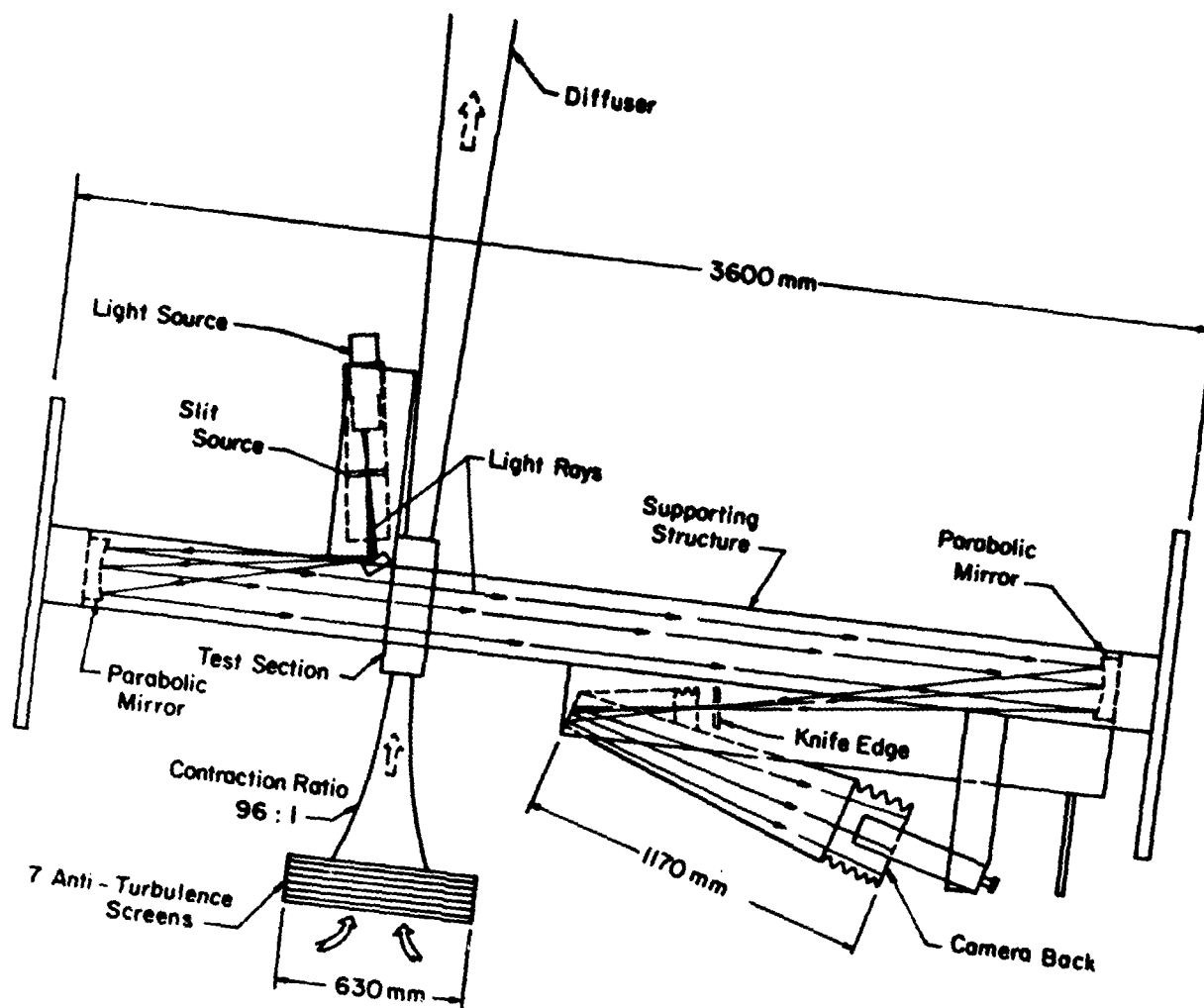


Figure 40. Schematic of Single Pass Schlieren System

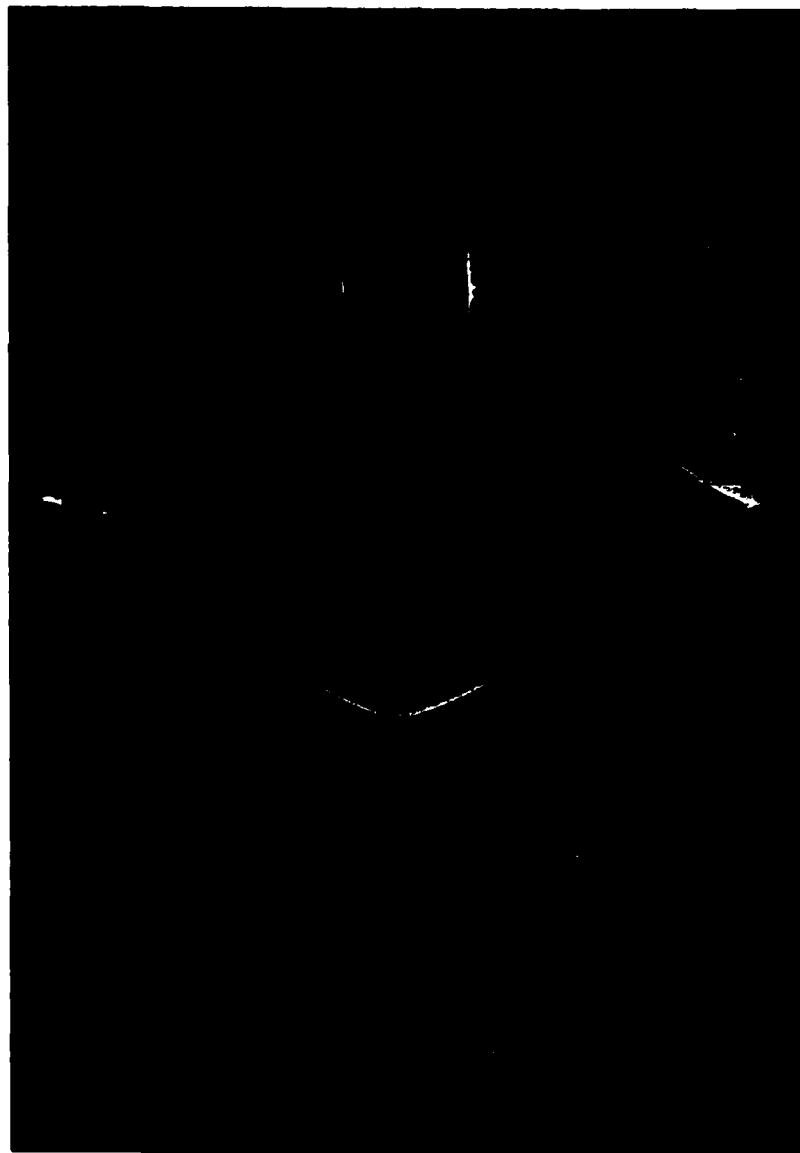


Figure 41. Opaque Stop Schlieren Photograph;  $9^\circ$  Double Wedge Model,  
 $M_\infty \approx 1.42$ .

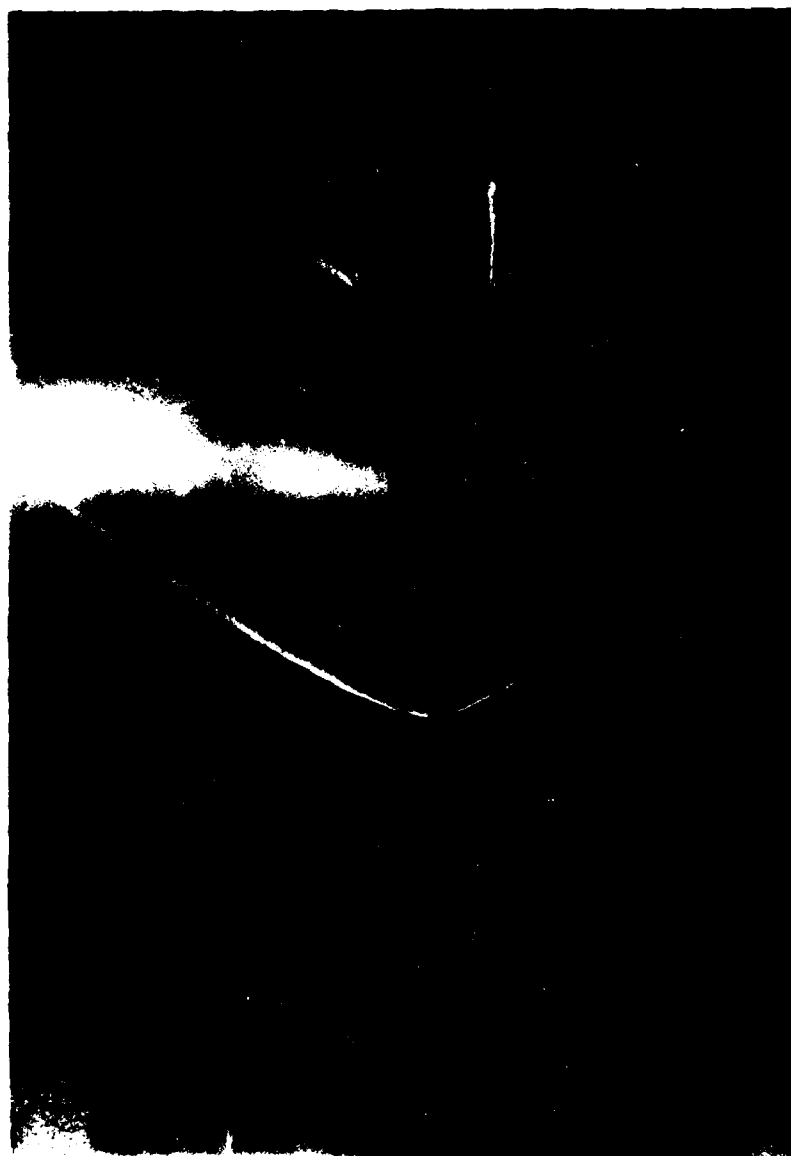


Figure 42. Simultaneous Smoke Flow/Opaque Stop Schlieren Photograph,  
9° Double Wedge Model,  $M_\infty \approx 1.42$ .

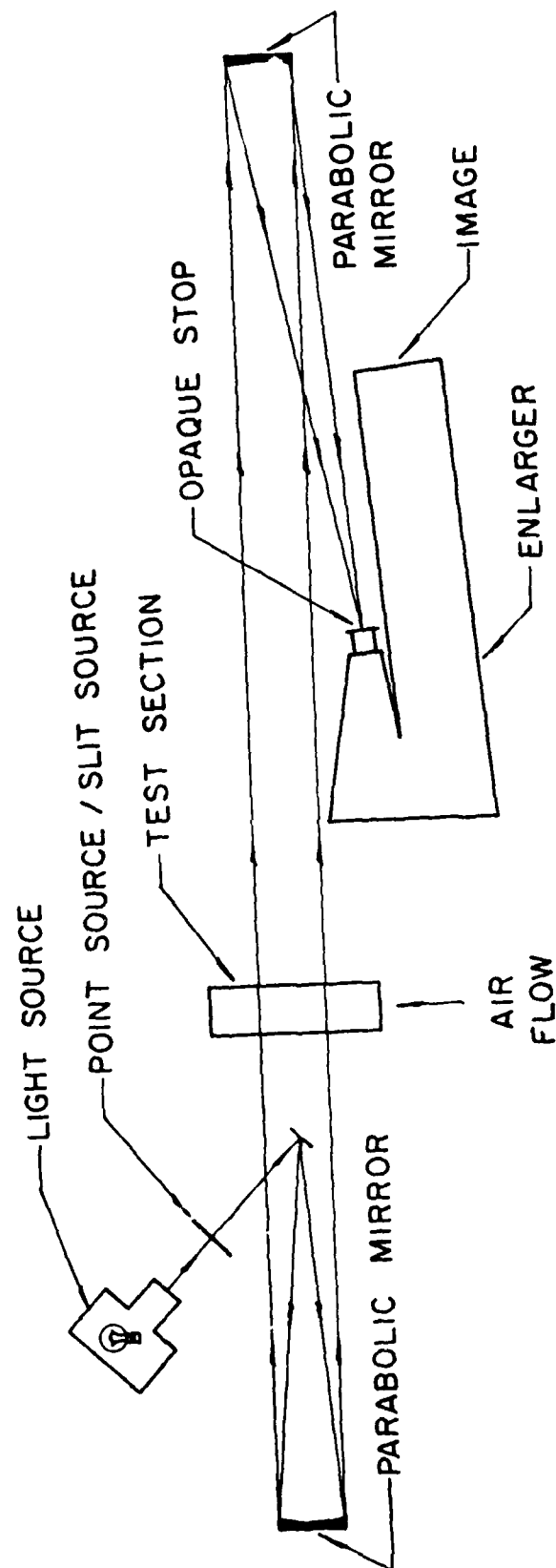


Figure 43. Modified Opaque Stop Schlieren System

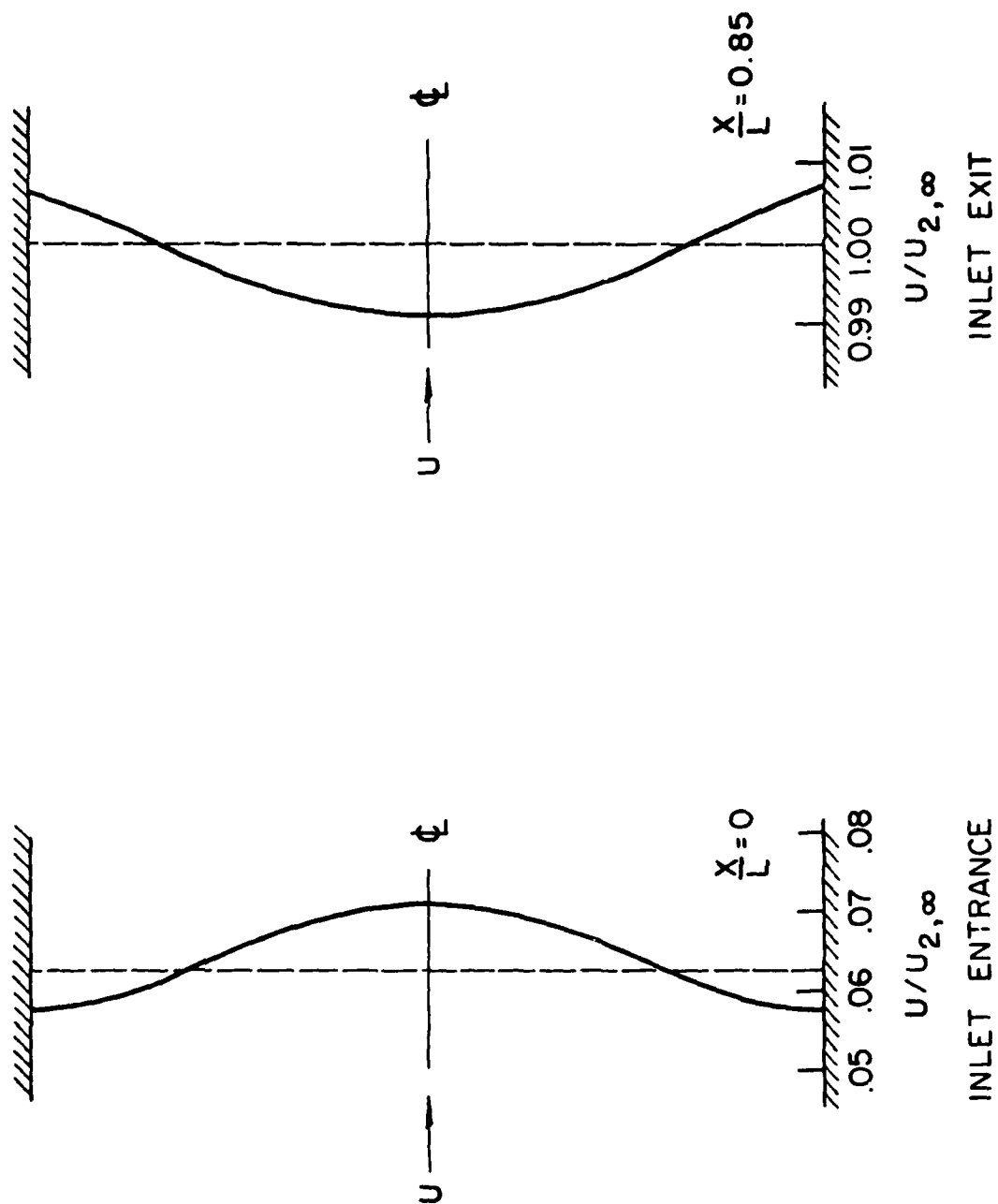


Figure 44. Inlet Entrance and Exit Velocity Profiles (Data from Reference 24).

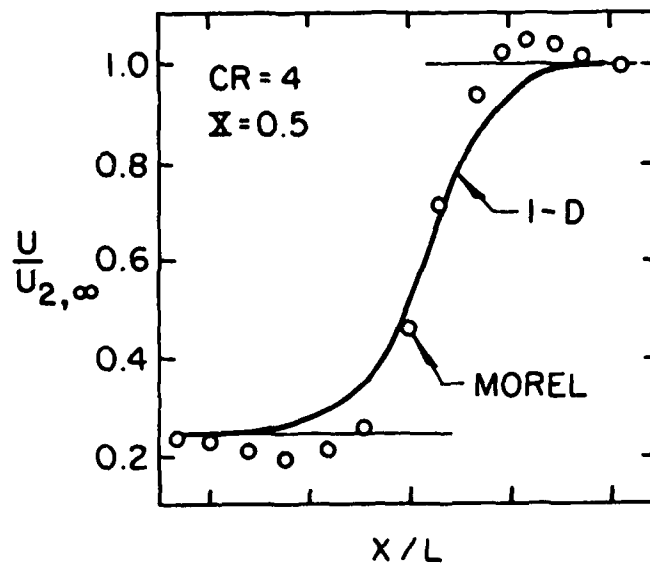


Figure 45. Inlet Wall Velocity Distribution, Comparison of One-Dimensional and Two-Dimensional Calculations.

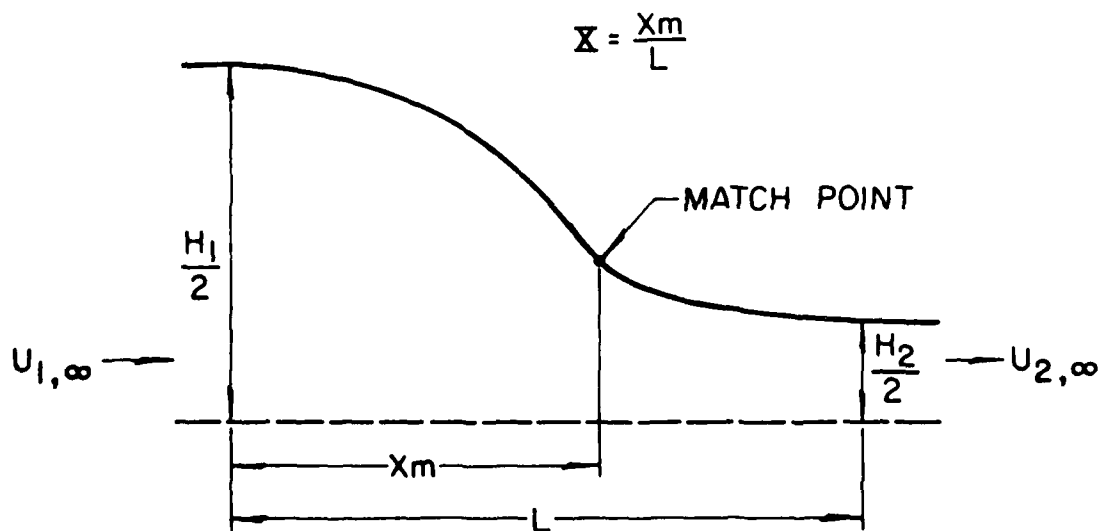


Figure 46. Geometry and Notation for Matched Cubic Inlet Shapes.

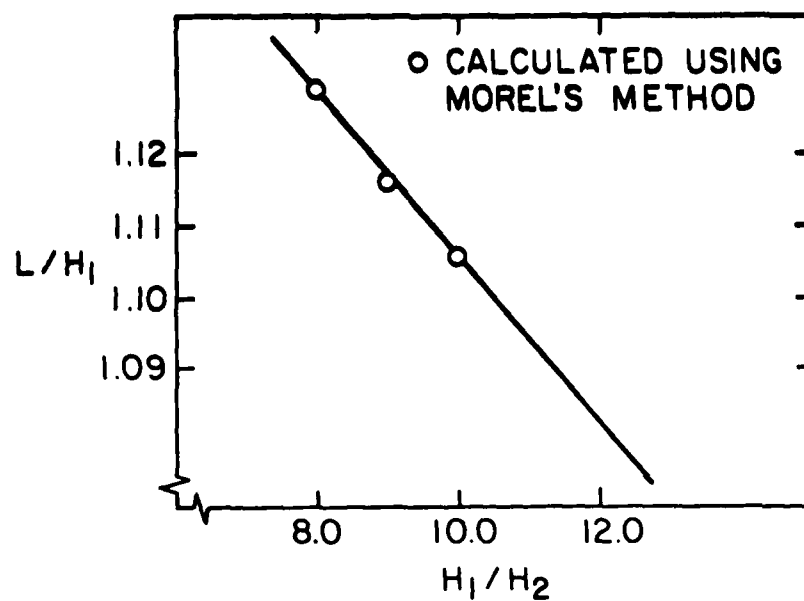


Figure 47. Non-Dimensional Inlet Length versus Contraction Ratio, Calculated Using Morel's Method.

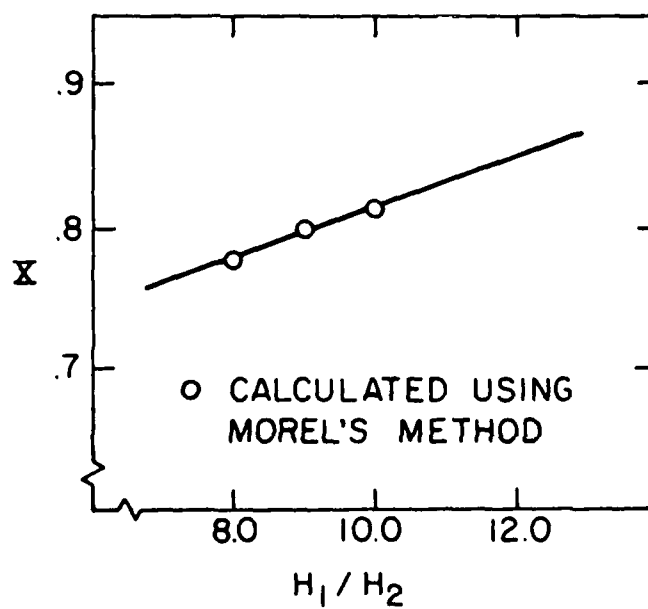


Figure 48. Location of Match Point versus Contraction Ratio, Calculated Using Morel's Method.

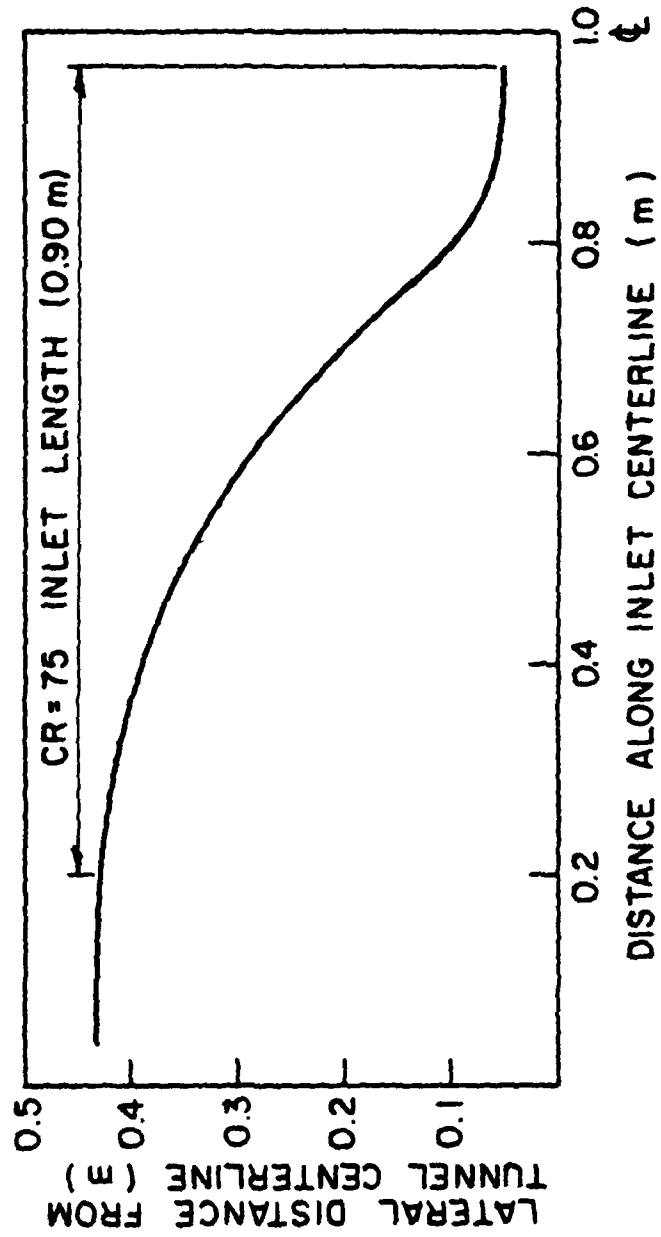


Figure 49. Inlet Profile, CR = 75 Inlet, Transonic Tunnel.



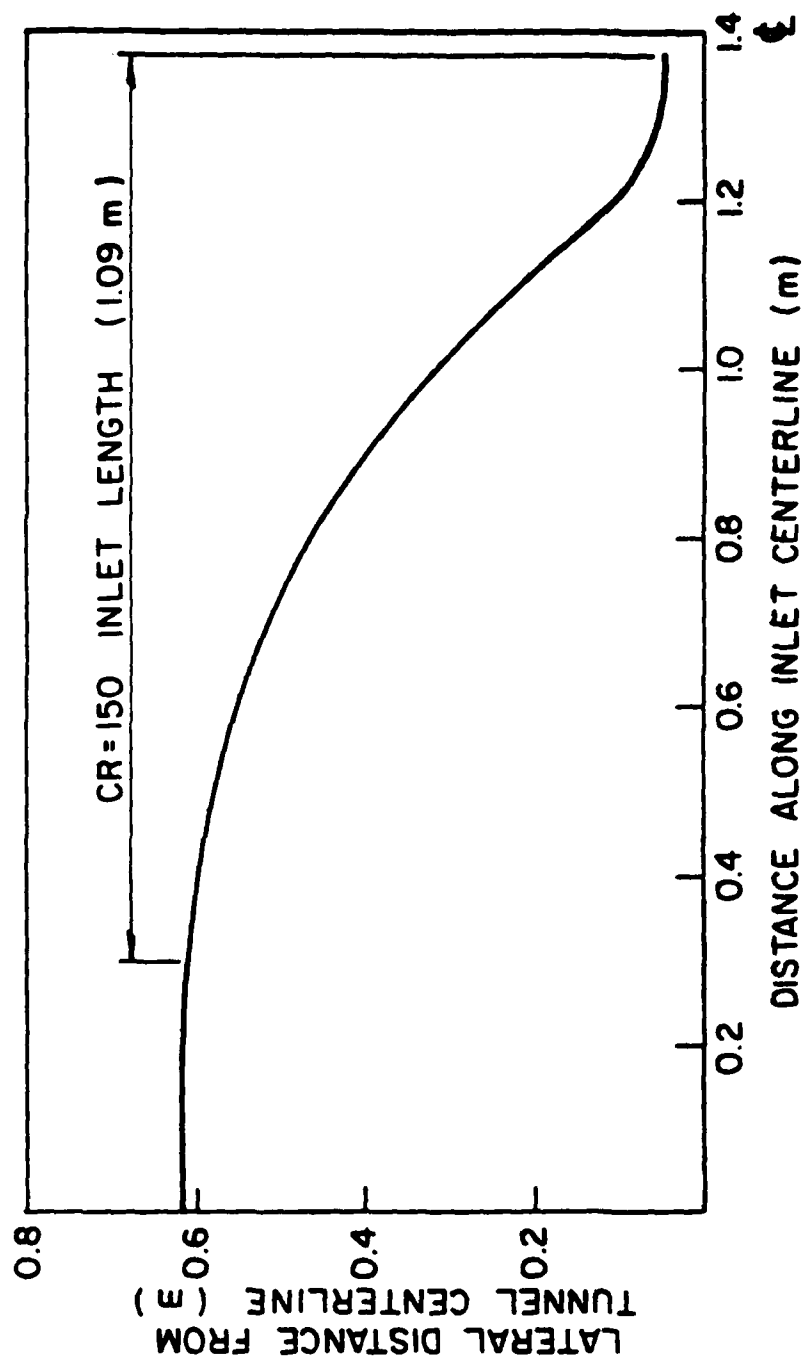


Figure 50. Inlet Profile, CR = 150 Inlet, Transonic Tunnel.

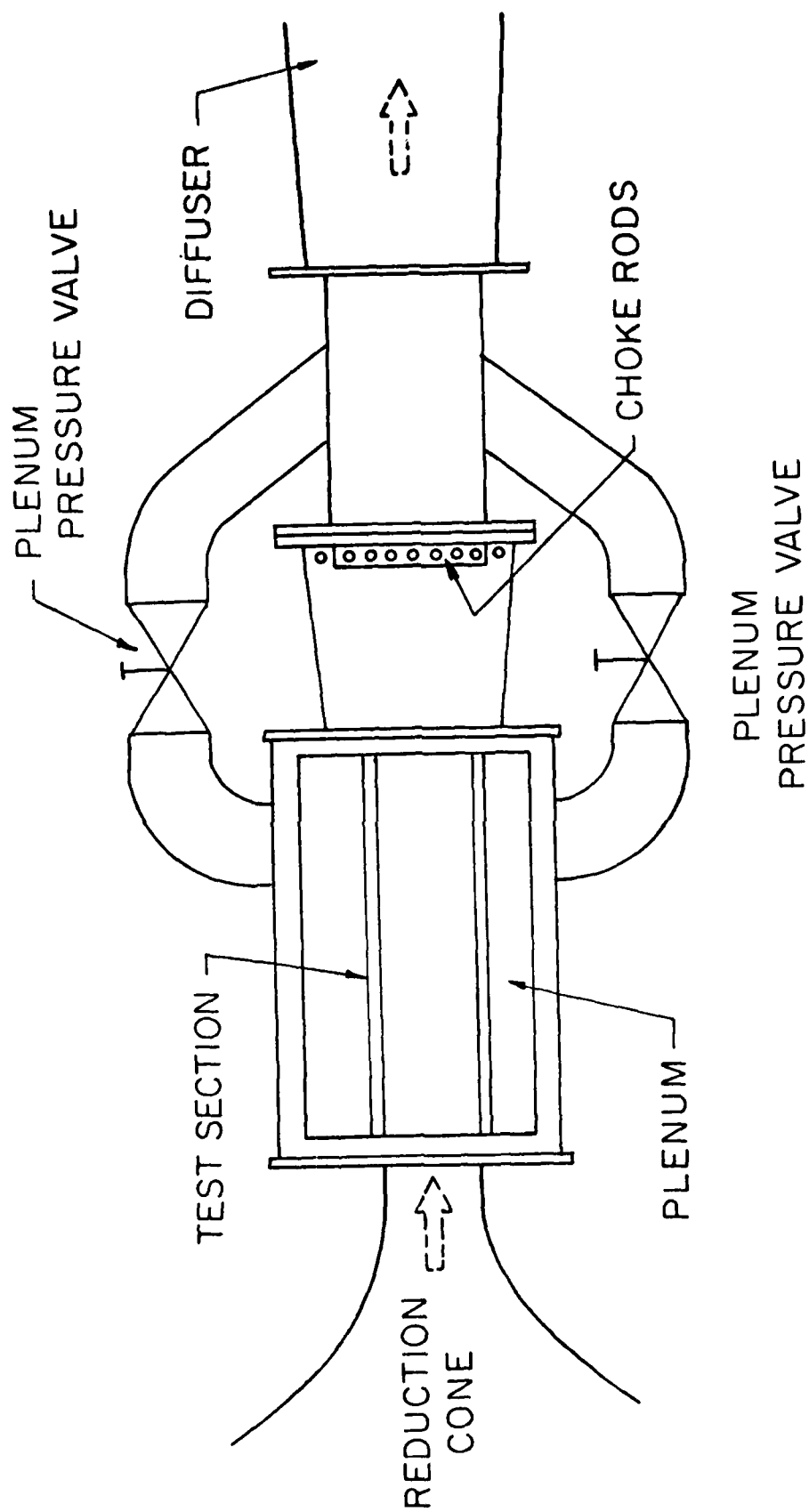
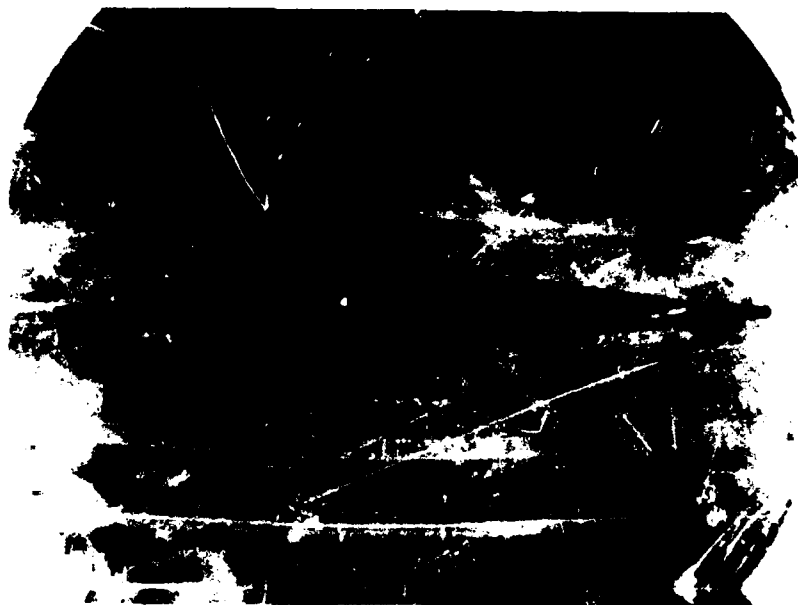
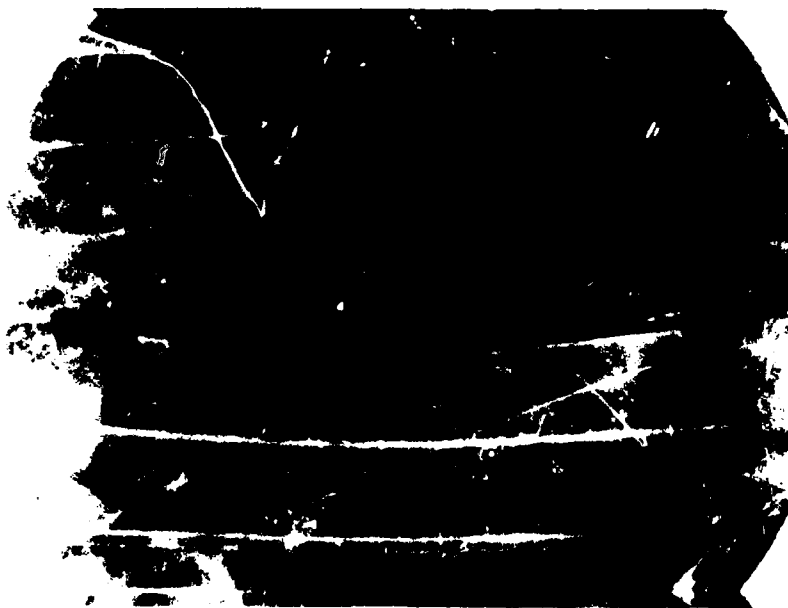


Figure 51. Schematic of Transonic Test Section



5 Screens



11 Screens

Figure 52. Screen Influence, Transonic Tunnel,  
CR  $\approx$  75 Inlet,  $M_{\infty} = 0.40$ .

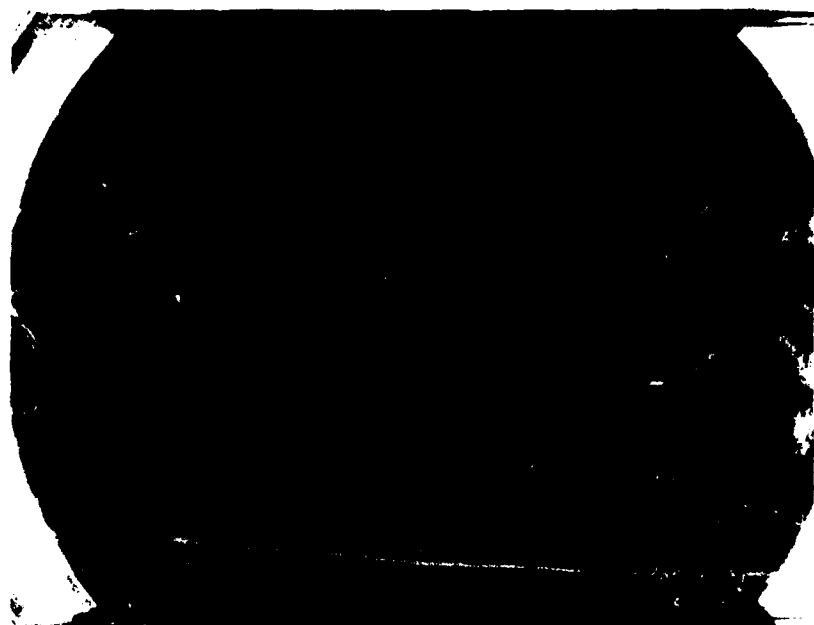


Valves Closed



Valves Open

Figure 53. Transonic Smoke Flow Visualization,  
CR = 75 Inlet,  $\alpha = 8^\circ$ ,  $M_\infty \approx 0.40$ .



Valves Closed



Valves Open

Figure 54. Transonic Smoke Flow Visualization,  
CR = 75 Inlet,  $\alpha = 15^\circ$ ,  $M_\infty \approx 0.40$ .



5 Screens



8 Screens

Fig. 55. Transonic Smoke Flow Visualization,  
CR = 150 Inlet,  $\alpha = 0$ ,  $M_\infty \approx 0.40$ .



11 Screens,  $M_{\infty} = 0.40$



11 Screens,  $M_{\infty} = 0.60$

Fig. 56. Transonic Smoke Flow Visualization  
CR = 150 Inlet,  $\alpha = 0^\circ$ .



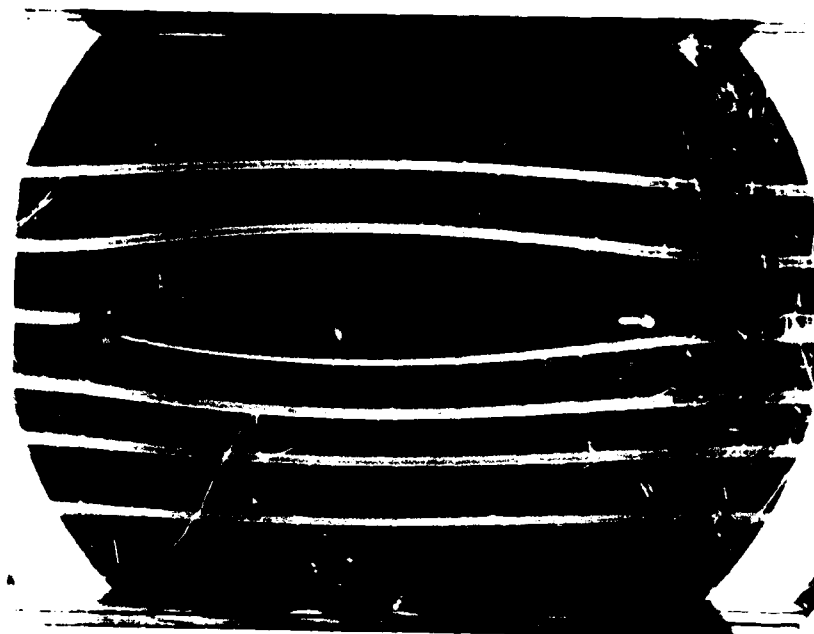
$\alpha = 0^\circ$



$\alpha = -13^\circ$

Fig. 57. Transonic Smoke Flow Visualization  
CR = 150 Inlet, 11 Screens,  $M_\infty \approx 0.72$ .



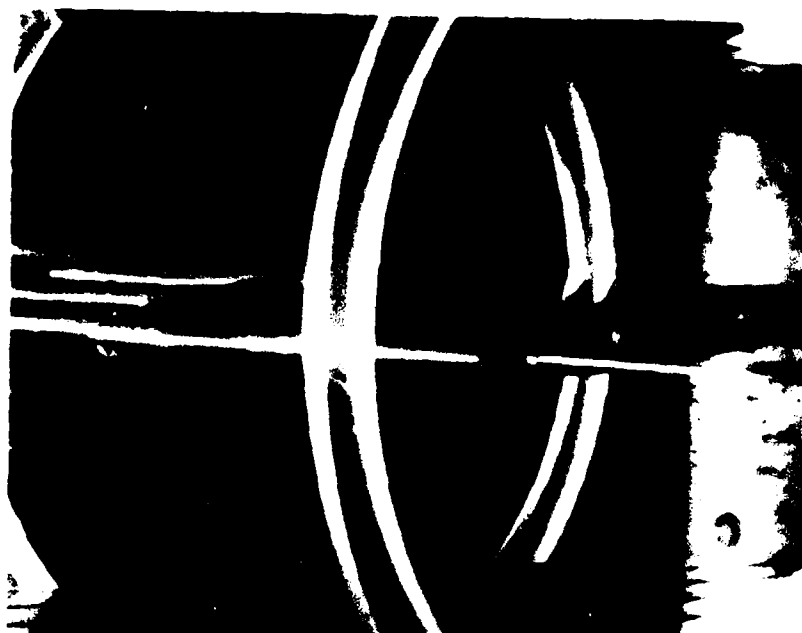


Valves Closed

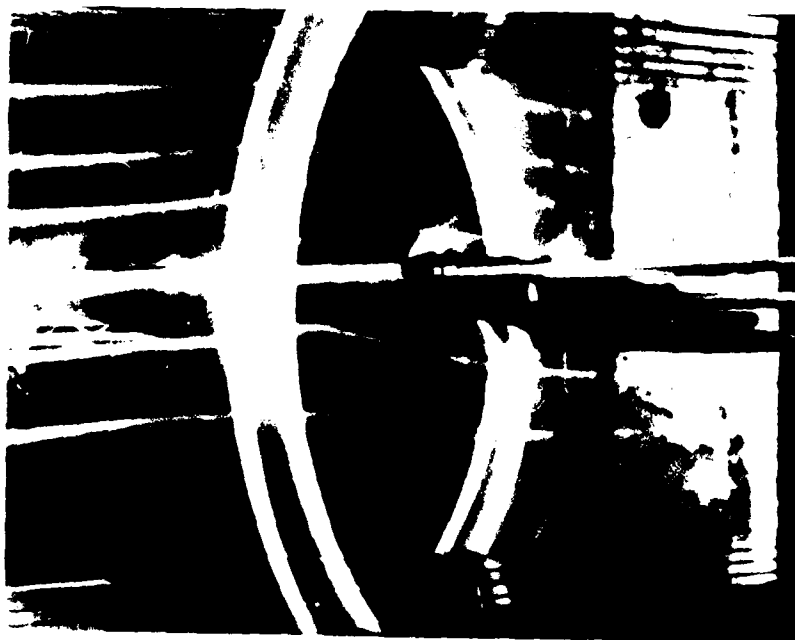


Valves Open

Fig. 58. Transonic Smoke Flow Visualization,  
CR = 150 Inlet, 11 Screens,  $M_\infty \approx 0.40$ .



Smoke-Rake Near Tunnel Centerline



Smoke-Rake Near Tunnel Wall

Figure 59. Transonic Smoke Flow Demonstration, Oblique View,  
CR = 150 Inlet,  $M_\infty \approx 0.40$ .

FILMED

— 8